The role of Hsp90 in the Wnt pathway of MCF7 breast cancer cells

A thesis submitted in fulfilment of the requirements for the degree of

MASTER OF SCIENCE
in Biochemistry

of

Rhodes University

Leanne Cooper
December 2010

In loving memory of my Mother, Susan Cooper, who fought a brave battle against cancer.

(7 December 1950 – 2 March 2010)

ABSTRACT

Breast cancer is one of the most common forms of cancer in not only South African women, but women all over the world. The molecular chaperone heat shock protein 90 (HSP90) is upregulated in cancer and is almost exclusively associated with proteins involved in intracellular signal transduction, thus it plays an important role in signalling pathways within the cell. In cancer, there is an aberrant activation of the Wnt signaling pathway, which results in stabilized β-catenin being able to translocate to the nucleus where it can trigger the transcription of oncogenes found to be involved in the self-renewal of cells. The level of β-catenin is usually kept in check by a destruction complex comprising glycogen synthase kinase 3-beta (GSK-3β), axin1, adenomatous polyposis coli (APC) which phosphorylate β-catenin, resulting in its ubiquitination and degradation. HSP90 has been found to be associated with GSK-3β, but whether this association is only transient is debatable. Very little is known about the association of HSP90 with other members of the Wnt pathway in breast cancer. In this study, we have attempted to further identify the direct associations between HSP90 and GSK-3β, β-catenin, p-β-catenin and axin1. Immunofluorescence and confocal microscopy co-localization studies suggested a potential association between HSP90 and these proteins. Treatment with HSP90 inhibitors, 17-AAG and novobiocin resulted in a shift of axin1 to what appeared to be the plasma membrane. The associations of HSP90 with GSK-3β, β-catenin, p-β-catenin and axin1 were confirmed biochemically by co-immunoprecipitation and inhibition using 17-AAG, geldanamycin and novobiocin. We showed, for the first time that HSP90 is associated in a possible complex with β-catenin, p-β-catenin and axin1 therefore is potentially involved in the modulation of p-β-catenin in the Wnt pathway through the stabilization of the destruction complex.

ACKNOWLEDGEMENTS

I would like to thank my indispensible supervisor, Professor Gregory Blatch for his unfailing encouragement and support over the years. His invaluable advice, contributions and helpful criticisms have certainly allowed for me to grow as a researcher and think critically. He has been an inspiration and a role model in research.

I am indebted to my co-supervisor, Dr Earl Prinsloo, for his endless patience, expertise and advice. He has been a fantastic colleague and mentor, and has encouraged me throughout all the challenges of research.

I also acknowledge the following contributions:

- Dr Sharon Prince for MCF7 cells and Dr C. Penny for HT29 cells,
- Professor Janet Hapgood for supplying glucocorticoid receptor antibodies,
- Dr Caroline Knox for her helpful suggestions for confocal microscopy analysis,
- Dr Adrienne L. Edkins for all her excellent ideas throughout my project; for giving up her precious time to assist me with cell culture and confocal microscopy; and for proof-reading a chapter of my thesis,
- Amy Kenyon for her assistance with confocal microscopy,
- Dr Petra Gentz for her organization and assistance of reagents and antibodies,
- Nicodemus Mautsa who assisted me with PCR,
- Dr Eva-Rachele Pesce who has given me sound advice throughout my project,
- My colleagues in BioBRU, in particular Buhle Moyo, Jo-Anne de la Mare and Ingrid Cockburn, for being dependent and humorous and for making each day of my laboratory experience enjoyable,
- My digsmates: Sean Edwards, Hailey Johnson, Lara Sciscio, Shan Ambrose, Matthys Kroon for being understanding and encouraging, especially during my periods of frustration and anxiety,
- My friends at Rhodes University for making the past 6 years very memorable,
- Cancer Research Initiative in South Africa (CARISA)
- Andrew Mellon Scholarship Foundation

I finally express my gratitude to my parents, Sue and John Cooper. Their unfailing love and support throughout my academics have inspired me to give of my best in everything that I do.

OUTPUTS

Conference outputs

Cooper, LC, Prinsloo, E, Blatch GL (2010).The role of HSP90 in Wnt Signaling in breast cancer and breast cancer stem cells. SASBMB 2010, Bloemfontein, 18-21 January 2010, Poster Presentation

Book chapter in press

Prinsloo E, Cooper LC, Moyo B, de la Mare J, Lawson JC, Edkins A, Blatch GL (2010). Heat shock proteins in normal and cancer stem cell biology: implications for regenerative and chemotherapeutic medicine. In: Stem Cell, Regenerative Medicine and Cancer, Singh SR (ed), pp 693-713. Nova Science Publishers Inc. New York, USA. ISBN: 978-1-61761-342-5.

Article in preparation

Cooper LC, Prinsloo E, Blatch GL (2010). β-catenin and its phosphorylated form: Potential HSP90α/β client proteins in MCF7 human breast cancer cells. To be submitted to Breast *Cancer Res*earch.

TABLE OF CONTENTS

LIST OF FIGURES

Chapter 1: Introduction

Chapter 3: Localization studies on Wnt protein members

Chapter 4: Association of members of the Wnt pathway with HSP90

Chapter 5: Effects on the Wnt pathway proteins by HSP90 inhibition

Chapter 6: Conclusion and future work

LIST OF TABLES

LIST OF ABBREVIATIONS

ATP	Adenosine 5´-triphosphate
17-AAG	17-Allylamino-17-demethoxygeldanamycin
APC	adenomatous polyposis coli
ATPase	Adenosine 5´-triphosphatase
BCL	B-cell lymphoma
BCL	CREB-Binding Protein
BRCA	Breast cancer gene
cAMP	cyclic adenosine monophosphate
Cdc37	cell division cycle 37
Cdk4	cell division kinase 4
CK	casein kinase
CREB	cAMP response element-binding protein
CSC	cancer stem cell
CSL	transcription factor
Dkk	Dickkopf
DMEM	Dulbecco's modified Eagle's medium
DMSO	dimethyl sulphoxide
DNA	Deoxyribose Nucleic Acid
Dvl	Disheveled
EDTA	ethylenediamine tetra-acetic acid
EMT	epithelial-mesenchymal transitions
ER α	estrogen receptor- α
ERK	Extracellular signal regulated kinase
FAP	familial adenomatous polyposis
FCS	Foetal calf serum
FKBP	FK506 binding protein
Fz	Frizzled
GA	geldanamycin
GAP	GTPase-activating protein
GBP	GSK-3 binding protein
gp130	Glycoprotein130
GSK-3β	glycogen synthase kinase 3β
HER-2	human epidermal growth factor receptor 2
HIF-1α	hypoxia inducible factor 1
HIFCS	heat inactivated fetal calf serum

HNPCC	hereditary nonpolyposis colorectal cancer
Hop	Hsp70/Hsp90 organizing protein
HSP40	Heat shock protein 40
HSP70	heat shock protein 70
HSP90	heat shock protein 90
HSPs	Heat shock proteins
IC_{50}	median inhibitor concentration (concentration that reduces the effect by 50 %)
IKK	IκB kinase
JAK	Janus kinase
KCl	Potassium chloride
LEF-1	lymphoid enhancer binding factor 1
LIF	Leukemia inhibitory factor
LRP	lipoprotein receptor protein
MMP	matrix metalloproteases
MMR	mismatch repair
mTOR	mammalian target of rapamycin
Na_2HPO_4	sodium hydrogen orthophosphate
NaCl	sodium chloride
NP40	Nonidet P40
N-terminus	amino terminus
PBS	phosphate buffered saline
PDK	pyruvate dehydrogenase kinase
PI3-K	phosphatidylinositol 3-kinase
PIAS3	protein inhibitor of activated STAT3
PMSF	Phenylmethylsulfonyl fluoride
PP2A	protein phosphatase 2A
Ptch 1	Patched 1
PTEN	phosphatase and tensin homolog
RAF1	v-raf-1 murine leukemia viral oncogene homolog 1
RIPA	radioimmunoprecipitation assay
RNA	ribonucleic acid
SCFβ-TrCP	SKP1-cullin 1-F-box
SDS	sodium dodecyl sulphate
SDS-PAGE	SDS-polyacrylamide gel electrophoresis
sFRP	secreted Fz related proteins
Shh	Sonic hedgehog

Smo	Smoothened
SP	side population
STAT3	signal transducer and activator of transcription 3
Sti-1	stress-inducible protein 1
TACE	tumour necrosis factor alpha converting enzyme
TBS	tris-buffered saline
TBST	TBS-tween
TCF	T-cell-specific factor
TPR	tetratricopeptide repeat
WIF-1	Wnt-inhibiting factor-1
Wnt	Wingless

LIST OF SYMBOLS

α	Alpha
β	Beta
°C	degree celcius
M	Molar
mM	millimolar
nM	nanomolar
µg	micrograms
µl	microlitres
L	litres
g	grams
mg	milligrams
kDa	kilo Daltons
min	minutes
mol	mole
ml	millilitre
%	percent or g/100 ml
U	units
V	volts
g	centrifugal force of gravity
rpm	revolutions per minute
S	svedberg
γ	gamma

Chapter 1: Introduction

1.1 Definition of Cancer

Cancer refers to a tumour formed by cells that multiply outside the limitations of tightly controlled pathways. These cells become malignant when they start to invade another part of the body that is normally occupied by other cells (Alberts *et al.*, 2002). Tumour transformation, invasion and metastasis relies on an intricate interconnected network of signals from the extracellular matrix as well as intracellular signal transduction pathways (Kumar and Weaver, 2009).

1.2 Epidemiology of Cancer

Cancer has been reported as second only to heart disease as the leading cause of death (Miniño *et al*., 2007). The number of deaths attributed to cancer exceeds that of heart disease for persons under the age of 85 years (Jemal *et al*., 2008). The Cancer Association of South Africa (CANSA, 2010, website 1) reported that there are approximately 80 000 cancer-related deaths each year in South Africa, of which breast cancer makes up 3 200 deaths (CANSA, 2010, website 1) and has been reported by the International Agency for Research on Cancer (IARC, 2010, website 2) as most pertinent type of cancer diagnosed in women. Colorectal cancer is the third most frequently diagnosed cancer, with 72 % of the cases being located in the colon, whilst the remaining is in the rectum (Jemal *et al.*, 2008). However, the statistics for sub-Saharan Africa are incomplete therefore these statistics could increase drastically.

Although there has been a gradual decline in the death rate from breast cancer since 1990, there are still more than 10 million known cases of cancer diagnosed each year (Eaton, 2003; Kakarala and Wicha, 2008). This decrease in deaths could be attributed to early detection instead of the effects of new treatments (Calvocoressi *et al.*, 2008). This holds true for colorectal cancer too, with a decrease in death rate since 1998 (Jemal *et al.*, 2008) not necessarily meaning a decrease in the cancer, but could be due to the removal of precancerous polyps (Cress *et al.*, 2006). Furthermore, it must be noted that there has been no significant change in the overall survival of women diagnosed with metastatic breast cancer (Miniño *et al.*, 2007) and recurrence of the disease still arises in an extensive proportion of women even after adjuvant therapy (Kakarala and Wicha, 2008).

1.3 Etiology of Cancer

There are three broad groups of risk factors that contribute to breast cancer, which include hereditary, hormonal & reproductive factors and environmental factors (Debruin and

Josephy, 2002). It was interesting to note that over 70 % of breast cancers are associated with environmental factors (Lichtenstein *et al*., 2000) and over 78 % of breast cancers are diagnosed in post-menopausal women, possibly due to long latency periods of chemical carcinogenesis (Debruin and Josephy, 2002).

Estrogens and progesterone are required for normal mammary development, but it is thought that their activation is linked to procarcinogenesis (Debruin and Josephy, 2002). Numerous identified risk factors for breast cancer can be attributed to their effects on lifetime exposure to estrogen and other hormones (Henderson and Feigelson, 2000). In addition to this, estrogens have been found to be metabolically converted to cytotoxic and genotoxic products, such as the oxidation of catechol estrogens to catechol quinones (Cavalieri *et al*., 1997).

Many breast cancers overexpress the nuclear hormone receptor estrogen receptor-α (ER-α). (Mastroianni *et al.* 2010). Mastroianni *et al.* (2010) proposed that ectopic Wnt signaling can substitute for estrogen to stimulate division of ERα-positive cells, resulting in estrogen-independent tumours.

Breast cancer is linked to oncogene activation and tumour suppressor gene inactivation (Russo and Russo, 2001). Overexpression of the proteins, human epidermal growth factor 2 (HER-2) (Hung and Lau, 1999) and Bcl-2 are involved in maintaining the oncogenic phenotype. Overexpression of the proto-oncogene product, Bcl-2 is linked to better prognosis whilst downregulation of *Bax* is associated with poor clinical outcome (Daidone *et al*., 1999; Schorr *et al*., 1999). Another gene that is mutated in 40 % of breast cancers is *p53*, which is involved in cell cycle regulation, DNA repair and apoptosis (Coles *et al*., 1992). Cancers that have mutated p53 have been found to be more aggressive and resistant to chemotherapy (Howard *et al*., 2004).

Hereditary factors are linked mainly with early-onset premenopausal breast cancer. Women who have mutations in the breast cancer gene (*BRCA*) *BRCA1* or *BRCA2* have an increased risk of developing breast cancer (Bennet *et al*., 1999). These genes are involved in transcriptional regulation, cell cycle control; apoptosis and DNA repair (Wang *et al*., 2001).

Epigenetics describes the study of alterations that occur during gene expression which are independent of the alterations in the primary DNA sequence (Sharma *et al*., 2010). Differentiation may be a consequence of these alterations which remain stable throughout numerous cell cycle divisions, allowing for the cells to have distinct identities (phenotypes)

whilst they contain the same genetic information (genotypes) (Sharma *et al*., 2010). Epigenetic alterations that occur include methylation of cytosine bases in DNA; and post-translational changes of histone proteins, in addition to changes in the nucleosome location along the DNA. This regulates what part of the gene can be used and therefore results in cellular diversity (Sharma *et al*., 2010). If these epigenetic changes are not kept in check, signaling pathways can become dysregulated, which ultimately leads to cancer (Jones and Baylin, 2002). It has also been proposed that epigenetic mutations that occur within normal stem and progenitor cells can lead to cancer (Feinberg *et al*., 2006). Reversal of epigenetic mutations forms the basis of novel cancer therapies (Yoo and Jones, 2006).

1.3.1 Etiology of Breast cancer

The mammary gland, unlike other organs in the body, undergoes morphological change during distinct developmental periods in an adult's life (Howard, 2000). These stages include fetal development, puberty, pregnancy and finally lactation. After lactation, expansive tissue remodeling occurs in the breast, whereby apoptosis allows for the glands to return to the same structure as that prior to pregnancy (Strange *et al.*, 2001). It can therefore be said that within the breast, there exists a compartment of cells that has the ability to differentiate and self-renew, so called adult stem cells, and these cells are required for multiple pregnancies to occur (Dontu *et al.*, 2004; Lawson *et al*., 2009). These cells are described as being stem cell-like, and are thought to be the origin of breast cancer, whereby mutations in these adult stem cells transform the cells into cancer stem cells (Dontu *et al.*, 2004). Since the adult breast stem cells are slow dividing and long lived cells, with a high potential to proliferate, mutations due to genotoxic agents can build up over an extensive period, thus leading to carcinogenesis (Dontu *et al.*, 2004; Lawson *et al*., 2009).

1.3.2 Etiology of Colorectal Cancer

Colorectal cancer starts off as noncancerous polyps with the majority of colorectal cancers being described as adenocarcinomas which form from glandular tissue (Stewart *et al.*, 2006). It has been estimated that more than 50 percent of a given population will develop one or more adenomas in a life time (Schatzkin *et al.*, 1994); however, a small percentage (5-10 %) of colorectal cancer patients have an inherited genetic mutation that causes the cancer (Lagerstedt Robinson *et al*., 2007). An example of such a syndrome is familial adenomatous polyposis (FAP) which is passed on as an autosomal dominant trait due to a mutation in the gene encoding for adenomatous polyposis coli (APC), whereby patients develop benign

polyps in the colorectal epithelium during early adulthood. Some of these polyps will develop into cancerous tumours that metastasize (Kotiligam *et al*., 2008). Another example is hereditary nonpolyposis colorectal cancer (HNPCC) (Lynch syndrome), whereby there is a mutation in one of the mismatch repair genes (MMR) (Vasen *et al*., 2007).

1.4 Cancer stem cells

Classic models of carcinogenesis describe cancerous tumours as "stochastic" or "random", in which any cell can be transformed by mutations (Martinez-Climent *et al.*, 2006). In contrast to this, there is growing evidence that malignant tumours are heterogeneous and comprise a subpopulation of cells with stem cell characteristics, and are thus termed cancer stem cells (CSCs) or tumour initiating cells (Korkaya and Wicha, 2007). Furthermore, within the cancer cell hierarchy (Figure 1.1) some tumours are similar to that of the tissue from which the tumour arose (Cariati and Purushotham, 2008). In addition, tumours formed from cancer stem cells, have been found to have the same heterogenic complexity as the original tumour (Al-Hajj *et al.*, 2003).

Normal stem cells and cancer stem cells share many important characteristics, including the ability to self-renew; the capacity to differentiate; active expression of telomerase; activation of anti-apoptotic pathways; increase in membrane transporter activity; and capacity to metastasize (reviewed in Wicha *et al.*, 2006). Furthermore, cancer stem cells are resistant to changes in temperature, pH as well as exposure to toxicants (Miyagi *et al.*, 2001; Woodward *et al.*, 2005). A possible explanation for this is that they possess high stress tolerances and are assisted by highly complexed heat shock proteins that are upregulated in cancer thus allowing for cancer cells to withstand environments that occur due to deregulated signaling pathways (Takayama *et al*., 2003; Whitesell and Lindquist, 2005).

There are two separate, but interlinked theories describing how cancer stem cells are formed. The first theory suggests that carcinogenic tumours are caused by rare cells that have stem cell properties, which are described as cancer stem cells/ tumour initiating cells. On the other hand, the second theory describes how cancer stem cells arise from deregulated self-renewal pathways in the normal stem/ progenitor cells (Graziano *et al.*, 2008; Campbell Marotta and Polyak, 2009).

Many cancerous tumours contain a rare population of cells, termed the side population (SP) cells that comprise a vast proportion of cancer stem-like cells (Kondo *et al.*, 2004; Hirschmann-Jax *et al.*, 2004; Patrawala *et al.*, 2005). *Ex vivo* cancer cell lines like the human

epithelial breast cancer line, MCF7 and the colorectal cell lines HT29 contain a subpopulation of cells (side population) that have stem cell-like characteristics. This SP have been shown to have a higher colony formation capacity in comparison to non-SP cells (Zhou *et al.*, 2007; Haraguchi *et al.*, 2008), thus could be used as models for cancer stem-like cell research.

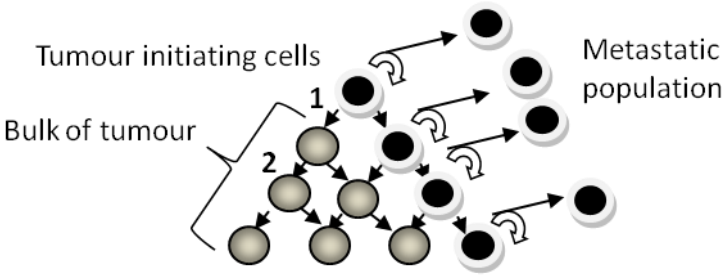

Figure 1.1. A schematic model of the hierarchical organization of the cancer tumour. The tumour initiating cells can sustain the tumour by self-renewal. In addition to this, it can differentiate into the different cancer cells comprising the bulk of the tumour, as well as form a metastatic population which can form new tumours. 1: asymmetric division. 2. symmetric division (adapted from Reya *et al.*, 2001).

Several important signaling pathways identified in both cancer stem cells and normal stem cells include human epidermal growth factor receptor 2 (HER-2), phosphatase and tensin homolog (PTEN), Notch, Hedgehog and Wingless (Wnt). Pathways involved in cell survival and proliferation of the MCF7 SP cells include phosphatidylinositol3-kinase (PI3-K)/ mammalian target of rapamycin (mTOR), PTEN, signal transducer and activator of transcription 3 (STAT3). Genes of the Wnt/β-catenin pathway were also upregulated in SP cells in comparison to non-SP cells (Zhou *et al.*, 2007). mTOR signaling positively regulates the STAT3 pathway, whilst the PTEN acts as a negative inhibitor of both the mTOR and STAT3 pathways (Zhou *et al.*, 2007). This evidence suggests the importance of studying the SP and its signaling pathways in order to elucidate the pathways important for cancer stem-like cell maintenance.

1.4.1 Cancer stem cells and chemotherapy

Conventional chemotherapies are aimed at targeting the bulk and cycling populations of tumours (Korkaya and Wicha, 2007). However, it has been found that cancer stem cells are resistant to current chemotherapeutic agents (Wicha *et al.*, 2006). There are several reasons for this resistance, which include the cell cycle kinetics of cancer stem cells, whereby cancer stem cells remain in the G_0 phase, and thus have increased resistance to cell cycle chemotherapeutic agents (Venezia *et al.*, 2004). Another explanation is that certain protective mechanisms are stimulated which prevent the cancer stem cell from senescence and

apoptosis. These mechanisms comprise: the stimulation of self-renewal pathways such as the Wnt/β-catenin pathway; expression of anti-apoptotic proteins such as B-cell lymphoma 2 (BCL-2); overexpression of drug-effluxing pumps which permits the cell to expel toxic drugs (Moserle *et al.*, 2010). A further explanation could be that cancer stem cells have increased resistance to DNA-damaging chemotherapeutic agents due to their asynchronous DNA synthesis as well as good DNA repair (Cairns, 2002).

Cancer stem cells are radio-resistant, and have been linked to repopulating the tumour during a relapse after radiation (Woodward *et al.*, 2007; Eyler and Rich, 2008). One of the mechanisms that is thought to be adapted to radiotherapy is the Wnt/β-catenin pathway, whereby DNA damage results in the stimulation of the Wnt/β-catenin pathway thus promoting genomic instability by converting non-tumourigenic stem cells into CSC or SP and enabling tumour cells to survive irradiation (Chen *et al.*, 2007; Shiras *et al.*, 2007).

It has been suggested that therapies aimed at targeting cancer stem cells should be incorporated into drug development (Wicha *et al.*, 2006; Moserle *et al.*, 2010). Cariati and Purushotham (2008) noted that targeting cancer stem cells instead of differentiated or transit amplifying cells would provide a long term cure for malignant tumours. Two approaches include: targeting molecular pathways which are over-activated in malignant stem cells and sensitizing cancer stem cells to standard therapies (Moserle *et al.*, 2010). It must be noted, however, that this could prove to be a challenge since many pathways are shared by both cancer stem cells and normal stem cells, especially those involved in self-renewal (Wicha *et al.*, 2006). An approach to drug design is "differentiation therapy" which induces differentiation in cancer tumours and has had some positive results (Spira and Carducci, 2003; Sell, 2004). It is thought that this differentiation therapy induces differentiation in cancer stem cells thus inhibiting the cancer stem cell's ability to self-renew (Korkaya and Wicha, 2007). However, as with targeted destruction of cancer stem cells, differentiation therapy may result in initiation of terminal differentiation of adult stem cell populations.

1.5 Signaling pathways in cancer

Signaling pathways involved in the differentiation and self-renewal of cancer cells are the Wnt, PTEN, Notch and Hedgehog pathways. Whilst in some instances, the pathways may act independently of one another for tissue self-renewal, proliferation and inhibition of differentiation, in other instances the different pathways may be interlinked in a hierarchical manner such that they influence one another (Figure 1.2) (Reya and Clevers, 2005).

Some studies (Liu *et al.*, 2005) have suggested that Hedgehog signaling acts downstream of Notch signaling, other studies have shown that Sonic hedgehog (Shh) acts upstream of Notch (Figure 1.2, step 1) (Morrow *et al*., 2009). Notch signaling prevents the differentiation of stem cells (Figure 1.2, step 2) (Dontu *et al.*, 2004), whilst Hedgehog signaling stimulates the self-renewal of cells (Figure 1.2, step 5) (Liu *et al*., 2006). These two pathways form a feedback loop that controls normal development, and deregulation of this loop could be associated with carcinogenesis (Liu *et al.*, 2005). The Wnt pathway acts downstream of Notch (Figure 1.2, step 3) and Hedgehog pathways (Figure 1.2, step 4) (Liu *et al.*, 2005) and has been found to be activated by transformation of the Notch pathway (Figure 1.2, step 3) (Kopper and Hadju, 2004). When the Wnt pathway is not stimulated, glycogen synthase kinase (GSK-3β) phosphorylates β-catenin (Figure 1.2, step 7) and prevents it from becoming stabilized and moving into the nucleus (Figure 1.2, step 8) (Kimelman and Xu, 2006). At the same time, GSK-3β inhibits mTOR kinase (Figure 1.2, step 9) (Inoki *et al*., 2006). In the presence of Wnt signal, GSK-3β is inhibited from phosphorylating β-catenin thus resulting in stabilized β-catenin moving into the nucleus to target genes involved in self-renewal (Figure 1.2, step 8) (Amit *et al*., 2002). PTEN prevents Akt from being activated (Figure 1.2, step 10). A reduction in PTEN results in Akt being activated by PI3-K (Figure 1.2, step 11) (Cross *et al*., 1995). Akt in turn inhibits GSK-3β (Figure 1.2, step 12) from phosphorylating β-catenin, resulting in an increase of stabilized β-catenin (Covey *et al*., 2010). In addition to this mTOR is stimulated (Figure 1.2, step 13) which can stimulate the signal transducer and activator of transcription (STAT3) pathway (Figure 1.2, step 14) resulting in the self-renewal of cells (Figure 1.2, step 15) (Zhou *et al*., 2007).

Elucidation of these pathways that regulate differentiation of stem cells and cancer has increased the understanding of how dysregulation of these tightly controlled processes could play a role in carcinogenesis. Additionally it would be important to understand the coordinated activity of these pathways such that they could offer a target for cancer prevention and therapy (Reya and Clevers, 2005; Kakarala and Wicha, 2008).

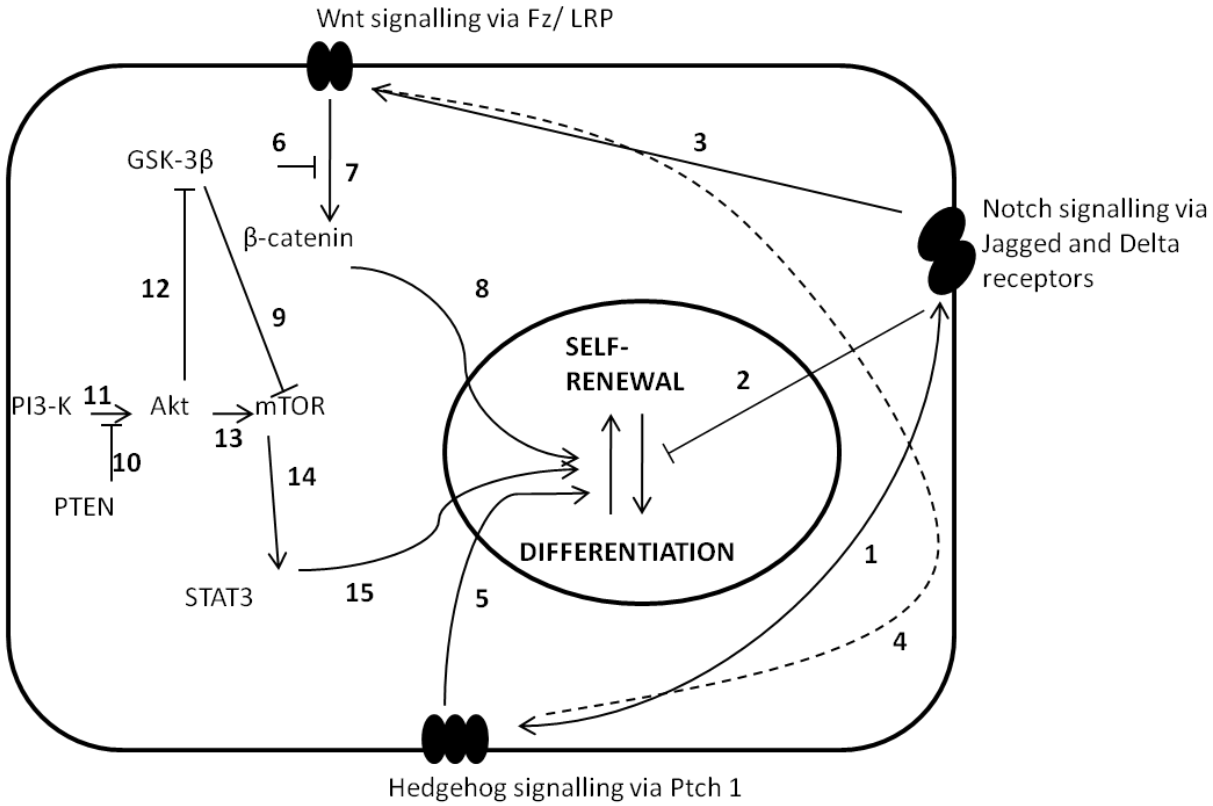

Figure 1.2. Schematic representation of the pathways involved in stem cell renewal and differentiation. See text for details. Arrow represents stimulated pathway, whilst blunted line represents inhibited pathway. Solid lines represent known interactions whilst dotted lines represent possible interactions GSK-3β: glycogen synthase kinase-3β. PI3-K: phosphatidylinositol 3-kinase. PTEN: phosphatase and tensin homolog mTOR: mammalian target of rapamycin. STAT3: signal transducers and activators of transcription 3. Ptch 1: Patched 1. Intricacies of the Akt pathway are discussed later in 1.6 (adapted from Liu *et al.*, 2005; Prinsloo *et al*., 2010).

1.5.1 Wnt Signaling

Wnt proteins comprise a family of 19 highly conserved glycoproteins that are associated with signaling pathways (reviewed in Angers and Moon, 2009). Cell surface Wnt receptors comprise a seven transmembrane protein of the Frizzled (Fz) family, and low density lipoprotein receptor proteins 5/6 (LRP5/6) (Polakis, 2000; Mao *et al.*, 2001). When the Wnt proteins bind to the receptors on the cell surface membrane, different pathways are stimulated. The non-canonical pathways, which are β-catenin independent, are stimulated when Wnt proteins bind to the Frizzled receptors in the absence of LRP5 or LRP6 (Angers and Moon, 2009). Other Wnt receptors include Ryk and ROR2 which can antagonize Wnt/β-catenin signaling (van Amerongen *et al*., 2008).

1.5.1.1 Wnt/β-catenin pathway

In normal cells, endogenous β-catenin is complexed with E-cadherin and α-catenin in cell junctions, and therefore plays a role in cell adhesion. Excess, newly synthesized β-catenin is

degraded by the destruction complex, comprising axin, APC, glycogen synthase kinase-3β (GSK-3β), protein phosphatase 2A (PP2A) and casein kinase 1 (CK1) (Price, 2006).

The canonical Wnt/β-catenin pathway is stimulated when the Wnt protein binds to the Fz/ LRP complex (Figure 1.3 and Figure 1.4A) (Hocevar *et al.*, 2003). It does this by bringing Frizzled and LRP together (Cong *et al*., 2004B). This in turn activates the cytoplasmic protein, Disheveled (Dsh) (Figure 1.3, step 1), which acts as a mediator by receiving signals from receptors and passing them on to the relevant effector molecules (Hocevar *et al.*, 2003). How this activation occurs is still not fully understood. It is, however, thought that phosphorylation by CK1 and CK2 at serine 45 of β-catenin may play a role in this process (Amit *et al.*, 2002).

There is much debate about whether β-catenin is stabilized by the direct inhibition of GSK-3β or whether it is due to axin degradation. One theory suggests that the activated Dsh complex inhibits β-catenin from being phosphorylated and degraded by another multiprotein complex comprising APC, axin, glycogen synthase kinase-3β (GSK-3β) and β-catenin (Figure 1.3, step 2) (Polakis, 2000; Wharton, 2003). It does this by associating with CK1, and preventing CK1 from priming β-catenin. This in turn prevents β-catenin from being phosphorylated by GSK-3β at serine 41, 37 and 33 (Amit *et al.*, 2002). In addition to this, Dsh recruits GSK-3 binding protein (GBP) (Figure 1.3, step 3) which is thought to separate GSK-3β from axin, therefore leading to the inhibition of phosphorylation of β-catenin (Li *et al*., 1999).

Another theory suggests that when Wnt binds to LRP5/6, GSK-3β and CK1γ phosphorylate LRP5/6 (Davidson *et al*., 2005; Zeng *et al*., 2005), which is a key event in receptor activation (Tamai *et al*., 2004). Both LRP5 and LRP6 have the motifs PPSPxS (P, proline, S, serine or threonine, x a variable residue) which, when phosphorylated, become docking sites for the axin complex (Figure 1.4A) (Tamai *et al*., 2004; Davidson *et al*., 2005). Although one study argued that upon Wnt stimulation, phosphorylation only occurs by CK1 (Davidson *et al*., 2005), there is growing evidence that GSK-3β primes the xS motif for phosphorylation by CK1 (Zeng *et al*., 2005; Khan *et al*., 2007). This results in axin being sequestered to the membrane where it associates with LRP5/6 since hyperphosphorylated LRP5/6 has a high affinity for axin. Sequentially, the inactive axin is dephosphorylated and degraded by an unknown mechanism (Mao *et al*., 2001). Axin, which is present in limiting levels within the cell (Lee *et al*., 2003), is the key scaffolding protein in the destruction complex, therefore without it, the destruction complex is rendered incapable of phosphorylating β-catenin

(Willert *et al*., 1999). In contrast, a recent study (Cselenyi *et al*., 2008) has shown that in the absence of axin degradation, LRP6 promotes the stabilization of β-catenin by directly inhibiting GSK-3β from phosphorylating β-catenin.

Interestingly, studies have shown that the Fz-Dsh interaction is important for the phosphorylation and activation of LRP6 (Bilić *et al*., 2007; Zeng *et al*., 2008). Since axin is recruited to the membrane via Dsh, it is proposed that when Fz recruits Dsh, the GSK-3β-axin complex is also recruited, subsequently allowing for GSK-3β to phosphorylate and activate LRP6 (Zeng *et al*., 2008). It can therefore be said that GSK-3β and axin play 2 antagonistic roles in the Wnt pathway; positive regulation via LRP phosphorylation and negative regulation via β-catenin phosphorylation (reviewed in Huang and He, 2008). Although the Dsh-Fz and Dsh-axin associations are weak (Wong *et al*., 2003; Schwarz-Romond *et al*., 2007B), both Dsh and axin have a DIX domain that allows for polymerization (Schwarz-Romond *et al*., 2007A). Subsequently, Dsh and axin can form large aggregates that form weak but dynamic protein associations. Furthermore, Wnt-stimulated receptor clustering needs the DIX domain (Schwarz-Romond *et al*., 2007A).

Stabilized β-catenin (Figure 1.3, step 4) can translocate to the nucleus to form a complex with the DNA binding proteins, T-cell-specific factor/ lymphoid enhancer binding factor 1 (TCF/ LEF-1) (Figure 1.3, step 5). The amino terminus of β-catenin modulates the stability of the protein (Barth *et al*., 1997), whilst the carboxy terminus acts as the transcriptional activator domain (Tutter *et al*., 2001). This in turn activates the transcription of genes involved in oncogenesis (Figure 1.3, step 6) (He *et al.*, 1998; Shtutman *et al.*, 1999). These genes include those involved in cell proliferation, such as *c-myc* (He *et al.*, 1998) and *c-jun* (Mann *et al.*, 1999); inhibition of apoptosis, such as *survivin* (Zhang *et al.*, 2001); and tumour metastasis such as (*matrix metalloprotease 7*) *MMP7* (Crawford *et al.*, 1999). β-catenin is involved in modulating the expression of a vast number of genes involved in cell proliferation, migration, invasion and morphogenesis, including those encoding for cyclin D1, the cell adhesion molecule L1-CAM, MMP and the metastasis gene *S100A4*, as well as *Fascin*, which has been found to be important for filopodia formation and cancer cell invasion (Vignjevic *et al*., 2007). Numerous co-activators of β-catenin have been identified, such as cyclic adenosine monophosphate (cAMP) response element-binding protein (CREB)-Binding Protein (CBP)/p300 (Ma *et al.*, 2005), Pygopus (Städeli and Basler, 2005) and BCL-9 (Hoffmans and Basler, 2005). They interact with the C-terminus of β-catenin, thus regulating the association of β-catenin with the TCF/LEF complex and the chromatin (Parker *et al*., 2008).

In the absence of the Wnt ligand (Figure 1.3, dotted arrows; Figure 1.4B), CK1 is recruited by axin, the scaffolding protein (Clevers, 2006), which results in the priming of β-catenin in preparation for phosphorylation by GSK-3β. GSK-3β is also recruited by axin to the multiprotein complex (Behrens *et al*., 1998). The subsequent phosphorylation of axin and APC by GSK-3β and CK1 increases the association of axin and APC with β-catenin (Figure 1.3, step 8) (Peifer and Polakis, 2000; Huang and He, 2008). The phosphorylation of β-catenin results (Figure 1.3, step 8) in its ubiquitination (Figure 1.3, step 9) by the ubiquitin-proteome pathway involving SKP1–cullin 1– F-box (SCFβ-TrCP the 26S proteosome 17) E3 ligase and to its degradation by the 26S proteosome (Figure 1.3, step 10) (Kimelman and Xu, 2006), thus reducing the level of cytosolic β-catenin (Kitagawa *et al.*, 1999).

In the resting state, low levels of β-catenin are present and the Wnt target genes are inhibited by the Groucho family of transcriptional repressors, which are bound to the lymphoid enhancer factor (LEF) and T cell factor (TCF) proteins (Angers and Moon, 2009). In normal and unstimulated cells, β-catenin is mainly localized to cell-cell junctions where it forms a complex with α-catenin and E-cadherin (Huber and Weis, 2001). This means that there are low levels of β-catenin in the cytoplasmic or nuclear regions due to its rapid turnover by the Dsh complex (Luu *et al.*, 2004). Upon Wnt activation, β-catenin translocates to the nucleus where it displaces Groucho and activates target genes (Daniels and Weis, 2005). It is thought that APC can also have a chaperoning effect, by exporting nuclear β-catenin into the cytoplasm for degradation (Henderson, 2000; Neufeld *et al.*, 2000). However, Eleftheriou *et al*. (2001) did not find that the chaperoning function was important and that β-catenin can move between the nucleus and cytoplasm without the aid of APC.

Extracellular antagonists and inhibitors also regulate the Wnt pathway (Figure 1.3, step 7). These include secreted Fz related proteins (sFRPs), Wnt inhibitory protein (WIF) (Bovolenta *et al*., 2008), Dickkopf (Dkk) (Aguilera *et al*., 2006; Semënov *et al*., 2001) and the Wise/SOST family (Li *et al*., 2005) which bind to Wnt ligands and are antagonistic to Wnt. These proteins have been found to have decreased expression in cancer (Suzuki *et al*., 2008). Interestingly, various self-regulatory loops have been found in the Wnt pathway, which are cell-specific. Examples include the proteins Fz, LRP6, axin2, TCF/LEF, Dkk1 being either negatively or positively regulated by TCF/β-catenin (Logan and Nusse, 2004; Chamorro *et al*., 2005; Khan *et al*., 2007)

Axin acts as a scaffolding protein in the destruction complex of β-catenin and is thus a negative regulator of the Wnt pathway. The two human homologs, axin1 (Axin homolog) and axin2 (Conductin homolog) share 45 % amino acid identity (Zeng *et al*., 1997; Mai *et al*., 1999). Whilst axin1 is constitutively expressed and thus maintains the basal level of Wnt pathway activity, axin2 is stimulated by an increase in β-catenin levels and thus regulates the intensity and extent of the Wnt/β-catenin signal (Lustig *et al*., 2002). Axin2 is also a downstream target of the Wnt pathway, and is possibly linked to controlling Wnt signaling via negative feedback (Lustig *et al*., 2002). Axin2 also contains TCF binding sites (Leung *et al*., 2002).

GSK-3β is constitutively active with phosphorylation of GSK-3β resulting in loss of its activity (Cole and Sutherland, 2008). Two isoforms of GSK-3 are identified, GSK-3β and GSK-3α which share 95 % similarity in their protein kinase catalytic domain (Woodgett, 1990). It has been found that GSK-3β can be substituted by GSK-3α in many of its kinase activities in the Wnt pathway (Manoukian and Woodgett, 2002). A recent study has identified another role of GSK-3β in the Wnt pathway which does not involve the phosphorylation of β-catenin. It is suggested that GSK-3β translocates to the nucleus, where it binds to axin and β-catenin, decreasing the levels of β-catenin/TCF transcription (Caspi *et al*., 2008). Sadot *et al*. (2002) proposed that β-catenin gets dephosphorylated rather than degraded when colon cancer cells are treated with LiCl, an inhibitor of GSK-3β.

Both protein phosphatase 1 (PP1) and PP2A are positive regulators of the Wnt pathway. PP1 associates with axin and dephosphorylates the CK1 primed sites on axin. This results in a conformational change of axin leading to the decrease in the association of GSK-3β with axin. β-catenin is therefore not phosphorylated (Luo *et al*., 2007). PP2A, on the other hand, dephosphorylates β-catenin (Zhang *et al*., 2009A). Another negative regulator of the Wnt pathway is the *Wilms Tumor* gene on the X chromosome (WTX) (Major *et al*., 2007). WTX associates with the destruction complex, causing the ubiquitination and degradation of β-catenin (Major *et al*., 2007).

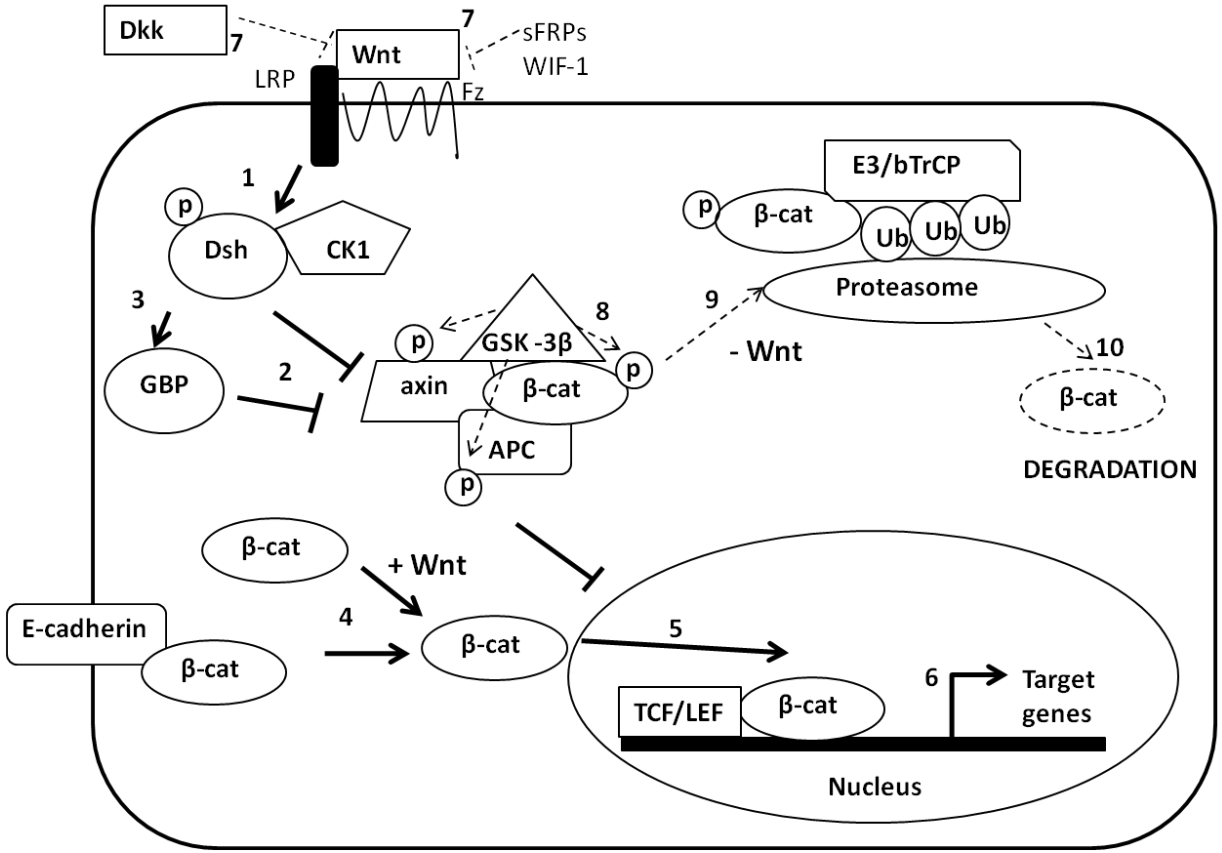

Figure 1.3. Simplified diagram of the canonical Wnt/β-catenin signaling pathway. Wnt proteins bind to receptors, Frizzled (Fz) and low density lipoprotein receptor-related proteins (LRP). This stimulates Disheveled (Dsh) (step 1) which leads to inactivation of a multiprotein complex (step 2) which normally renders β-catenin unstable. GBP is also recruited by Dsh (step 3) which can dislodge glycogen synthase kinase-3β (GSK-3β) from axin. Stabilized β-catenin (Step 4) can therefore move into the nucleus (step 5) to activate target genes (step 6). When the Wnt signals are inhibited (step 7) by Dickkopf (Dkk) or secreted Fz related proteins (sFRPs), phosphorylation within the multiprotein complex comprising axin, adenomatous polyposis coli (APC), and GSK-3β occurs (step 8). Subsequently, β-catenin gets phosphorylated (step 8) and is targeted for ubiquitination (Ub) by the E3 ligase and TrCP (E3/TrCP) leading to its degradation by proteosome (step 10). CK1: casein kinase 1, GBP, GSK-3 binding protein, TCF: T cell factor protein, LEF: lymphoid enhancer factor Arrows represent pathways stimulated. Blunted lines represent pathways inhibited. Solid arrow and blunted line represent signaling in the presence of Wnt, whilst dotted arrows and dotted blunted lines represent signaling when Wnt is not present (adapted from Brown, 2001; website 3).

1.5.1.2 Wnt Signaling in normal cells

Wnt signaling is involved in many cellular processes including cell fate, cell proliferation versus differentiation, cell survival vs apoptosis, cell behavior and migration (Logan and Nusse, 2004), as well as the self-renewal and differentiation of stem cells (Kakarala and Wicha, 2008). Not only is it involved in regulating the stem cell population of the crypts of the small and large intestine (Hoppler and Kavanagh, 2007), but is also important for mammary gland development. A loss of Wnt signaling results in mammary developmental defects, possibly due to the mammary gland stem cell population being compromised (Lindvall *et al*., 2007).

1.5.1.3 Wnt signaling in cancer

Aberrant activation of the Wnt/β-catenin pathway is associated with cancer (Figure 1.4C). This can be caused by mutations in the Wnt pathway (Table 1.1) or overexpression of the Wnt ligands (Table 1.1) (Brown, 2001; Polakis, 2007). Mutations have been found in genes encoding for β-catenin (Morin *et al*., 1997), APC (Schlosshauer *et al*., 2000) and axin (Jin *et al*., 2003), resulting in the stabilization of β-catenin which becomes Wnt independent and thus can translocate to the nucleus to activate target oncogenes (Figure 1.4C) (Hoppler and Kavanagh, 2007). Interestingly, nuclear localization of β-catenin is linked to epithelial-mesenchymal transitions (EMTs) which are identified by the loss of E-cadherin (Brabletz *et al*., 2001) and increase in mesenchymal markers such as fibronectin (Kirchner and Brabletz, 2000). EMT is the key event in metastasis, whereby the cell transforms from epithelial phenotype to a mesenchymal phenotype which is capable of migrating to another site of metastasis formation (Thiery, 2002). Loss of intercellular adhesion is linked to increased motility of the cancer cell and hence increased metastatic ability (Hiscox *et al*., 2006).

Table 1. 1 Mutations in the Wnt pathway that result in cancer.

Mutated gene	Function	Effect of mutation	Reference
Axin1	tumour suppressor	loss of function	Oates *et al*., 2006; Satoh *et al*., 2000)
Axin2	tumour suppressor	loss of function	Lammi *et al*., 2004 ; Liu *et al*., 2000)
APC	tumour suppressor	loss of function	Schlosshauer *et al*., 2000
β-catenin	oncogene	gain of function	Morin *et al*., 1997

Phosphorylation sites on the N-terminus of β-catenin have been found to be mutated, thus resulting in an increase in the nuclear mutated protein (Morin *et al*., 1997; Rubinfeld *et al*., 1997; Wong *et al*., 2001). The mutations are thought to be located around the binding site of the ubiquitin proteosome, thus inhibiting the ubiquitination and degradation of β-catenin (Wong *et al*., 2001). Of the serine/ threonine mutations that occur, the residues, serine 32 and 45, were the most commonly mutated (Wong *et al*., 2001). Amit *et al.* (2002) suggested that serine 45 is phosphorylated by CK1 and axin, which primes β-catenin for phosphorylation by GSK-3β. Therefore, a change in the serine or threonine residues inhibits the phosphorylation and degradation of β-catenin, thus increasing its stability (Morin *et al*., 1997).

In cancer, there is a defined decrease in the expression or inactivation of the Wnt antagonists, Dkk, Wnt-inhibiting factor-1 (WIF-1) and sFRP due to hypermethylation of their promoters (Suzuki *et al*., 2004; Gehrke *et al*., 2009). Not only has a decrease in sFRP1 been reported in breast cancer (Wong *et al*., 2002), but also WIF-1, whereby its RNA expression was decreased up to 60 % (Wissmann *et al*., 2003). Gehrke *et al.* (2009) suggested a possible therapeutic strategy could be employed that would use demethylating agents (an epigenetic therapy) to reinduce the gene expression. This would allow for the expression of Dkk, WIF-1 and sFRP which would negatively regulate Wnt/β-catenin signaling and inhibiting tumourigenic target gene expression.

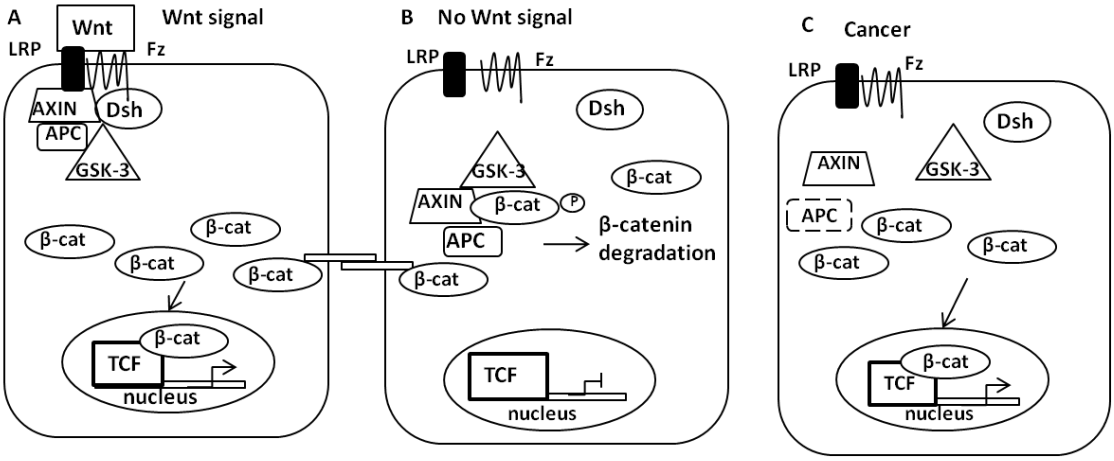

Figure 1.4. Comparison of the Wnt/β-catenin pathway in the presence of Wnt (A), absence of Wnt (B) and in cancer (C). Wnt proteins bind to receptors, Frizzled (Fz) and low density lipoprotein receptor-related proteins (LRP). The destruction complex comprises axin, adenomatous polyposis coli (APC) and glycogen synthase kinase-3β (GSK-3). In the presence of Wnt (A), signaling via Disheveled (Dsh) and/or axin leads to the inactivation of the destruction complex resulting in β-catenin stabilization and accumulation in the cytosol where it translocates to the nucleus and binds to the proteins T-cell factor (TCF)/ lymphoid enhancer factor-1 (LEF1) family, initiating the transcriptions of target genes. In the absence of Wnt (B), the destruction complex phosphorylates β-catenin leading to its degradation. In cancer (C), the Wnt pathway is aberrantly activated due to a number of factors including mutations within the destruction complex. Wnt, wingless-type integration site family member (adapted from Brown, 2001; website 3).

1.5.1.4 Wnt signaling in colon cancer

In more than 80 % of colon cancer diseases, the *APC* gene is mutated, generally in the centre of the *APC* gene (reviewed in Henderson and Fagotto, 2002) resulting in a truncated protein. Since APC is involved in the negative regulation of the Wnt pathway, the functional loss of APC results in the accumulation of β-catenin in the nucleus, which constitutively associates with TCF4 (Korinek *et al.*, 1997). This can result in cancer (Yang *et al*., 2006). Not only is the ability of the truncated protein to bind to other regulatory proteins compromised, but its association with microtubules is also disrupted, resulting in a decrease in the microtubule stability (Polakis, 2000; Henderson and Fagotto, 2002; Kroboth *et al*., 2007). Although the truncated protein can bind weakly to β-catenin, it does not induce degradation of β-catenin. This is because the other members of the destruction complex are not bound. It must be noted, however, that APC is only necessary when axin levels are limiting, and that when axin expression is increased in cancer cells that lack APC, the activity of the destruction complex is returned to normal (reviewed in Clevers, 2006).

When one of the tumour suppressor *APC* alleles is mutated, the inherited disorder familial adenomatous polyposis (FAP) results, which is characterized by numerous formations of β-catenin-enriched adenomas in the intestine in early adulthood (Miyoshi *et al*., 1992; Clevers, 2006). If there are mutations in both alleles, sporadic colorectal cancer arises (Kohler *et al*., 2009). Individuals with mutations in the gene encoding for axin2 are predisposed to colorectal cancer (Lammi *et al.*, 2004).

LEF-1 is not typically expressed in the adult human colon, yet, in colon cancer, full length LEF-1 isoforms are expressed (Hovanes *et al.*, 2001). Due to more active TCF/LEF present in cancer, more Wnt target gene expression can occur (Hoppler and Kavanagh, 2007).

The phosphorylation of β-catenin and its degradation ensures that the cytoplasmic levels of β-catenin are kept in check. Colonospheres are a group of colon cancer cells that have cancer stem cell-like characteristics. In these cells, the expression levels of axin1 and p-β-catenin are found be lower than that of normal colon cancer cells (Kanwar *et al*., 2010). In contrast the expression levels of β-catenin (immunohistochemical staining) and phosphorylated GSK-3β are higher in the colonospheres in comparison to the normal colon cancer cells indicating that the Wnt pathway plays a key function in growth and maintenance of colonospheres (Kanwar *et al*., 2010).

1.5.1.5 Wnt signaling in breast cancer

Nuclear/ cytoplasmic accumulation of β-catenin has been found in more than 60 % of breast cancers (Lin *et al*., 2000; Nakopoulou *et al*., 2006) suggesting that the Wnt pathway is aberrantly activated. On the other hand, there are studies that have found little or no nuclear/cytoplasmic β-catenin (Gillett *et al*., 2001; Wong *et al*., 2002; Dolled-Filhart *et al*., 2006). Further evidence supporting the theory that the Wnt pathway is activated in breast cancer comes from the activation of the Wnt pathway by truncation of the *APC* gene in mice, which leads to tumours forming in the mouse mammary tissues (Moser *et al*., 2001). In murine breast cancer, the gene encoding for Wnt-1 was identified as an oncogene that was activated by the mouse mammary tumour virus (Nusse and Varmus, 1992). More recently, Schlange *et al*. (2007) confirmed that the Wnt pathway is constitutively active in breast cancer cells by identifying that there were consistent expression levels of phosphorylated Dsh, a downstream constituent of the activated pathway.

In addition to mutations in the Wnt pathway, alterations to the Wnt pathway can occur by other means, such as at the Wnt-ligand interface (Collu *et al*., 2009). Examples include the overexpression of Wnts (Milovanovic *et al*., 2004), decrease in *sFRP1* expression (Veeck *et al*., 2006 and 2008), and the overexpression of *Dsh1,* whose gene product is required in the canonical pathway (Nagahata *et al*., 2003; Milovanovic *et al*., 2004). Furthermore, treatment of breast cancer cells with purified sFRP resulted in cell proliferation being inhibited by as much as 30 % and a decrease in active β-catenin in some cell lines, whilst other cell lines, such as MCF7 cells were not affected (Schlange *et al*., 2007). Another study linked Wnt signaling to cell motility in the breast cancer cell line, MDA-MB-231, such that treatment of the cells with sFRP1 decreased the motility (Matsuda *et al*., 2009).

Downregulation of Dsh resulted in a decrease in β-catenin as well as the Wnt target, c-Myc in some of the breast cancer lines (Schlange *et al*., 2007). As expected, the transcriptional activity due to the β-catenin-TCF association increases in some breast cancer cell lines (Lin *et al*., 2000). An example is Cyclin D1, which is overexpressed in half of the breast cancer patients. Since the gene encoding for cyclin D1 has a T cell factor (TCF4) binding site, it is thought there is some link between its expression and the β-catenin/TCF4 pathway (Kelleher

et al., 2006). Indeed, an association was found between the activation of β-catenin and cyclin D1, which resulted in poorer clinical outcome (Lin *et al*., 2000).

The differences in the Wnt pathway mutations, if any, could be attributed to different tissues and organs requiring redundant proteins for different uses (Brown, 2001). An example of this is axin and APC, which are necessary members of the destruction complex in the liver and colon, whilst their homologs, Conductin and APC2 might be essential in breast tissue (Brown, 2001). However, studies on these mutations are not well documented. Another explanation could be that in breast cancer, there are mutations upstream of the axin complex, such as in the Wnt receptors which could account for the nuclear β-catenin staining (Brown, 2001). An example is the *Wnt10b* gene, which is expressed at low levels under normal circumstances and when overexpressed causes murine mammary breast cancer. A similar link has been found between the overexpression of the human *WNT10B* gene and breast cancer (Bui *et al*., 1997). The Wnt pathway in breast cancer may also be stimulated by other regulators of the pathway (Brown, 2001).

Although there are many theoretical approaches to inhibiting the Wnt/β-catenin pathway, it is rare that they have been put to use in the human system due to the risk of side effects (Gehrke *et al*., 2009). These could arise if the signaling pathway is interrupted too far upstream. It has however been shown that inhibiting the components further downstream has been linked to anti-neoplastic effects with a reduction in side effects (Gehrke *et al*., 2009. It is thus interesting to see if selective disruption of the Wnt signaling will have an effect on cancer treatment (Gehrke *et al*., 2009).

1.6 Other Signaling pathways

1.6.1 PTEN

Akt is involved in cell proliferation and survival and is overexpressed in many cancers such as breast, prostate, lung, pancreatic, ovarian, and colorectal cancers (Vivanco and Sawyers, 2002). It is stimulated by upstream kinases, PI3-K and pyruvate dehydrogenase kinase (PDK) 1 (Zhang and Burrows, 2004) and is counteracted by PTEN through a dephosphorylation process. Decrease in PTEN stimulates Akt, mTOR, inhibiting PI3-K and resulting in the deactivation of GSK-3β by phosphorylation and increase in stabilized β-catenin (Figure 1.2) (Cross *et al*., 1995). Akt has also been found to be a client protein of HSP90; depending on HSP90 for its stability and activity (Basso *et al*., 2002A and B).

In a similar manner, GSK-3β affects mTOR independently of β-catenin (Inoki *et al*., 2006) (Figure 1.2). When Wnt is not present, GSK-3β phosphorylates tuberin which activates the GTPase-activating protein (GAP) activity of tuberin, leading to the inhibition of mTOR kinase. Therefore, when Wnt is present, GSK-3β is inhibited resulting in an upregulation of mTOR activity (Wullschleger *et al*., 2006).

1.6.2 Notch Signaling

Notch signaling plays a key role in cell fate determination, apoptosis and proliferation during mammary development by inhibiting the differentiation of stem/progenitor cells (Dontu *et al.*, 2004). It has been suggested that aberrant activation of Notch signaling is associated with carcinogenesis (Stylianou *et al.*, 2006). Furthermore, inhibition of Notch signaling can change the transformed phenotype of human breast cancer cell lines (Stylianou *et al.*, 2006), giving an implication of the benefits of inhibiting this signaling for therapeutic designs (Stylianou *et al.*, 2006). The Notch and Wnt pathway are linked in breast cancer, whereby ectopic Wnt-1 expression resulted in the transformation of human mammary epithelial cells by a mechanism that involved the upregulation of Notch signaling (Ayyanan *et al*., 2006). Furthermore, Notch1 has been found to bind directly to β-catenin (Hayward *et al*., 2006) and both the Wnt pathway and Notch pathway share common cofactors (Alves-Guerra *et al*., 2007), GSK-3β phosphorylates Notch which regulates its activity (Espinosa *et al*., 2003), and β-catenin activation of the Notch ligand by transcription (Rodilla *et al*., 2009).

When the ligands, Delta and Jagged bind to Notch receptors, three proteolytic cleavages are initiated (Figure 1.5). These include two cleavages in the extracellular domain followed by one in the plasma membrane by the complex γ-secretase complex. This results in the release of the intracellular domain of the receptor into the cytoplasm where it translocates to the nucleus to act on target genes (Frisén and Lendahl, 2001). Certain therapies have been developed that target the inhibition of the γ-secretase complex, which has been shown to inhibit Notch signaling and decrease the stem cell population or slow the γ-secretase growth of some tumours (Fan *et al.*, 2006).

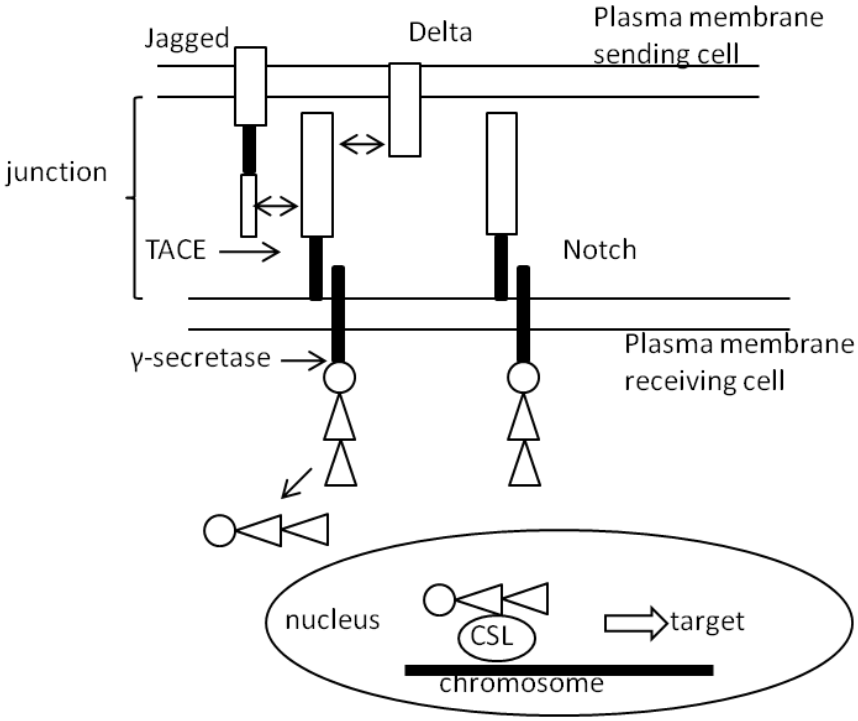

Figure 1.5. Schematic representation of Notch signalling. Notch is activated by the binding of its ligands Delta and Jagged to the ligand receptors. This results in the cleavage of the Notch extracellular domain by TACE, following which γ-secretase cleaves the intracellular domain from the membrane. The Notch intracellular domain then moves to the nucleus where it interacts with the CSL to activate transcription of target genes. TACE, tumour necrosis factor alpha converting enzyme, CSL, transcription factor (adapted from Hambardzumyan *et al.*, 2008).

1.6.3 Hedgehog Signaling

Hedgehog signaling comprises three ligands Sonic, Desert and Indian. Hedgehog signaling is involved in the self-renewal of both normal and malignant mammary stem cells and deregulation of the pathway is linked to cancer (Liu *et al.*, 2006). Furthermore, an inhibitor of the Hedgehog pathway, cyclopamine has been shown to reduce the rate of mammary tumour cells *in vitro* (Kubo *et al.*, 2004). However, MCF7 cells were found to be more resistant to cyclopamine (Kubo *et al.*, 2004).

The pathway is highly organized and kept inhibited by the transmembrane protein Patched1 (Ptch 1). Activation of the pathway occurs when Shh binds to the receptor (Figure 1.6), Ptch 1 which in turn activates the transmembrane protein Smoothened (Smo). This sequesters the release of Gli which translocates to the nucleus and activates the target genes (Ingham and McMahon, 2001).

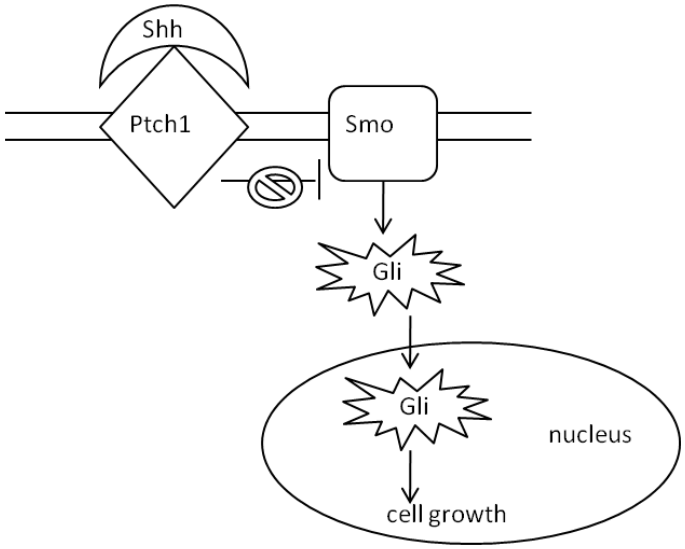

Figure 1.6. Schematic representation of Sonic hedgehog (Shh) signaling pathway. When Shh binds to the receptor, Ptch1, Smo is activated to activate Gli, which translocates to the nucleus and activates the target genes (adapted from Hambardzumyan *et al.*, 2008). Ptch 1, Patched 1; Smo, Smoothened; Gli, transcriptional activator.

1.7 Molecular chaperones and HSP90

Heat shock proteins (HSPs) are chaperones that have an increased expression in tissues that are exposed to proteotoxic stressors such as elevated temperatures, heavy metals, hypoxia and acidosis (Whitesell and Lindquist, 2005). In addition to this, Westerheide and Morimoto (2005) reviewed that there is an increased expression of HSPs when cells undergo mutations or are exposed to environmental stress, such as inflammation, tissue repair, cancer, and neurodegenerative diseases. In spite of the name "heat shock protein", most chaperones are constitutively expressed under normal conditions and their adaptive response ensures cell survival (Whitesell and Lindquist, 2005).

Heat shock protein 90 (HSP90) is a 90 kDa protein which is one of the most abundant chaperones and is highly conserved in prokaryotes and eukaryotes (Borkovich *et al.*, 1989; Ferrarini *et al.*, 1992) and, under normal physiological conditions, is required for important cellular processes, which include hormone signaling, self-renewal and differentiation (Helmbrecht *et al.*, 2000). In addition to this, it assists with protein folding and translocation (Young *et al*., 2001; Picard, 2002; Wandinger *et al*., 2008).

Five isoforms of HSP90 have been identified, which include HSP90α, HSP90β, HSP90N, Grp94 and Trap1 (reviewed in Li *et al*., 2009). HSP90β is constitutively expressed whilst HSP90α is induced by stress and both are cytosolic (Sreedhar *et al.*, 2004). The membrane

associated HSP90N completely lacks the N-terminus which is involved in ATPase activity (Grammatikakis *et al*., 2002). Grp94, associated within the endoplasmic-reticulum and Trap1, associated with the mitochondria, have only been described in higher eukaryotes (Felts *et al*., 2000; Ni and Lee, 2007).

Studies of the crystal structures of yeast HSP90 (Ali *et al*., 2006) and Grp94 (Dollins *et al*., 2007) provide evidence that HSP90 exists primarily as a homodimer, although heterodimerization of HSP90α and HSP90β can occur (Neckers *et al*., 1999). Each monomer comprises three highly conserved domains: the amino terminal domain (N-terminal), middle domain and the carboxy terminal domain (C-terminal) (Figure 1.7) (Pearl and Prodromou, 2006). The N-terminal domain has an ATP-binding pocket with ATPase activity (Dutta and Inouye, 2000). The middle domain is also involved in client protein binding (Hawle *et al*., 2006), whilst the C-terminal dimerization domain reinforces the association between the two N-terminal domains of the monomers (Terasawa *et al*., 2005). The C-terminal domain of eukaryotic, cytosolic HSP90 has a pentapeptide (-MEEVD) which binds to the tetratricopeptide repeat (TPR) domain of HSP90 co-chaperones, such as HSP70/90 organizing protein (Hop) (Terasawa *et al*., 2005; Pearl *et al*., 2008).

The HSP90 dimer undergoes a conformational change that allows it to associate with its client protein (Figure 1.7). In the "open" conformation, the N-terminal domains are separate allowing for the binding of a client protein (Richter *et al*., 2008) (Figure 1.7A). When ATP binds to the N-terminal domains, a conformational change results in the N-terminal domains coming together and "clamping" the client protein (Richter *et al*., 2008) (Figure 1.7B). The ATPase activity of HSP90 drives the chaperone cycle (Kamal *et al*., 2004).

The chaperone cycle starts with the nascent protein binding to the Hsp70/Hsp40 complex, which is associated with the "open" HSP90 conformation via Hop, which binds to both HSP90 and Hsp70 (Pearl *et al*., 2008). Hop not only binds to the –MEEVD region of HSP90, but also to the N-terminal, preventing HSP90 from "closing" so that the client protein can be transferred to HSP90 from Hsp70 (Terasawa *et al*., 2005). Upon ATP binding to HSP90, Hop is displaced by p23 and immunophilins, and the intermediate chaperone complex is transformed to the mature complex (Neckers, 2003). Activator of HSP90 ATPase (Aha1), binds to the middle domain of HSP90, assisting with the HSP90 conformational change so that ATP can bind (Meyer *et al*., 2004). ATP hydrolysis stimulates the release of the client protein from HSP90 (Terasawa *et al*., 2005).

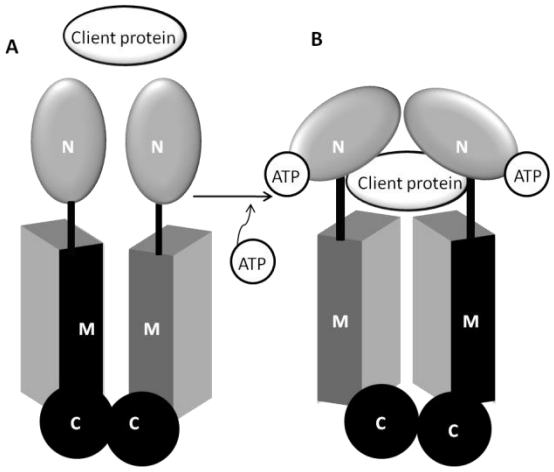

Figure 1.7. Schematic diagram of the binding of HSP90 to its client protein via its ATP-molecular clamp. HSP90 exists as a dimer, with each monomer comprising C-terminal domain (C), middle domain (M) and N-terminal domain (N). (A) When ATP is not bound, an antiparallal dimer is formed by the C-terminal domain, with the N-terminal domains open for capture of the client protein. (B) When ATP binds to the N-terminal domain, a conformational change causes the N-terminal domains to clamp over the client protein (adapted from Brown *et al*., 2007).

1.8 HSP90 and cancer

There is an increased expression of HSP90 in tumours and cancers in comparison to normal tissues, such that it comprises as much as 4-6 % of the total protein in cancer cells in comparison to 1-2% in normal cells (Chiosis and Neckers, 2006). It has been found that HSP90 is in a highly complexed state with high ATPase activity in tumours in comparison to normal cells where it is relatively uncomplexed and in a latent state (Kamal *et al*., 2003; Chiosis and Neckers, 2006). This suggests its potential roles in assisting the tumour cells with maintaining homeostasis, as well as regulating growth and survival in a hostile environment (Solit and Chiosis, 2008). HSP90 stabilizes and protects oncogenic client proteins from proteosomal degradation and assists in oncogenesis and malignant transformation (Grbovic *et al.*, 2006).

HSP90 plays an important role in the oncoproteins involved in cell proliferation and survival of cancer cells (Table 1.2). These client proteins include serine/ threonine kinases (Akt) and protein expressed from v-raf-1 murine leukemia viral oncogene homolog 1 (RAF-1); human epidermal growth factor receptor 2 (HER-2) and hypoxia inducible factor 1/ signal transducer and activator of transcription 3 (HIF-1α/STAT3) in addition to p53, casein kinase 2 (CK2), cell division kinase 4 (Cdk4) and mutated p53 (Kim *et al.*, 2008). For a more extensive list of HSP90 interactors see Appendix A9. The inhibition of HSP90 has been linked to cancer cell differentiation (Goetz *et al.*, 2003).

It is well known that chaperones and client proteins are involved in senescence programs in cancer (Restall and Lorimer, 2010). An example of a protein that is associated with the HSP90 complex is cell division cycle 37 (Cdc37), which has been found to be up-regulated in cancer (Stepanova *et al.*, 2000). Cdc37 is involved in cell division and maintenance of signaling pathways associated with kinases such as Src, RAF-1 and Cdk4 (Stepanova *et al.*, 1996). The immunophilins, FK506-binding protein (FKBP) 52 FKBP52 and FKBP51 are also upregulated in cancer cells (Periyasamy *et al.*, 2007) and mouse embryonic stem cells. Another particularly interesting protein is mortalin, which inhibits p53 (Wadhawa *et al.*, 1998) and thus is involved in tumour formation. Furthermore, p53 inhibits the phosphorylation of STAT3, whilst STAT3 down regulates the expression of p53 in cancers (Lin *et al.*, 2002; Niu *et al.*, 2005).

STAT3 is linked to the activation of the Wnt pathway. Leukemia inhibitory factor (LIF) and the interleukin 6 family bind to their receptors, gp130 on the cell surface membrane, triggering a signal cascade, in which the STAT3 becomes phosphorylated, resulting in the transcription of genes involved in stem cell proliferation, such as *WNT5A* (Darnell *et al.*, 1994; Katoh and Katoh, 2007). The WNT5A in turn activates the canonical Wnt signaling pathway (reviewed in Katoh and Katoh, 2007), and an upregulation of *WNT5A* has been found in breast cancer (Iozzo *et al.*, 1995). WNT5A is upregulated in the initial stages of primary tumours due to tumour-stromal interaction. Studies have shown that inhibition of HSP90 disrupted the STAT3 pathway, such that there was a decrease in phosphorylation of STAT3 which was associated with a decrease in tumour growth (Lang *et al.*, 2007). A possible explanation for this could be that the inhibition of the phosphorylation of STAT3 by HSP90 resulted in the inhibition of the transcription of *WNT5A*, a key gene in cancer cell proliferation (Katoh and Katoh, 2007).

Although HSP90 is required for both cancer and normal cells, cancer cells appear to have a higher sensitivity to inhibition of the HSP90 chaperone function (Park *et al.*, 2003). Inhibitors of HSP90 could thus be used in addition to or as an alternative to chemotherapy (Pick *et al.*, 2007). On the other hand, it must be noted that to compromise the HSP90 function could result in exposing the underlying genotypic diversity, such as the cancer stem-like cells, resulting in an acceleration of malignancy in advanced cancers (Whitesell and Lindquist, 2005). It can therefore be said that timing of cancer therapies is a key factor. There is suggestion for the potential role of HSP90 as a prognostic marker since high HSP90 expression is associated with decreased survival in primary breast cancer (Pick *et al.*, 2007).

Table 1.2 HSP90 client proteins involved in proliferation and survival of cancer cells

Client protein	Function of client protein and association with HSP90	Reference
mutated p53	Tumour suppressor protein. Abrogated p53 interacts with HSP90/p23 to form stable complex	Zhau *et al.*, 2000; Vousden and Lu, 2002
p60v-src	HSP90 associates with p60v-src and assists with the translocation of its inactive form to the plasma membrane	Brugge, 1983
CK2	Involved in cell proliferation. HSP90 binds to CK 2 and is involved in kinase activity, preventing self aggregation	Miyata and Yahara, 1992
Cdk4/ Cdk6	Involved in cell progression through G1 phase. HSP90 folds and maintains Cdk4 in an primed, inactive state	Stepanova *et al.*, 1996
STAT3	Inhibits apoptosis and increases cell transformation. HSP90 stabilizes STAT-transporter interactions	Kim *et al.*, 2008

p60v-src, tyrosine kinase of Rous sarcoma virus, CK, casein kinase, Cdk4, cyclin dependent kinase 4, STAT3, signal transducer and activator of transcription 3

1.9 HSP90 inhibitors

A number of HSP90 inhibitors have been investigated, which are separated into four classes according to their method of inhibition (Table 1.3). Benzoquinone ansamycins, such as geldanamycin, bind to the N-terminus of HSP90, competing with ATP. HSP90 is thus kept in its ADP-bound conformation and therefore prevented from clamping around a client protein, resulting in the degradation of the client protein (Blagg and Kerr, 2006; Neckers, 2006). In a similar manner, novobiocin binds to the C-terminus of HSP90 and therefore results in the degradation of client proteins (Marcu *et al*., 2000).

HSP90 receives client proteins from HSP70/HSP40 with the aid of Hop and client protein association is increased in the presence of other co-chaperones such as p23 and Cdc37 (Richter and Buchner, 2001). In comparison to targeting the ATP binding, HSP90 inhibitors that target the co-chaperone association with HSP90 or HSP90 and client protein association,

provide a better target of inhibition since the progression of the chaperone cycle is inhibited (Pearl *et al*., 2008).

Table 1.3. Examples of HSP90 inhibitors and their mode of action (adapted from Prinsloo *et al*., 2010)

HSP90 Inhibitor	**Inhibitor mode of action**
Geldanamycin[1], 17-AAG[2], IPI-504[3], Radicocol[1], 17-DMAG[3]	Competitive inhibition of ATP at N-terminus
Novobiocin[4], chlorobiocin[4], coumermycin A1[5]	Competitive inhibition of ATP at C-terminus
Celastrol[6]	Targeting of HSP90/ co-chaperone association
Shepherdin[7]	Targeting of HSP90/ client protein association
Tubocapsenolide A[8]	Interference with post-translational modification of HSP90

[1] Roe *et al*., 1999. [2] Goetz *et al*., 2003. [3] Hollingshead *et al*., 2005. [4] Marcu *et al*., 2000. [5]Burlison and Blagg, 2006. [6] Zhang *et al*., 2009B. [7] Plescia *et al*., 2005. [8] Chen *et al*., 2008

There are currently 13 HP90 inhibitors in clinical trial (Kim *et al*., 2009), such as 17-AAG, which has been used in Phase 1 trials since 1999 (Pacey *et al*., 2006) and is now being tested in Phase 2 clinical trials (Ronnen *et al*., 2006). Together with trastuzumab, 17-AAG has shown promising anti-tumour activity (Modi *et al*., 2007). However, it must be noted that 17-AAG has a few disadvantages, such as low water-solubility, instability in solution and decreased oral bioavailability (Messaoudi *et al*., 2008).

Different client proteins respond differently to HSP90 inhibitors, with some exhibiting more sensitivity than others. For example, HER-2 is more sensitive than Akt in response to HSP90 inhibition by ansamycin antibiotics (Basso *et al*., 2002A). Client proteins that are rapidly degraded are more likely to require HSP90 for stability (Liu and Carpenter, 1993; Xu *et al*., 2001). A factor that may influence the sensitivity and kinetics of a client protein for HSP90 is the affinity of the protein for the HSP90 complex as well as the intracellular concentration of the protein in the cell (Zhang and Burrows, 2004). Therapies targeted at the inhibition of HSP90 alone could be counter-intuitive since other co-chaperones could be upregulated as a result. Instead, therapies should be aimed at targeting the co-chaperone interaction (reviewed in Prinsloo *et al*., 2010).

1.10 Cytosolic HSP90 and the Wnt pathway

Very little is known about the role of HSP90 in the Wnt signaling pathway in breast cancer. One study suggested that HSP90 assisted in the correct folding of GSK-3β, preventing the kinase from degradation (Banz *et al*., 2009). It was also shown to be involved in the autophosphorylation of GSK-3β in rabbit reticulocyte lysate; a process which occurs as GSK-3β matures. HSP90-induced inhibition by geldanamycin had an effect on the transitional intermediate of GSK-3β, but did not affect the mature, phosphorylated GSK-3β (Lochhead *et al.*, 2006). More recently, HSP90 has been found to be associated with GSK-3β in human hepatocellular carcinoma Hep3B cells, thus indicating the importance of HSP90 for the serine/threonine activity of the mature GSK-3β (Banz *et al*., 2009).

IκB kinase (IKK) has been found to be associated with HSP90 and Cdc37 (Chen *et al*., 2002). IKK regulates β-catenin by phosphorylation resulting in degradation (Lamberti *et al*., 2001) therefore providing a link between HSP90 and the Wnt pathway. Zhang and Burrows (2004) reviewed that because β-catenin is involved in cell-cell adhesions and plays a role in the association of E-cadherin with intracellular actins, inhibition of HSP90 could influence these events of cell adhesion.

More recently, Kurashina *et al*. (2009) showed that upon 17-AAG and D-MAG treatment, there was a decreased expression of the downstream target gene encoding for TCF7L2 in adult T cell leukemia/lymphoma (ATL) cells. They hypothesized that treatment with HSP90 inhibitors cause the dephosphorylation of Akt, thus activating GSK-3β, which in turn phosphorylates β-catenin for ubiquitination.

Other potential HSP90 clients involved in the Wnt pathway include casein kinase 2 (CK2), which is linked to the phosphorylation of Cdc37 in the HSP90-Cdc37 complex (Miyata, 2009). Since Cdc37 mediates the recruitment of HSP90 to kinases (Hinz *et al*., 2007), Prinsloo *et al.* (2010) proposed that the CK2-HSP90-Cdc37 complex is associated with the Wnt destruction complex by GSK-3β.

It would be important to characterize the possible association between HSP90 and the components of the Wnt signaling pathway in breast cancer in order to provide a mechanistic understanding of the fundamental regulation of the Wnt pathway. In would thus allow for an understanding of where to target therapeutic HSP90 inhibitors to disrupt the Wnt pathway.

1.11 Problem statement and knowledge gap

The multichaperone complex requires clarification in the Wnt pathway in breast cancer. HSP90 has been found to be associated with GSK-3β but little is known about the involvement of HSP90 with other members of the Wnt pathway in breast cancer. In addition to this, the interactions between HSP90 and the Wnt pathway proteins, particularly β-catenin and p-β-catenin require clarification in breast cancer.

1.12 Hypothesis

HSP90 plays a significant role in the Wnt pathway through the modulation of the disheveled complex and p-β-catenin in breast cancer.

1.13 Objectives

The broad objective is to characterize the interaction between HSP90 and the Wnt pathway components in the breast cancer line MCF7, with a comparative analysis of expression levels in the colon cancer line HT29.

1.13.1 Specific Objectives

- Culturing MCF7 and HT29 cells and comparing the protein expression levels between the two cell lines.
- Identification of associations between HSP90 and the members of the Wnt pathway, such as GSK-3β, axin1, β-catenin and p- β-catenin, by co-immunoprecipitation, will be performed.
- Identification of the effects of HSP90 inhibition by geldanamycin, 17-AAG and novobiocin on protein expression levels of the members of the Wnt pathway.
- Identification of localization and co-localization of HSP90 and the members of the Wnt pathway, and the effect of HSP90 inhibitors on the localization of these proteins.

Chapter 2: Materials and Methods

2.1 Materials

All chemicals, culture media, molecular biology reagents, suppliers, catalogue numbers and equipment are listed in Appendix A5-8. The antibodies used in this study are listed below (Table 2.1-2.3). Unless stated otherwise, all reagents were of the highest grade and purity.

Table 2.1. List of primary antibodies used for Western analysis and confocal microscopy

Antibody	Company	catalogue	dilution for Western detection	dilution for confocal microscopy
mouse anti-human HSP90α/β IgG_{2a} monoclonal antibody	Santa Cruz Biotechnologies	sc 13119	1:1000	1:100
rabbit polyclonal anti-human GSK-3β	Santa Cruz Biotechnologies	sc 9166	1:1000	1:100
rabbit polyclonal anti-human β-catenin	Santa Cruz Biotechnologies	sc 7199	1:1000	1:100
rabbit polyclonal anti-human axin1	Santa Cruz Biotechnologies	sc 14029	1:1000	1:100
rabbit polyclonal anti-actin	Sigma-Aldrich	A 2103	1:2000	
mouse monoclonal anti-phospho-β-catenin (pSer33/pSer37)	Sigma-Aldrich	C 4231	1:800	1:100
mouse monoclonal anti-human p-STAT3 $IgG2_b$	Santa Cruz Biotechnologies	sc 8059	1:1000	
rabbit polyclonal anti-human STAT3 IgG	Santa Cruz Biotechnologies	sc 482	1:1000	
rabbit polyclonal anti-human Akt1/2/3	Santa Cruz Biotechnologies	sc 8312	1:1000	

Table 2.2. Secondary antibodies for Western detection

Antibody	Company	Catalogue	Dilution
Goat anti-mouse IgG $F(ab')_2$ Polyclonal Antibody, HRP	KPL	474 1806	1:5000
Donkey anti-rabbit IgG polyclonal antibody, HRP	GE Healthcare	NA 934V	1:5000

Table 2.3. Secondary antibodies for confocal microscopy

Antibody	Company	Catalogue	Dilution	Colour
Alexa Fluor® 488 chicken anti-rabbit IgG (H+L)	Invitrogen	A21441	1:1000	green
Alexa Fluor® 546 donkey anti-mouse IgG (H+L)	Invitrogen	A10036	1:1000	red
Alexa Fluor® 633 donkey anti-goat IgG (H+L)	Invitrogen	A21082	1:1000	purple

2.2 Methods

2.2.1 Mammalian tissue culture

2.2.1.1 Routine maintenance of MCF7 breast cancer epithelial cells

The MCF7 human breast epithelial cancer cells (a gift from Dr Sharon Prince, Department of Human Biology, University of Cape Town, Cape Town, South Africa) were initially seeded onto 25 cm^3 tissue culture flasks (T25, Corning) to increase cell confluency as determined by light microscopy. The cells were then passaged by trypsinization onto 75 cm^3 tissue culture flasks (T75, Corning) and maintained in complete media comprising Dulbecco's modified Eagle's medium (DMEM), 5 % (v/v) heat inactivated fetal calf serum (HIFCS), 50/50 penicillin/streptomycin (100 U/ml). The cells were incubated in a humidified incubator at 37 °C, in a 9 % CO_2 atmosphere.

Cell cultures were split 1:2 once 80 % confluency was attained, as judged by light microscopy. Cells were split by washing with phosphate buffered saline (PBS) pH 7.4, following which trypsin/ethylenediaminetetraacetic acid (EDTA) was added for a few minutes at 37 °C to generate a single cell suspension. Complete media was added to the trypsin suspension to inhibit further trypsinization, and the cell suspension was transferred to a sterile 15 ml tube. A small aliquot was removed from the cell suspension which was used for cell counting using a volume hemocytometer. Trypan Blue was used to stain the cells, with blue cells being identified as dead. Centrifugation of the cell suspension was carried out at 720 *g*, at 4 °C for 2 minutes. The supernatant was poured off the pelleted cells, and the cells were resuspended in the residual volume to create a single cell suspension, before more complete media (20 ml) was added. The cells were then seeded onto 2 x 75 cm^3 tissue culture flasks. All cell cultures were routinely checked for *Mycoplasma* (see Appendix A1 for protocol).

2.2.1.2 Routine maintenance of human colorectal cancer line HT29

Human colorectal cancer line, HT29 (a gift from Dr C. Penny, Wits University, Johannesburg, South Africa) were maintained in the same way as the MCF7 cells (see section 2.2.1.1). The cells were split 1:4 and more frequently than MCF7 cells. HT29 cells were found to be contaminated with *Mycoplasma* prior to immunoprecipitation studies therefore were only used as a comparative cell line for determining the expression level of Wnt pathway proteins.

2.2.1.3 Cryopreservation of mammalian cells

Following trypsinization (see section 2.2.1.1), cells from one confluent T75 flask were resuspended in complete media, followed by centrifugation at 720 *g*. The pelleted cells were resuspended in 1 ml cryopreservation media (10 % (v/v) dimethyl sulphoxide [DMSO] in HIFCS). The solution was transferred to 1 cryo vial, kept on ice for about half an hour before being stored at -80 °C.

2.2.2 Association of members of the Wnt pathway and HSP90 in MCF7 and HT29 cells

2.2.2.1 Harvesting cells for immunoprecipitation

Four flasks (T75) of MCF7 cells (approximately 2-3 x 10^7 cells) were harvested at approximately 100 % confluency. The cells were washed with PBS (pH 7.4) before trypsinization. Further trypsinization was inhibited by adding complete media. A small aliquot of cell suspension was then removed to be used for cell counting. Cells were pooled and pelleted by centrifugation at 720 *g*, 4 °C, for 2 minutes. The pooled, pellet of cells was resuspended in 1 ml PBS pH 7.4 and transferred to a sterile 1.5 ml microcentrifuge tube.

2.2.2.2 Cell lysate preparation

Trypsinized cells were immediately pelleted at 720 *g*, for 2 minutes. After centrifugation, the supernatant was removed and the pelleted cells were resuspended in the residual volume before 200 µl of ice cold radioimmunoprecipitation assay (RIPA) buffer (50 mM Tris-HCl pH 7.4, 150 mM NaCl, 1 mM EDTA, 1mM Na_3VO_4, 1 % (v/v) Nonidet P40 (NP40), 1 mM sodium deoxycholate, 1 mM PMSF, 2 µg/ml protease inhibitor cocktail) was added. Lysis was allowed to occur on ice, on a rocking platform for 30 to 60 minutes. Cell debris was discarded by centrifugation at 12 000 *g*, 4 °C for 30 minutes, and the supernatant used for immunoprecipitation.

2.2.2.3 Immunoprecipitation

Lysate aliquots (100 µl) were transferred to 2 separate 1.5 ml microcentrifuge tubes. The remaining residual volume was aliquoted (10 µl) and stored at -20 °C to be used as the positive control. A preclearing step was performed during which protein A/G PLUS-agarose immunoprecipitation reagent (Santa Cruz Biotechnologies, USA) (20 µl) was added to the lysates and the resulting slurries were incubated for 1 hr on a rotating shaker at 180-200 rpm

at 4°C. Centrifugation at 1000 *g* for 5 mins was performed, and the supernatants were transferred to a new 1.5 ml microcentrifuge tube. Primary antibodies (4 μg), such as anti-human GSK-3β, anti-human HSP90α/β and anti-human β-catenin antibodies (see Table 2.1 for details of the antibodies), were added to the test sample and incubated for 2 hrs at 4 °C on a rotating shake at 180-200 rpm. After incubation, protein A/G PLUS agarose immunoprecipitation reagent (40 μl) was added to the sample and incubation was continued overnight on ice on a rocking platform at 180-200 rpm. The control samples included lysate being subjected to immunoprecipitation without antibody; and protein A/G PLUS-agarose and antibody, without lysate. In each case, the volumes were kept constant by the addition of RIPA lysis buffer.

Following overnight incubation, the complexes were centrifuged at 1000 *g* for 5 mins at 4 °C, and the pellet washed 4 times with PBS pH 7.4, repeating the centrifugation steps. The final pellet was resuspended in 5 X sodium dodecyl sulphate (SDS) sample loading buffer (0.063 M Tris, 10 % glycerol, 2 % SDS, 2.5 % bromophenol blue, 6 % β-mercaptoethanol) (50 μl) and the sample boiled for 10 min. After boiling, the sample (10 μl) was resolved by SDS-polyacrylamide gel electrophoresis (PAGE) (12 % acrylamide) according to Laemmli (1970) (see section 2.2.3) for Western blot analysis (see section 2.2.4).

2.2.2.4 Immunoprecipitation using Invitrogen (Dynal bead separations) Dynabeads co-immunoprecipitation kit

Rabbit polyclonal anti-human GSK-3β (5 μg) antibody (Table 2.1) was coupled to Dynabeads® M-270 Epoxy (5 mg) overnight according to manufacturer's instructions (Invitrogen). Bovine serum albumin (5μg) was coupled to Dynabeads® M-270 Epoxy (5 mg) overnight as the control. Four T75 flasks (approximately 2-3 x 10^7 cells) of MCF7 cells were harvested (see Section 2.2.2.1) and the resulting pellet was weighed before lysing the cells in the calculated volume of extraction buffer for 15 minutes on ice. Co-immunoprecipitation was carried out on the supernatant according to manufacturer's instructions. Immunoprecipitation using bovine serum albumin coupled to Dynabeads® M-270 Epoxy instead of antibody coupled to the beads was performed in exactly the same manner as a control. In the final step, the protein complex was eluted in 60 μl elution buffer, after which 20 μl of 5 X SDS sample loading buffer was added to the sample. Samples were boiled for 10 minutes at 100 °C before the 10 μl aliquots were resolved by SDS-PAGE (12 % acrylamide; see section 2.2.3) and Western blot analysis (see section 2.2.4).

2.2.3 SDS-PAGE

Discontinuous SDS-PAGE (12 % acrylamide: bis-acrylamide 30:1) analysis was carried out according to Laemmli (1970). Proteins were resolved on an SDS gel (4 % acrylamide stacking gel, pH 6.8, 12 % acrylamide resolving gel, pH 8.8) (see Appendix A6 for recipe) at 200 V, 64 mA for approximately 1 hour 10 minutes in 1 X SDS-PAGE running buffer (0.3 M (w/v) Tris, 1.44 % (w/v) glycine, 0.1 % (w/v) SDS). The gel was stained overnight using Coomassie Brilliant Blue staining (0.2 % Coomassie R-250, 40 % (v/v) methanol, 10 % (v/v) glacial acetic acid), and destained in destain solution (40 % (v/v) methanol, 10 % (v/v) glacial acetic acid). Samples were treated with 5 X SDS-PAGE sample loading buffer (0.063 M Tris, 10 % glycerol, 2 % SDS, 2.5 % bromophenol blue, 6 % β-mercaptoethanol) and heated for 5 – 10 minutes at 100 °C on a heating block, before loading onto the gel (12 % acrylamide: bis-acrylamide 30:1).

2.2.4 Western blot analysis

Western blot analysis was performed according to Towbin *et al*. (1979). Samples were resolved on 12 % acrylamide gel by SDS-PAGE. Prior to electroblotting, the gel was washed in ice cold transfer buffer (25 mM Tris, 192 mM glycine and 20 % (v/v) methanol) to remove excess SDS. Transfer of the resolved proteins was performed onto Trans-Blot® transfer nitrocellulose membrane (BioRad, South Africa) in transfer buffer for 1 hr 30 min at 100 V (500 mA) with stirring and cooling. Ponceau (0.1 % (w/v) Ponceau S, 1 % (v/v) glacial acetic acid) staining was used to confirm protein transfer and the stained membrane was photographed. Non-specific binding sites were blocked for 1 hr in 5 % blocking solution (5 % (w/v) fat free milk powder in tris-buffered saline (TBS) (0.8 % (w/v) NaCl, 0.24 % (w/v) Tris, pH 7.6) in plastic zip-lock bags on a shaker at 180-200 rpm at 4 °C. Primary antibody (see Table 2.1) was added to the 2 % blocking solution and the membrane was further incubated overnight on the shaker at high speed at 4 °C. The membrane was then washed for 1 hour in TBS with 0.1 % tween (TBS-T), at 15 min intervals followed by incubation with secondary antibody (see Table 2.2) for 45 minutes at 4 °C on the shaker. Three 15 minute rinses were performed before detection using the ECL Advanced Western Blotting Kit (Amersham Biosciences, GE Healthcare, UK) in Chemidoc^{TM} EQ (BioRad, UK).

2.2.4.1 Stripping and reprobing Western blots

Stripping and reprobing was executed according to the ECL Kit™ (Amersham Biosciences, GE Healthcare, UK) protocol. Briefly, the stripping buffer (100 mM 2-mercaptoethanol, 2 % (w/v) SDS, 62.5 mM Tris-HCl pH 6.8) was preheated to 50 °C before covering the membrane for 10 minutes in an incubator at 50 °C. For a more stringent strip, the membrane was incubated with the stripping buffer for 30 minutes. Two 10 minute washes using TBS-T were performed at room temperature before the membrane was blocked for 1 hr in blocking solution (5 % (w/v) fat free milk powder in TBS). The procedure was performed as previously described (Section 2.2.4).

2.2.5 Inhibition studies

2.2.5.1 Treatment with 17-Allylamino-17-demethoxygeldanamycin (17-AAG)

MCF7 and HT29 cells were seeded onto 6 well culture plates (Corning, USA) at a density of 5 x 10^5 cells per well, fed with 2 ml complete media and allowed to adhere to the plate overnight at 37 °C, 9 % CO_2. The following day, the cells were serum-starved for 1 hour prior to 17-AAG treatment. 17-AAG stocks (Sigma-Aldrich, USA) were prepared in DMSO (1M). Different concentrations of 17-AAG (1 μM, 5 μM, 10 μM) were made up from the stock (1M) in complete media and added to the different wells. Media containing only DMSO, no 17-AAG, was used as the control. The cells were treated for 72 hours at 37 °C, 9 % CO_2. Following treatment, the media was removed from the cells and non-adherent floating cells were pelleted at 720 *g* for 2 minutes. The adherent and pelleted cells were washed with PBS pH 7.4 to removed excess FCS in the media. Lysis was allowed to occur by adding 250 μl 5 x SDS-PAGE sample loading buffer to the adherent cells for 15 minutes at 4 °C, followed by scraping of the lysate into the microcentrifuge tubes containing the pelleted cells. The microcentrifuge tubes were boiled for 10 minutes at 100 °C. The samples were stored at -20 °C prior to being resolved by SDS-PAGE and Western transfer and analysis.

2.2.5.2 Treatment with geldanamycin

MCF7 and HT29 cells were seeded as previously described (see Section 2.2.5.1). The following day, the cells were serum starved for 1 hour prior to geldanamycin treatment. Geldanamycin stock solutions (BioMol International, USA) (5 mM) were made up in DMSO and stored at -20 °C. Working solutions of geldanamycin at 0.1 μM, 0.5 μM, 1 μM, 10 μM were made up in complete media and added to the different wells. Media containing only

DMSO, no geldanamycin, was used as the control. The cells were treated for 24 hours at 37 °C, 9 % CO_2. Following treatment, the media was removed from the cells and the floating cells were pelleted at 720 *g* for 2 minutes. The same lysis procedure, using 500 µl 5 x SDS-PAGE sample loading buffer, was performed as previously described (see Section 2.2.5.1).

2.2.5.3 Treatment with novobiocin

Fresh stock solutions of novobiocin (10 mM) were made up in distilled water and filter sterilized (0.22 µM). The same procedure was carried out as in section 2.2.5.2 with concentrations of 100 µM, 260 µM, 500 µM novobiocin being used to treat the cells for 24 hours. Media without novobiocin was used as the control.

2.2.6 Comparison of the levels of Wnt pathway proteins between MCF7 and HT29 cells

Each cell line was trypsinized and the single cell suspension was transferred to a 1.5 ml microcentrifuge tube in 1 ml PBS. Whole cell lysates were made by lysing the cells in 5 X SDS sample loading buffer at a final concentration of 1 x 10^5 cells/µl and boiling for 10 min at 100 °C. The protein samples (5 µl) were resolved by SDS-PAGE and Western blot analysis was performed. The Ponceau stained membranes and actin levels were used as the loading control.

2.2.7 Localization of Wnt protein members and co-localization studies between Wnt members and HSP90

2.2.7.1 Treatment of cells for confocal microscopy

Each cell line was seeded (1 X 10^5 cells/ well) on borosilicate glass cover slips in 4 well culture plates (Nunclon^{TM}, Nunc), and allowed to adhere overnight at 37 °C, 9 % CO_2. The following day, the cells were treated for 5 hours with complete medium containing either novobiocin (500 µM final concentration), or 17-AAG (10 µM final concentration). Untreated complete medium was used as the control for novobiocin experiments. Completed medium containing only DMSO, no 17-AAG was used as the control for 17-AAG experiments. Following treatment, complete medium was aspirated, and the cells were washed with PBS pH 7.4, before fixing with ice cold methanol (100 % (v/v)). The cells were allowed to dry before blocking with filter-sterilized (0.22 µM) blocking solution (1 % bovine serum albumin (BSA/ PBS) for 30 mins at room temperature. The cells were then incubated with primary antibody (1:100 (v/v) in 0.1 % BSA/PBS solution) (see Table 2.1) overnight at 4 °C.

Following overnight incubation, the secondary antibody (1:1000 (v/v) in 0.1 % BSA/PBS solution) (see Table 2.3) was incubated at room temperature for 1 hour in the dark, before 2 washes of 5 minutes were performed with 0.1 % (w/v) BSA/PBS solution. Nuclear material was stained with Hoechst 33342 solution (1:1000 in water (v/v)) and the cover slips were dried before mounting with Dako fluorescent mounting medium (Dako, USA). The same procedure was performed, without primary antibody, as a control.

Samples were analysed using the Zeiss LSM 510 confocal microscope with 40 X or 60 X oil objective with the relevant wavelengths (see Table 2.4). Images were recorded digitally using the LSM software (Zeiss, Germany). With each image capture, care was taken that the same parameters were used. The inhibitor study images were enhanced by changing the brightness and contrast in ImageJ v1.421 (MacroBiophotonics, USA) so that if any change in localization occurred, the change could be seen (see Appendix A2, Figures A2.1-A2.3 for original images). Cross sections of the cells were analyzed using LSM Image Browser v4.2.121 (Zeiss, Germany) to identify the location of the proteins by analyzing the intensity of the staining relative to nuclear staining. Non-specific staining was not observed upon staining with secondary antibodies only.

Table 2.4 Excitation and emission wavelengths of the antibodies used in Confocal Microscopy

Secondary antibody	Colour	Excitation wavelength (nm)	Emission Wavelength (nm)
Alexa^{Fluor} 488	green	499	519
Alexa^{Fluor} 546	red	561	572
Alexa^{Fluor} 633	purple	632	648

2.2.7.1.1 Quantification of co-localization studies

Quantitative analysis of the co-localization studies on 3 separate, unedited images was performed by calculating the average of the Pearson's correlation coefficient (Rr), Mander's overlap coefficient (R) and the coefficients M_1 and M_2 in the program ImageJ v1.421 (MacroBiophotonics, USA).

In addition to this, the colocalization coefficients, M_1 (for red signal) and M_2 (for green signal) were used to identify how well each channel overlapped with the other. These coefficients could be used to determine if a red signal overlapped considerably with a green signal (Bolte and Cordelières, 2006).

Chapter 3: Localization studies on Wnt protein members

3.1 Introduction

It is well known that molecular chaperones are involved in the modulation of folding and assembly of target proteins (Pearl and Prodromou, 2001). Previous studies have shown that HSP90 is important for signaling pathways (Schulte, *et al*., 1995) and it has been suggested that HSP90 is involved in the Wnt pathway by association with GSK-3β in Hep3B cells (Banz *et al*., 2009). However, Lochhead *et al*. (2006) noted that this association in rabbit reticulocyte lysates only takes place for the maturation of GSK-3β, and the mature form of GSK-3β does not require HSP90.

3.1.1 Cytoplasmic localization of proteins

In this study, cytoplasmic localization incorporates both the cytosol and cytoplasm. HSP90α/β is mainly localized in the cytoplasm (Taherian *et al*., 2007), whilst the isoforms HSP90N has been found to be associated with the membrane (Grammatikakis *et al*., 2002), Grp94 in the endoplasmic-reticulum (Ni and Lee, 2007) and Trap1 in the mitochondria (Felts *et al*., 2000).

The members of the Wnt pathway including: β-catenin (López-Knowles *et al*., 2010), p-β-catenin (Nakopoulou *et al*., 2006), GSK-3β and axin1 have also been found to be localized mainly to the cytoplasm (Wiechens *et al*., 2004; Caspi *et al*., 2008). Two isoforms of axin have been identified, which include axin1 and axin2. Axin1 is constitutively expressed and regulates the basal level of Wnt signaling, whilst axin2 is upregulated when there is an increase in the β-catenin level thus it plays a role in the duration and intensity of a Wnt signal (Yan *et al*., 2001; Lustig *et al*., 2002). It is thought that axin1 is associated with microtubules and is involved in the regulation of the microtubules stability through Dsh (Ciani *et al*., 2004). Endogenous axin has been found to be located in small, punctate structures in the cytoplasm that shift closer to the plasma membrane when cells are treated with LiCl which inhibits GSK-3β (Levina *et al*., 2004; Wiechens *et al*., 2004). Since axin recruited other members of the destruction complex into these structures, it is thought that these structures may be important for β-catenin degradation (Faux *et al*., 2008). Upon Wnt stimulation, axin relocates from the cytoplasm to the plasma membrane in a Dsh dependent manner (Neo *et al*., 2000).

β-catenin forms cell-cell contacts in a complex with E-cadherin and α-catenin at the plasma membrane (Kam and Quaranta, 2009). In breast carcinoma cells, β-catenin has been found to

be localized in the cytoplasm and plasma membrane (López-Knowles *et al*., 2010). High cytoplasmic β-catenin expression has been associated with poor clinical outcome, high-grade tumours with increased rate of proliferation, ER-negative and HER-2 positive breast cancers (López-Knowles *et al*., 2010). β-catenin can become stabilized in the cytoplasm in breast cancer due to low APC expression (Ozaki *et al*., 2005), methylation of the APC promoter (Prasad *et al*., 2008) or APC truncation (Schlosshauer *et al*., 2000). Studies have suggested that cytoplasmic accumulation of β-catenin is linked to endocrine therapy resistance (Hiscox *et al*., 2006; López-Knowles *et al*., 2010). On the other hand, cytoplasmic localization of p-β-catenin is linked to good prognosis in breast cancer patients (Nakopoulou *et al*., 2006).

3.1.2 Nuclear localization of proteins

Heat stress and hypoxic shock cause the shift in localization of HSP90α/β to the nucleus (Katschinski *et al*., 2002; Langer *et al*., 2003). A shift in some of the proteins of the Wnt pathway is also seen after Wnt stimulation (Polakis, 2000). This includes the nuclear localization of dephosphorylated, stabilized β-catenin (Chan *et al*., 2002; Staal *et al*., 2002). An increase in nuclear β-catenin can also be seen when stable β-catenin is overexpressed in transgenic mice (Harada *et al*., 1999) or in cell lines (Morin *et al*., 1999), as well as by using inhibitors to prevent β-catenin degradation (Simcha *et al*., 1998; Henderson *et al*., 2002).

GSK-3β and axin1, although mainly localized in the cytoplasm have also been found to occur in the nucleus (Salahshor and Woodgett, 2005; Caspi *et al*., 2008). Nuclear GSK-3β is thought to play a role in decreasing the expression level of β-catenin in the Wnt pathway that is independent of its phosphorylation of β-catenin (Caspi *et al*., 2008). It does this by decreasing the level of β-catenin/TCF dependent transcription (Caspi *et al*., 2008). Adenocarcinomas and tumours have also been found to have nuclear axin1 and axin2 (Salahshor and Woodgett, 2005). Since axin1 can move between the cytoplasm and nucleus, it is suggested that it acts as a chaperone for β-catenin such that it is required for the shuttling of β-catenin from the nucleus into the cytoplasm (Cong *et al*., 2004A; Wiechens *et al*., 2004).

P-β-catenin has also been located in the nucleus of cancers including: melanoma (Kielhorn *et al*., 2003), colorectal (Chung *et al*., 2001) and breast cancer (Nakopoulou *et al*., 2006) which could be a result of overexpression of the protein and oversaturation of the degradation complex such that nuclear localization results (Nakopoulou *et al*., 2006). Furthermore, nuclear p-β-catenin has been linked to poor clinical outcome due to its association with aggressive and invasive tumour phenotypes (Nakopoulou *et al*., 2006).

Immunofluorescence and confocal microscopy are used to identify the spatial distribution of molecules within a cell. Based on antigen specificity and the development of multiple fluorophores, protein presence and location can detected by immunofluorescence (Paddock, 2005). Co-localization occurs when a signal is emitted at the same pixel position in different fluorescence microscopy images (Zinchuk *et al*., 2007). It gives insight into the structural and functional characteristics of proteins analyzed, although not necessarily providing direct evidence of their functional relationship (Zinchuk *et al*., 2007). The Pearson's correlation coefficient (Rr) describes the similarity between the patterns of the intensity distribution, but does not factor the intensities of the signals. The values range from -1 to 1, where 0 represents no significant correlation and a value from 0.5 to 1 represents co-localization. A disadvantage of the Pearson's correlation coefficient is that it is restricted to samples with approximately equal number of densities in each channel (Manders *et al*., 1992). To overcome this, the Mander's overlap coefficient was also used which describes the degree of localization by assessing the overlap of the signals. The values range from 0 to 1, with 0.5 representing 50 % overlap between the pixels in each image (Zinchuk *et al*., 2007). Values from 0.6 to 1 for Mander's overlap coefficient indicate co-localization.

In this study, immunostaining of MCF7 cells was performed to identify whether there is an overlap of signals between HSP90 and the components of the Wnt pathway, including GSK-3β, axin1, β-catenin and p-β-catenin, to see if a possible association of HSP90 exists with these proteins. Treatment of MCF7 cells with the HSP90 inhibitors, geldanamycin, 17-AAG and novobiocin, was performed to identify whether a change in the localization of the Wnt pathway members would occur.

3.2 Results

3.2.1 Localization of HSP90 and the Wnt members, GSK-3β, axin1, β-catenin and phospho-β-catenin in MCF7 cells

3.2.1.1 GSK-3β and HSP90α/β

Using indirect immunofluorescence and confocal microscopy, GSK-3β was found to be localized mainly in the cytoplasm in all of the cells, although apparent weak nuclear localization was identified in some cells assayed (Figure 3.1A). HSP90α/β was found to be localized in the cytoplasm in all of the cells, with some nuclear localization (Figure 3.1A). The staining profiles for HSP90α/β and GSK-3β were similar (Figure 3.1B), with both proteins having peak intensities outside the nucleus, in the cytoplasmic region.

Immunofluorescence and confocal microscopy also suggested that HSP90α/β was situated in a similar location within the cell as GSK-3β (Figure 3.1A, merged).

Quantitative analysis of the immunofluorescence signals gave a Pearson's correlation coefficient (Rr) of 0.78 (±0.008) and Mander's overlap coefficient (R) of 0.91 (±0.004), suggesting co-localization of HSP90α/β and GSK-3β. Furthermore, the M_1 (0.996 ±0.002) and M_2 (0.994 ± (0.002) values indicated that there was a strong overlap between the red and green channels, representative of HSP90α/β and GSK-3β staining, respectively.

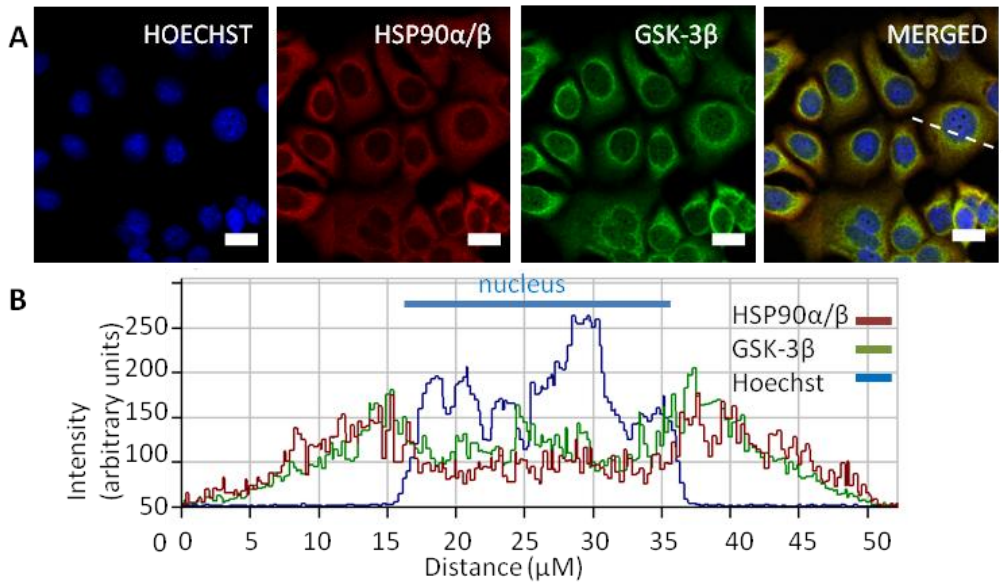

Figure 3.1. HSP90α/β and GSK-3β co-localize. A. Confocal microscopy images of stained MCF7 cells captured using a Zeiss LSM 510 confocal microscope. Hoechst: blue nuclear staining. HSP90α/β (red) using anti-human HSP90α/β antibody. GSK-3β (green) using anti-human GSK-3β. Merged: the overlap of Hoechst, GSK-3β and HSP90α/β signals with the yellow area highlighting co-localization of GSK-3β and HSP90α/β. B. Cross section of a MCF7 cell representing the similar staining profiles for GSK-3β and HSP90α/β. Profiles were obtained using the program Zeiss LSM Image Browser. The blue line represents Hoechst staining of the nucleus, the green line represents the signaling for GSK-3β staining and the red line represents the signal for HSP90α/β staining. Scale bars represent 20 μm. Dotted line represents cross section of cell used for intensity profile.

3.2.1.2 Axin1 and HSP90α/β

Immunofluorescence and confocal microscopy illustrated how axin1 was localized throughout the MCF7 cell in most of the cells (Figure 3.2A), however, the axin1 signal was weak. In accordance with section 3.2.1.1, HSP90α/β was found to be localized mainly in the cytoplasm in all of the cells assayed, with some nuclear HSP90α/β localization in some of the cells (Figure 3.2A). The signals for HSP90α/β staining showed that HSP90α/β appeared to be localized mainly in the cytoplasm, with some nuclear localization (Figure 3.2B). The signal

for axin1 staining was low and did not change in the different locations throughout the cell. (Figure 3.2B). It was difficult to analyze the co-localization between axin1 and HSP90α/β since the axin1 staining was weak and there was a difference in the signal intensities of the staining of the 2 proteins (Figure 3.2B).

Quantitative analysis of the immunofluorescence signals gave a low Pearson's correlation coefficient of 0.237 (±0.1). In contrast, the Mander's overlap coefficient of 0.636 (±0.07) showed that there was about 64 % co-localization between HSP90α/β and axin1. The coefficients, M_1 (0.95 ±0.06) and M_2 (0.8 ±0.1) values illustrated that there was a higher overlap between the red signal of HSP90α/β with the green signal of axin1 than there was vice versa.

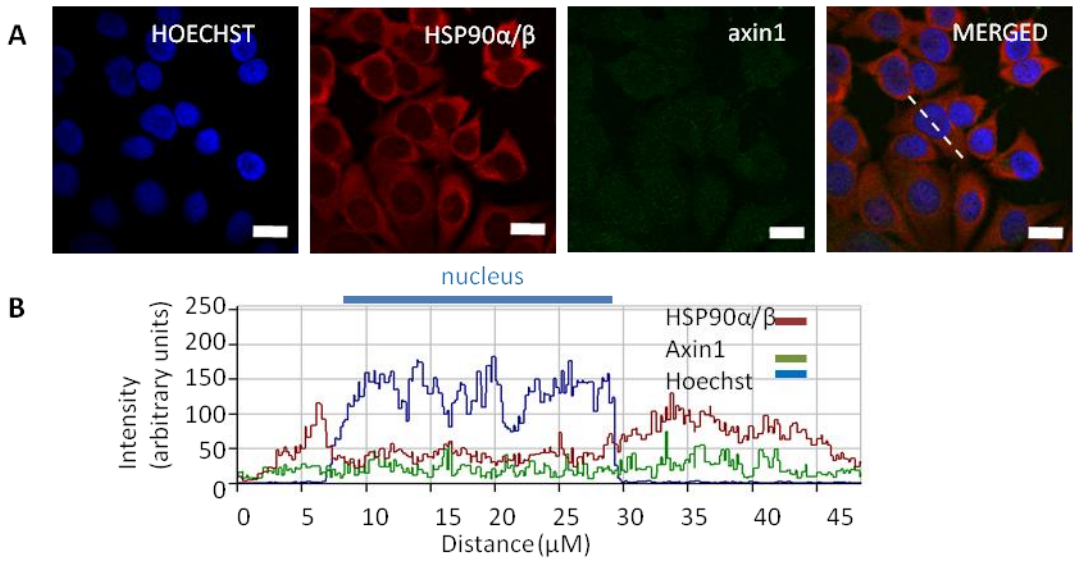

Figure 3.2. Co-localization of HSP90α/β and axin1. A. **C**onfocal microscopy images of stained MCF7 cells captured using a Zeiss LSM 510 confocal microscope. Hoechst: blue nuclear staining. HSP90α/β (red) using anti-human HSP90α/β antibody. Axin1 (green) using anti-human axin1. Merged: the overlap of Hoechst, axin1 and HSP90α/β signals. B. Cross section of MCF7 cell representing the similar staining profiles for axin1 and HSP90α/β. Profiles were obtained using the program Zeiss LSM Image Browser. The blue line represents Hoechst staining of the nucleus, the green line represents the signaling for axin1 staining and the red line represents the signal for HSP90α/β staining. Scale bars represent 20 μm. Dotted line represents cross section of cell used for intensity profile.

3.2.1.3 β-catenin and HSP90α/β

Immunofluorescence confocal microscopy revealed that β-catenin was localized to distinct punctate structures just outside the nucleus in all of the MCF7 cells (Figure 3.3A, arrow), whilst there was some localization within the cytoplasm and membranes. The signal intensities representative of β-catenin staining were highest just outside the nucleus and at the

membrane (Figure 3.3B). On the other hand, HSP90α/β had diffuse cytoplasmic staining with some perinuclear staining in most of the cells (Figure 3.3A, top right panel), with high signal intensities, representative of HSP90α/β staining, outside the nucleus (Figure 3.3B).

Quantitative analysis of the immunofluorescence signals gave high values for both the Mander's overlap coefficient (R=0.819 ±0.03) and the Pearson's correlation coefficient (Rr=0.654 ±0.1). The M_1 (0.98 ±0.02) and M_2 (0.98 ±0.02) coefficients suggested that there was about a 98 % overlap in signals between the red and green signals representing HSP90α/β and β-catenin staining, respectively.

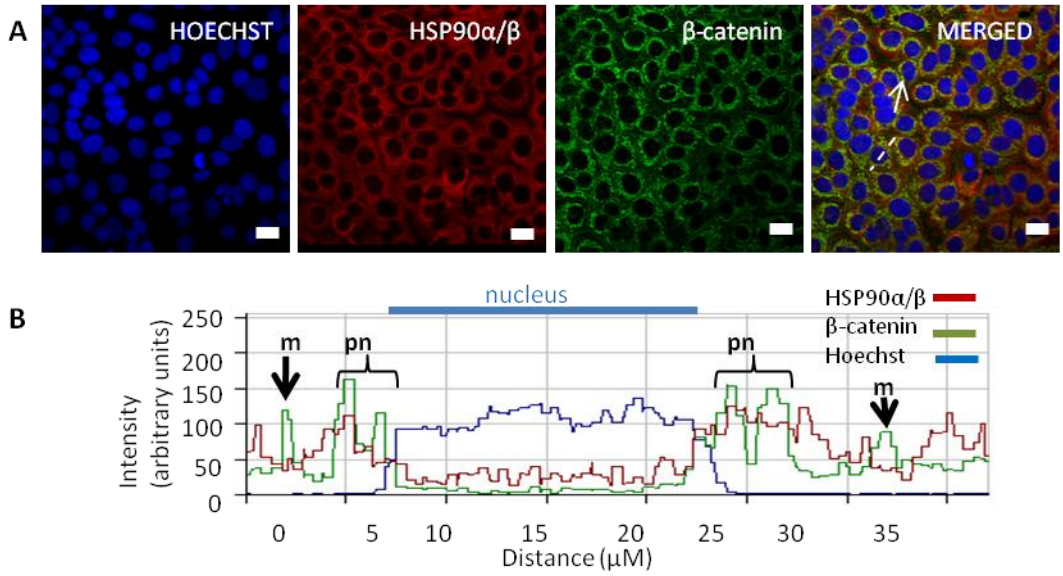

Figure 3.3. Co-localization analysis of total β-catenin and HSP90α/β. A. Confocal microscopy images of stained MCF7 cells captured using a Zeiss LSM 510 confocal microscope. Hoechst: blue nuclear staining. HSP90α/β (red) using anti-human HSP90α/β antibody. β-catenin (green) using anti-human β-catenin. Merged: the overlap of Hoechst, β-catenin and HSP90α/β signals. B. Cross section of MCF7 cell representing the staining profiles for β-catenin and HSP90α/β. Profiles were obtained using the program Zeiss LSM Image Browser. The blue line represents Hoechst staining of the nucleus, the green line represents the signaling for total β-catenin staining and the red line represents the signal for HSP90α/β staining. Scale bars represent 20 μm. Dotted line represents cross section of cell used for intensity profile. Arrows point toward punctate structures. m represents β-catenin that is predicted to be at the plasma membrane. pn represents β-catenin that is predicted to be in the perinuclear region.

3.2.1.4 Phospho-β-catenin and HSP90α/β

Using immunofluorescence microscopy staining, both p-β-catenin and HSP90α/β were localized mainly in the cytoplasm in all of the cells (Figure 3.4). Both proteins had similar localizations (Figure 3.4, merge) and the intensity signals representative of p-β-catenin and HSP90α/β staining were highest in the cytoplasm (Figure 3.4B).

Quantitative analysis of the immunofluorescence signals gave a Pearson's correlation coefficient of 0.427 (±0.05) and a Mander's overlap coefficient of 0.78 (±0.02) suggesting that there was 78 % co-localization between p-β-catenin and HSP90α/β. Both the coefficients M_1 (0.97 ±0.01) and M_2 (0.94 ±0.02) showed a high correlation between the red and green signals representative of the staining of HSP90α/β and p-β-catenin respectively.

These results suggested that there was a high possibility of co-localization between HSP90α/β and p-β-catenin. Co-immunoprecipitation of HSP90α/β and p-β-catenin would be needed to confirm this finding.

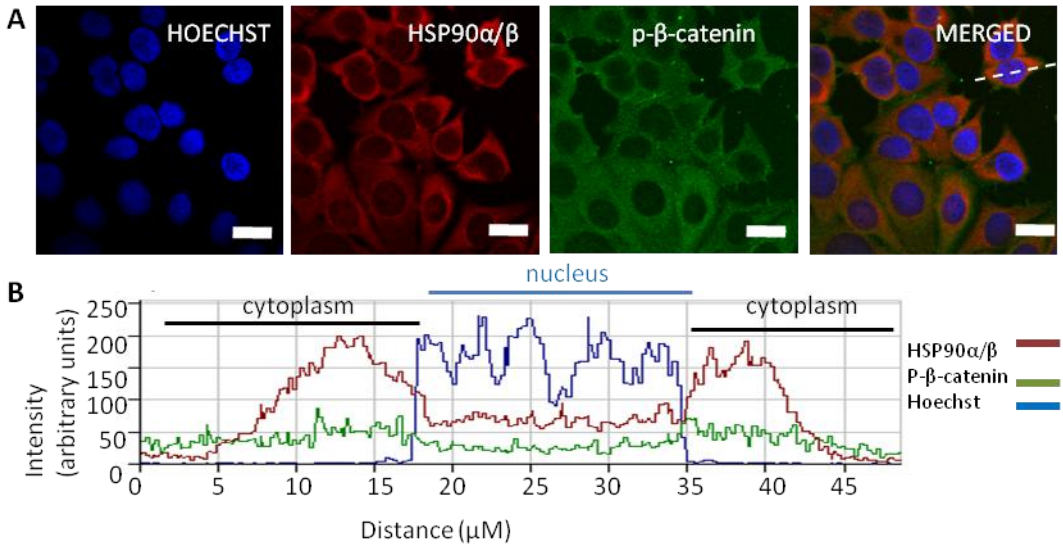

Figure 3.4. Co-localization analysis of HSP90α/β and p-β-catenin. A. Confocal microscopy images of stained MCF7 cells captured using a Zeiss LSM 510 confocal microscope. Hoechst: blue nuclear staining. HSP90α/β (red) using anti-human HSP90α/β antibody. P-β-catenin (green) using anti-human p-β-catenin. Merged: the overlap of Hoechst, p-β-catenin and HSP90α/β signals. B. Cross section of MCF7 cell representing the staining profiles for p-β-catenin and HSP90α/β. Profiles were obtained using the program Zeiss LSM Image Browser. The blue line represents Hoechst staining of the nucleus, the green line represents the signaling for p-β-catenin staining and the red line represents the signal for HSP90α/β staining. Scale bars represent 20 µm. Dotted line represents cross section of cell used for intensity profile.

3.2.2 Effects of HSP90 inhibitors, 17-AAG and novobiocin on the localization of HSP90α/β, GSK-3β, axin1, β-catenin and p-β-catenin

MCF7 cells were treated with the compounds, 17-AAG and novobiocin, to identify if HSP90 inhibition had an effect on the localization of the Wnt pathway members, GSK-3β, axin1, β-catenin and p-β-catenin.

3.2.2.1 GSK-3β and HSP90α/β

Using immunofluorescence and confocal microscopy, it was found that in untreated MCF 7 cells, HSP90α/β and GSK-3β were localized in the cytoplasm of most of the cells (Figure 3.5A). Treatment of MCF7 cells with the HSP90 inhibitor, novobiocin (500 μM) (Figure 3.5B) resulted in very little change in the localization of HSP90α/β and GSK-3β in comparison to untreated cells (Figure 3.5A), although it did appear that there was a slight shift of HSP90α/β to the perinuclear region in some of the cells after novobiocin treatment (Figure 3.5C). Exposure to 17-AAG (10 μM), resulted in a morphological change in most of the MCF7 cells whereby the cells had a smaller, rounded phenotype in comparison to untreated cells (Figure 3.5C). As a result of this, it appeared that there was a slight shift of localization to the perinuclear region for HSP90α/β and GSK-3β in most of the cells (Figure 3.5C).

The signal intensity profiles of the pattern distribution of HSP90α/β and GSK-3β (Figure 3.5D-F) were obtained by taking cross sections of the merged images of HSP90α/β and GSK-3β (Figure 3.5G-I). In each of the studies: untreated (Figure 3.5D), novobiocin treated (Figure 3.5E) and 17-AAG (Figure 3.5F) treated MCF7 cells, there was an overlap in the pattern of distribution of HSP90α/β and GSK-3β staining. The signal intensity profile of untreated cells showed that there was a similar pattern of distribution between HSP90α/β and GSK-3β (Figure 3.5D). The highest signal for HSP90α/β and GSK-3β staining, in untreated cells, was located outside the nucleus, in what appeared to be the cytoplasmic region, although signals were detected within the nucleus (Figure 3.5D). The signal intensity profile of novobiocin treated cells showed that there was a slight shift of signals representing HSP90α/β and GSK-3β staining, to what appeared to be the perinuclear region (Figure 3.5E). This could be due to the morphological change of the cells, whereby the cells appeared to be large and flattened (Figure 3.5H). There was a slight shift of the pattern of HSP90α/β and GSK-3β staining to what appeared to be the perinuclear region in 17-AAG treated cells, with some cytoplasmic staining (Figure 3.5I).

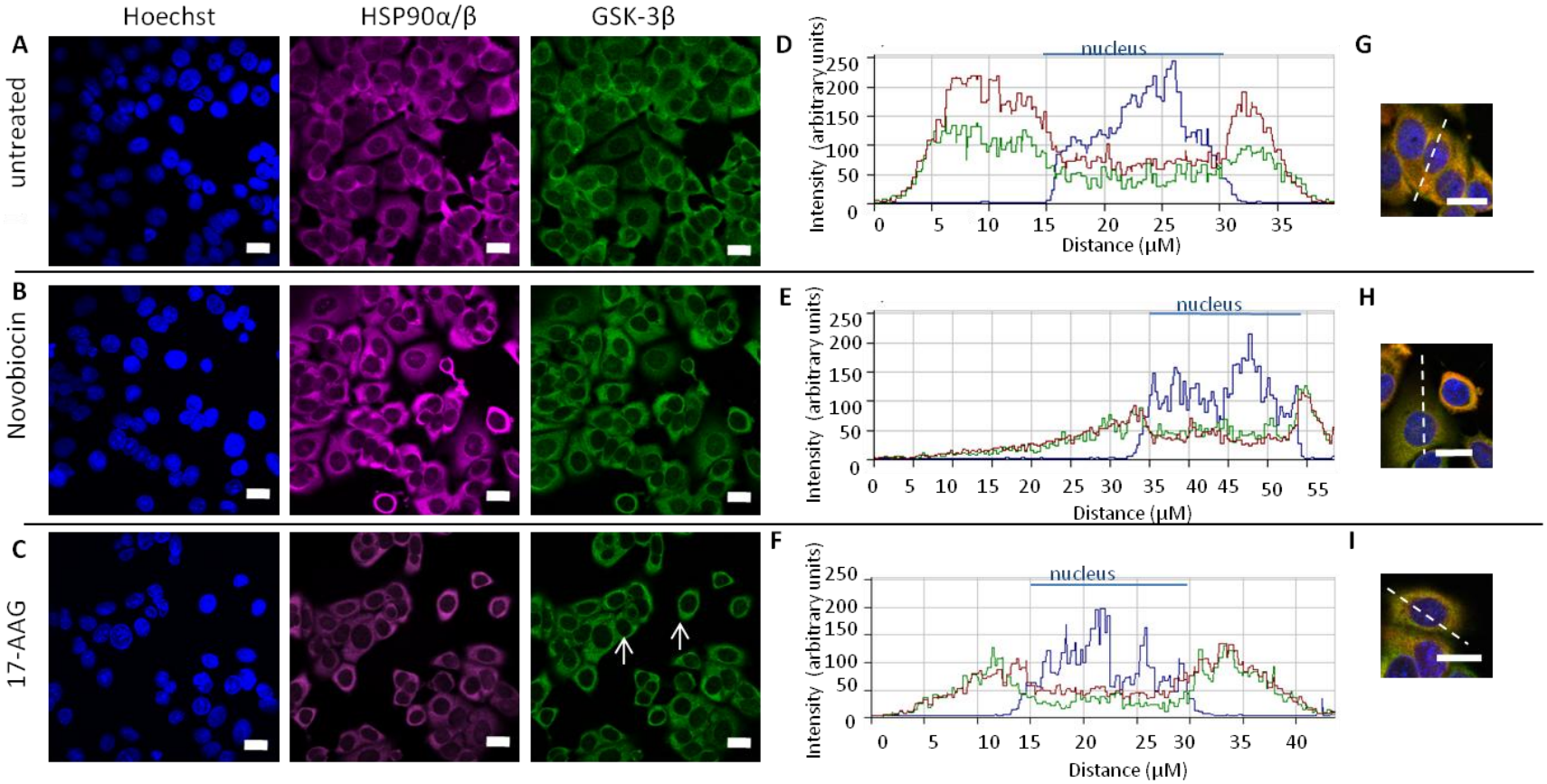

Figure 3.5. Effects of HSP90 inhibitors on the localization of HSP90α/β and GSK-3β. MCF7 cells were serum-starved for 1 hour prior to 5 hour treatment with inhibitors. Confocal microscopy images of stained MCF7 cells captured using a Zeiss LSM 510 confocal microscope. A. Untreated MCF7 cells. B. Novobiocin (500 μM) treated MCF7 cells. C. 17-AAG (10 μM) treated MCF7 cells. Hoechst: blue nuclear staining. HSP90α/β (purple) using anti-human HSP90α/β antibody. GSK-3β (green) using anti-human GSK-3β antibody. D, E, F: Intensity profile studies of GSK-3β (green), HSP90α/β (red), Hoechst (blue) for: untreated MCF7 cells (D), Novobiocin (500 μM) treated MCF7 cells (E); and 17-AAG (10 μM) treated MCF7 cells (F). The blue line represents Hoechst staining of the nucleus, the red line represents the signal for HSP90α/β staining and the green line represents the signal for GSK-3β staining. G, H, I: Immunofluorescence confocal microscopy images representing the merged images of HSP90α/β, GSK-3β and Hoechst. Scale bars represent 20 μm. Dotted line represents cross sections of cells used for intensity profiles. Arrows point towards morphological change to "rounded" phenotype after 17-AAG treatment. Images were enhanced by adjusting contrast and brightness using MacBiophotonics ImageJ for better identification of localization patterns.

3.2.2.2 Axin1 and HSP90α/β

Immunofluorescence and confocal microscopy revealed that axin1 appeared to be localized throughout most of the untreated cells (Figure 3.6A), although the intensity of the staining was very weak. After novobiocin treatment, there appeared to be an increase in the localization of axin1 at what appeared to be the plasma membrane in most of the cells (Figure 3.6B, arrows). However, this would need to be confirmed with antibodies that stain membrane structures. Although it appeared that axin1 appeared to localize more to what appeared to be the perinuclear region, after 17-AAG treatment, this could also be attributed to the rounder phenotype of the MCF7 cells (Figure 3.6C). HSP90α/β had similar localization patterns as was previously described (Section 3.2.2.1), with what appeared to be cytoplasmic localization in most of the untreated cells (Figure 3.6A) and a slight shift to what appeared to be the perinuclear region in novobiocin (Figure 3.6B) and 17-AAG (Figure 3.6C) treated MCF7 cells.

Signal intensity profiles were obtained from the cross sections of the merged images of HSP90α/β and axin1 (Figure 3.6G-I). In untreated cells, the signal intensity of axin1 staining was much lower than that of HSP90α/β staining (Figure 3.6D). Furthermore, the signal intensity of axin1 staining was the same throughout the cell in untreated MCF7 cells (Figure 3.6D). In novobiocin treated cells, the signal intensity of axin1 staining was also lower than that of HSP90α/β staining, and remained constant throughout the cell (Figure 3.6E). The increase in signal intensity corresponding to axin1 staining at what appeared to be the plasma membrane (Figure 3.6H), was difficult to see since the intensity of staining was so low (Figure 3.6E). There appeared to be a similar staining profile for axin1 and HSP90α/β after 17-AAG treatment (Figure 3.6F), with most of the signal for axin1 staining being located outside the nucleus in what appeared to be the cytoplasmic region (Figure 3.6F). The signal intensity profiles for HSP90α/β were similar to those previously described (Section 3.2.2.1).

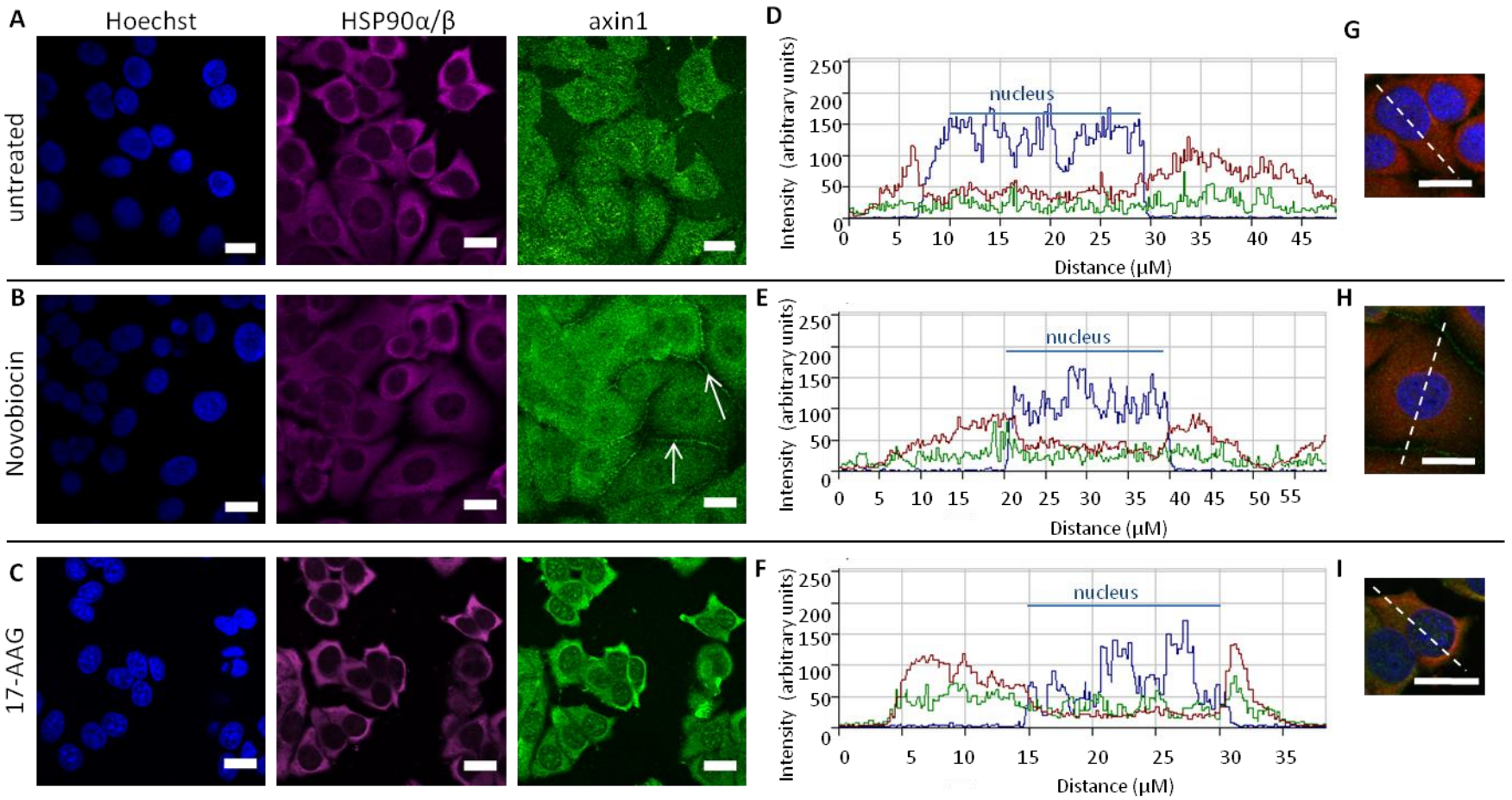

Figure 3.6. Effects of HSP90 inhibitors on the localization of HSP90α/β and axin1. MCF7 cells were serum-starved for 1 hour prior to 5 hour treatment with inhibitors. Confocal microscopy images of stained MCF7 cells captured using a Zeiss LSM 510 confocal microscope. A. Untreated MCF7 cells. B. Novobiocin (500 μM) treated MCF7 cells. C. 17-AAG (10 μM) treated MCF7 cells. Hoechst: blue nuclear staining. HSP90α/β (purple) using anti-human HSP90α/β antibody. Axin1 (green) using anti-human axin1 antibody. D, E, F: Intensity profile studies of axin1 (green), HSP90α/β (red), Hoechst (blue) for: untreated MCF7 cells (D) (same image as Figure 3.2B), Novobiocin (500 μM) treated MCF7 cells (E); and 17-AAG (10 μM) treated MCF7 cells (F). The blue line represents Hoechst staining of the nucleus, the red line represents the signal for HSP90α/β staining and the green line represents the signal for axin1 staining. G, H, I: Immunofluorescence confocal microscopy images representing the merged images of HSP90α/β, axin1 and Hoechst. Scale bars represent 20 μm. Dotted line represents cross sections of cells used for intensity profiles. Arrows point toward what appears to be the plasma membrane. Images were enhanced by adjusting contrast and brightness using MacBiophotonics ImageJ for better identification of localization patterns.

3.2.2.3 p-β-catenin and β-catenin

Immunofluorescence and confocal microscopy revealed that p-β-catenin had what appeared to be diffuse cytoplasmic staining in most of the untreated and HSP90 inhibitor-treated MCF7 cells (Figure 3.7A-C). Neither novobiocin (Figure 3.7B) nor 17-AAG (Figure 3.7C) treatment caused any notable change in the localization of p-β-catenin in MCF7 cells. β- was localized to punctate structures in what appeared to be the perinuclear region in all of the untreated cells (Figure 3.7A, arrow). There was also diffuse cytoplasmic staining of β-catenin in most of the untreated cells (Figure 3.7A), with some localization at what appeared to be the plasma membrane (Figure 3.7A). There was no distinct change in the localization pattern of β-catenin after treatment with novobiocin (Figure 3.7B) or 17-AAG (Figure 3.7C); however it did appear that there was a slight shift in β-catenin to what appeared to be the perinuclear region after novobiocin treatment (Figure 3.7B).

Cross sections of MCF7 cells (Figure 3.7A-C, dotted lines) were used to create signal intensity profiles (Figure 3.7D-F) of p-β-catenin and β-catenin staining. The level of signal intensity for p-β-catenin staining was low in all of the MCF7 cells (Figure 3.7D-F), although it appeared to be slightly higher in what appeared to be the cytoplasmic region in most of the cells (Figure 3.7D-F). Treatment with novobiocin and 17-AAG did not cause any notable change in the distribution pattern of the signal intensities for p-β-catenin (Figure 3.7E and F). The signal intensities for β-catenin staining were highest at what appeared to be the perinuclear region in both untreated (Figure 3.7D) and treated (Figure 3.7E and F) MCF7 cells. There was no notable change in the distribution pattern of β-catenin staining after novobiocin (Figure 3.7E) or 17-AAG treatment (Figure 3.7F).

3.2.2.4 p-β-catenin and HSP90α/β

The signal intensity profiles of p-β-catenin and HSP90α/β staining in MCF7 cells (Figure 3.8A-C) were obtained by taking cross-sections of immunofluorescence merged images of p-β-catenin and HSP90α/β staining (Figure 3.8D-F). The signal intensity profile of HSP90α/β staining was the same as previously described (Section 3.2.2.1) with the signal for HSP90α/β staining being highest in what appeared to be the cytoplasm, with some nuclear staining in the untreated (Figure 3.8A) and treated (Figure 3.8B and C) MCF7 cells. The signal intensity profile for p-β-catenin staining was also the same as previously described (Section 3.2.2.3). The staining patterns of p-β-catenin and HSP90α/β are different to each other for untreated

(Figure 3.8A) and novobiocin treated (Figure 3.8B) MCF7 cells; however they appear similar after treatment with 17-AAG (Figure 3.8C).

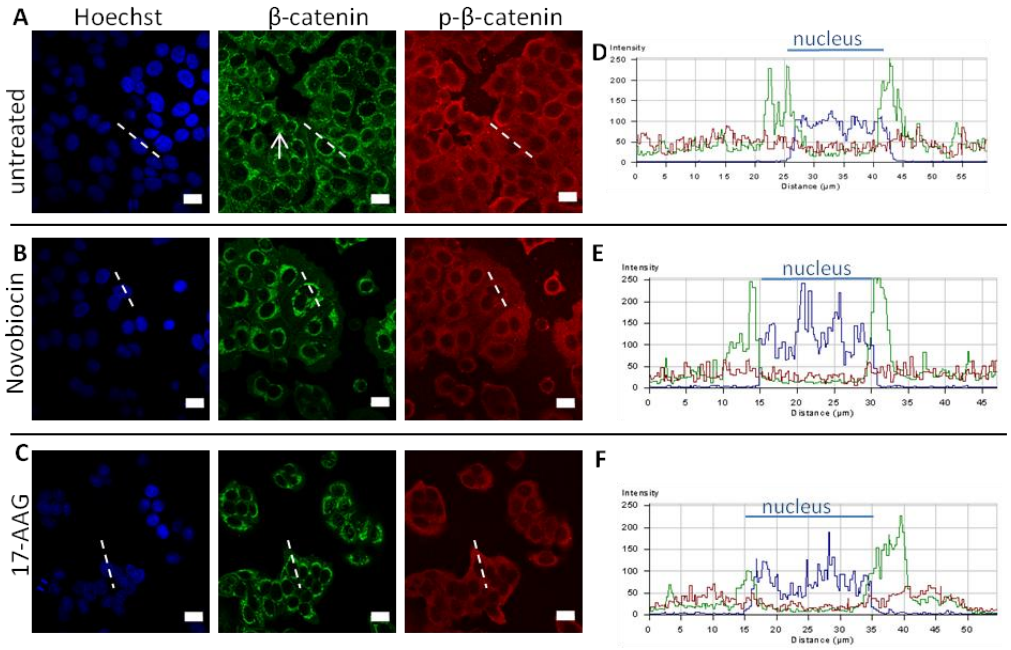

Figure 3.7. Effects of HSP90 inhibition on the localization of p-β-catenin and β-catenin. MCF7 cells were serum-starved for 1 hour prior to 5 hour treatment with inhibitors. Immunofluorescence confocal microscopy images of stained MCF7 cells captured using a Zeiss LSM 510 confocal microscope. A. Untreated MCF7 cells. B. Novobiocin (500 μM) treated MCF7 cells. C. 17-AAG (10 μM) treated MCF7 cells. Hoechst: blue nuclear staining. β-catenin (green) using anti-human β-catenin antibody. p-β-catenin (red) using anti-human p-β-catenin antibody. Cross sections of MCF7 cell representing the staining profiles for: β-catenin for untreated cells (D); novobiocin (500 μM) treated MCF7 cells (E); 17-AAG (10 μM) treated MCF7 cells (F). Profiles were obtained using the program Zeiss LSM Image Browser. The blue line represents Hoechst staining of the nucleus; the green line represents the signaling for β-catenin staining. The red line represents the signaling for p-β-catenin staining. Scale bars represent 20 μm. Dotted line represents cross section of cell used for intensity profile.

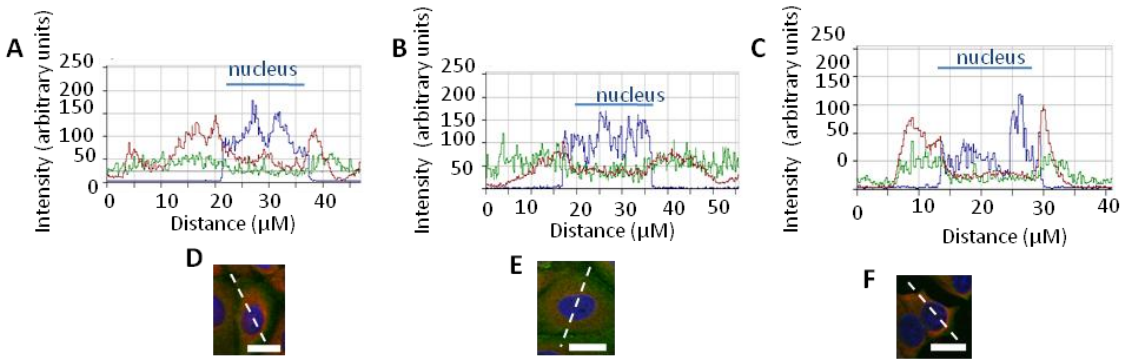

Figure 3.8. Intensity profile studies of the subcellular localization change of p-β-catenin and HSP90α/β in response to HSP90 inhibition. MCF7 cells were serum-starved for 1 hour prior to 5 hour treatment with inhibitors. Immunofluorescence and confocal microscopy images of stained MCF7 cells were captured using a Zeiss LSM 510 confocal microscope. Cross sections of MCF7 cell representing the staining profiles for HSP90α/β for: untreated cells (A); novobiocin (500 μM) treated MCF7 cells (B); and 17-AAG (10 μM) treated MCF7 cells (C). The blue line represents Hoechst staining of the nucleus, the red line represents the signal for HSP90α/β staining and the green line represents the signal for p-β-catenin staining. Confocal microscopy images representing the merged images of HSP90α/β, p-β-catenin and Hoechst of untreated MCF7 cells (D), novobiocin treated MCF7 cells (E) and 17-AAG treated cells (F). Scale bars represent 20 μm. Dotted line represents cross section of cell used for intensity profile**.**

3.3 Discussion

HSP90α/β was found to be localized mainly in the cytoplasm in untreated MCF7 cells which concurs with literature where HSP90α/β is mainly located in the cytoplasm (Borkovich *et al*., 1989; Taherian *et al.*, 2007). As expected, GSK-3β was also localized mainly in the cytoplasm where it could interact with the destruction complex of the Wnt pathway. However, nuclear localization was observed in some of the cells which could be as a result of GSK-3β being involved in the regulation of β-catenin independently of the Wnt destruction complex (Caspi *et al*., 2008). Axin1 was localized throughout the cell at a low concentration which could be due to axin being the limiting factor in the Wnt pathway and thus found at low concentrations (Lee *et al*., 2003). It must be noted, however, that this could also be a result of the primary antibody not being as sensitive as the other antibodies for confocal microscopy.

P-β-catenin was found to be localized in the cytoplasm where it gets targeted for degradation by the destruction complex. Furthermore, high levels of cytoplasmic p-β-catenin have been linked to good clinical outcome in breast cancer patients (Nakopoulou *et al*., 2006). On the other hand, total β-catenin was localized to distinct punctate structures in the cytoplasm (Figure 3.3), close to the nucleus. Studies have shown that β-catenin exists in different subcellular locations within the cell, which include the plasma membrane (Ozawa, 1989), cytoplasm (López-Knowles *et al*., 2010), cytosol or nucleus (Kikuchi, 2000; Morin *et al*., 1999). In normal ducts of myoepithelial cells, β-catenin is localized to the plasma membrane, whilst breast carcinoma cells have both cytoplasmic and plasma membrane localized expression of β-catenin (López-Knowles *et al*., 2010). Kikuchi (2000) identified cytosolic β-catenin to be complexed with the destruction complex, whilst Faux *et al.* (2008) found that punctate structures were the sites of these destruction complexes. Schwarz-Romond *et al*. (2005) recognized these structures as protein assemblies instead of vesicles within the cytoplasm. Again, they found Dsh to be associated with these complexes providing further evidence that these structures are the site of destruction complexes. It can therefore be proposed that in this MCF7 cell line, β-catenin was associated with destruction complexes close to the nucleus.

This study showed that there was possible co-localization between HSP90α/β and GSK-3β (Figure 3.1) which concurs with literature since HSP90α/β is required for the autophosphorylation of GSK-3β (Lochhead *et al*., 2006; Schlange *et al*., 2007). Furthermore,

since the signals of axin1 and HSP90α/β staining did overlap, as did p-β-catenin and HSP90α/β, it is possible that there was some association between HSP90α/β and these proteins. Although β-catenin was localized in distinct punctate structures, quantitative analysis revealed that there was partial co-localization with HSP90α/β indicating a possible association between the two proteins.

When MCF7 cells were treated with HSP90 inhibitors, 17-AAG and novobiocin, very little change occurred in the subcellular localization of GSK-3β (Figure 3.5), β-catenin (Figure 3.7) or p-β-catenin (Figure 3.7), although the morphology of the cells did change with both 17-AAG and novobiocin treatment in most of the cells. Interestingly, a shift of axin1 to what appeared to be the plasma membrane was seen after the MCF7 cells were treated with novobiocin (Figure 3.6B). A possible explanation for this localization change could be that the interaction between HSP90α/β and axin1 was disrupted by novobiocin such that the destruction complex was no longer stabilized by HSP90α/β, and axin1 located to the membrane.

In conclusion, analysis by confocal microscopy revealed that there was a possible association of HSP90α/β with GSK-3β and possibly with axin1 and p-β-catenin since they appeared to share similar subcellular localizations to HSP90α/β. It must be noted, however, that the signal intensities of both axin1 and p-β-catenin were very low therefore no definite conclusion could be drawn from the study. HSP90 inhibition caused a shift in the localization of axin1 which gives further evidence of a possible association between axin1 and HSP90α/β. Although β-catenin had a different localization pattern in comparison to HSP90α/β, there was an overlap of signals. It would therefore be necessary to validate these claims biochemically by performing co-immunoprecipitation studies, which will be described in the next chapter.

Chapter 4: Association of members of the Wnt pathway with HSP90

4.1 Introduction

It is well-known that the Wnt pathway is in a "switched on" state in colon cancer lines due to mutations in the destruction complex (Morin *et al*. 1996; Moon *et al*., 2004). Although mutations within the Wnt pathway in breast cancer have not been identified, other factors, such as sFRP1 downregulation and Dsh upregulation may play a role in aberrantly activating the pathway (Schlange *et al*., 2007). Interestingly, in MCF7 cells, treatment with sFRP1 did not affect the cell proliferation or result in a reduction in active β-catenin levels, nor did knockdown of Dsh have any effect (Schlange *et al*., 2007). These results indicate that in MCF7 cells, some other factor influences the activation of Wnt pathway. It is an interesting study to determine the levels of the proteins involved in the Wnt pathway in both breast cancer and colon cancer to determine if there is a difference. HT29 is a colorectal cancer cell line that is extensively used for research because it has maintained its biologic and physiologic features of normal colorectal epithelial cells (von Kleist *et al*., 1975). In this study, the expression levels of the proteins involved in the Wnt pathway in MCF7 and HT29 cells were determined by Western Blot analysis to ensure that the proteins were detectable prior to performing immunoprecipitation studies.

The association of HSP90 with members of the full Wnt pathway needs to be established. The previous study (section 3) gave preliminary evidence that a possible association between HSP90 and GSK-3β, axin1 and p-β-catenin since they were localized to similar positions within the cell. To further verify these associations in MCF7 cells, co-immunoprecipitation experiments were performed to isolate complexes containing Hsp90α/β, β-catenin, GSK-3β and axin1. The proteins were resolved by SDS-PAGE and Western Blot analysis was performed to identify the complexed proteins. To ensure that each immunoprecipitation had worked, the immunoprecipitation samples were subjected to Western analysis for detection of the expected protein, before analysis of co-precipitated proteins.

4.2 Results

4.2.1 Protein expression levels of MCF7 in comparison to HT29 cells

Equal numbers of MCF7 and HT29 cells were loaded on the SDS gel by loading the same quantity of lysate (see Section 2.2.1). Western blot analysis of the proteins expressed indicated that Akt (Figure 4.1A) was expressed at a slightly higher level in MCF7 cells in comparison to HT29 cells, whilst HSP90α/β expression levels appeared to be similar between

the 2 cell lines (Figure 4.1B). Furthermore, GSK-3β also appeared to be expressed at a similar level in both MCF7 and HT29 cells (Figure 4.1C). The higher molecular weight protein of axin1 appeared to be expressed at a higher level in HT29 cells in comparison to MCF7 cells (Figure 4.1D). A lower molecular weight signal was identified for axin1 which could be a degradation product or truncated form of the protein. HT29 cells expressed higher levels of both total β-catenin (Figure 4.1E, H) and p-β-catenin (Figure 4.1F) in comparison to MCF7 cells (Figure 4.1E and F, M).

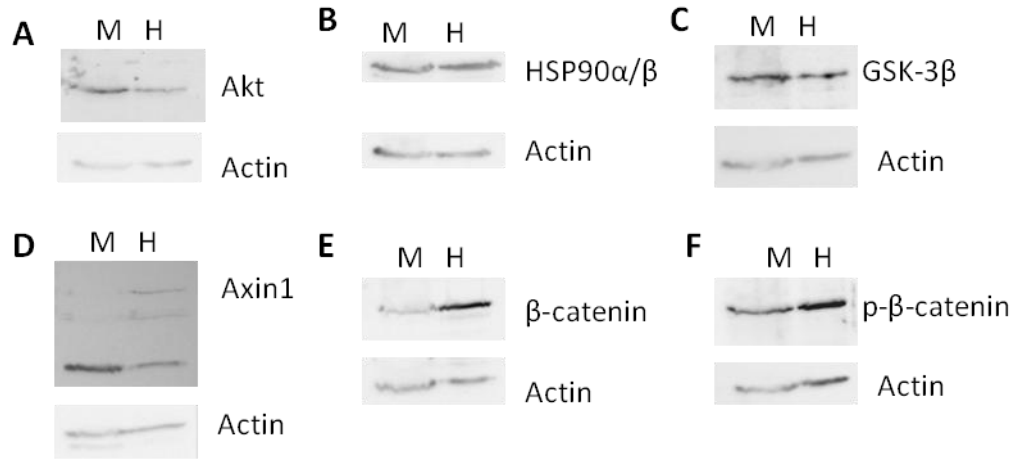

Figure 4.1 Wnt pathway is switched on in colorectal cancer line. Western analysis of cell lysates of MCF7 (M) HT29 cell lysates (H). Equivalent number of cells was loaded per lane. A. Detection of Akt (56 kDa) using anti-human Akt antibody. B. Detection of HSP90α/β (90 kDa) using anti-human HSP90α/β antibody. C. Detection of GSK-3β (43 kDa) using anti-human GSK-3β antibody. D. Detection of axin1 (95 kDa) using anti-human axin1 antibody. E. Detection of β-catenin (94 kDa) using anti-human β-catenin antibody. F. Detection of p-β-catenin (94 kDa) using anti-human p-β-catenin antibody. Actin was used as the loading control.

4.2.2 Association of members of the Wnt pathway with HSP90 by co-immunoprecipitation

Immunoprecipitation using anti-HSP90α/β antibodies was successful (Figure 4.2A, lane 4) since a signal corresponding to HSP90α/β (Figure 4.2A, lane 1) was identified in the immunoprecipitation sample (Figure 4.2A, lane 4). This signal was not detected in either of the negative controls (Figure 4.2A, lane 2 and 3) which meant that HSP90α/β did not bind non-specifically to the beads. Heavy chain (Figure 4.2, Hc) and light chain (Figure 4.2A, Lc) IgG bands were identified in the negative control and immunoprecipitation sample (Figure 4.2A, lane 3 and 4).

Immunoprecipitation using β-catenin antibodies was also successful since β-catenin was identified in the immunoprecipitation sample (Figure 4.2B, lane 4) and positive control of free lysate (Figure 4.2B, lane 1) but not in either of the negative controls (Figure 4.2B, lane 2

and 3). Heavy chain (Figure 4.2, Hc) and light chain IgG bands (Figure 4.2A, Lc) were identified in the negative control and immunoprecipitation sample (Figure 4.2B, lane 3 and 4).

Axin1 was detected as 2 bands in the positive control of free MCF7 lysate (Figure 4.2C, lane 1), with the lower molecular weight band appearing darker than the higher molecular weight band. The higher molecular weight band did not appear in the immunoprecipitation sample (Figure 4.2C, lane 4), and the lower molecular weight band may have been masked by the heavy chain IgG (Figure 4.2C, lane 4).

Although GSK-3β was identified in the free MCF7 lysate (Figure 4.2D, lane 1), it was difficult to identify whether GSK-3β was successfully isolated by the immunoprecipitation experiment since the heavy chain IgG signal potentially masked the GSK-3β signal (Figure 4.2D, lane 4). The negative control (GSK-3β antibody coupled to protein A/G-PLUS beads only) was not performed in this experiment; therefore the size of the heavy chain IgG could not be confirmed.

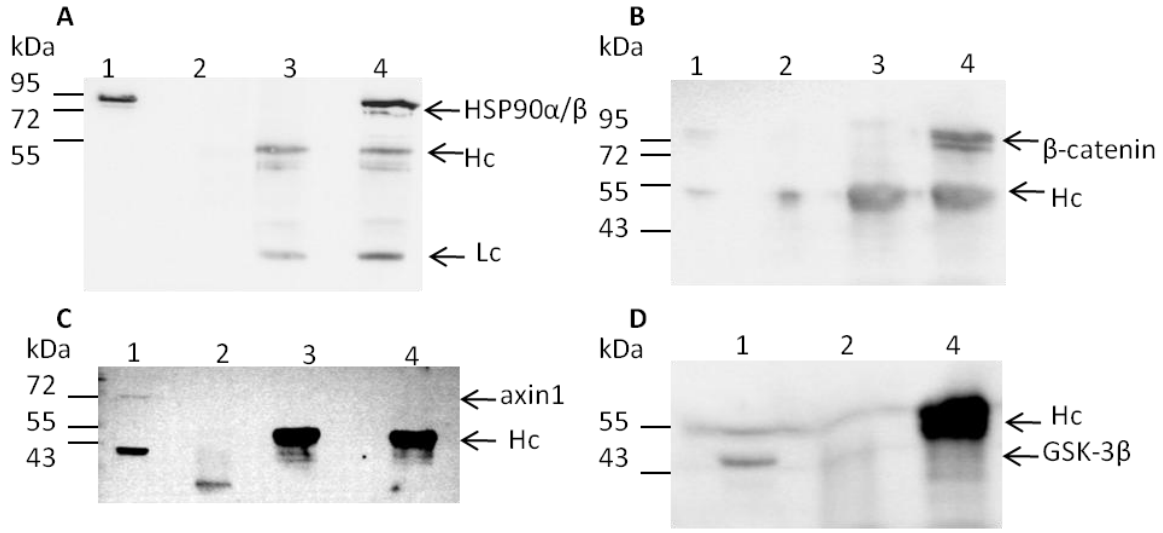

Figure 4.2. Validation of antibodies to Wnt pathway proteins and HSP90 in IP assays. Western Blot analyses of immunoprecipitation samples carried out in MCF7 lysates. A. Western detection of HSP90α/β after immunoprecipitation using an anti-human HSP90α/β antibody. B. Western detection of β-catenin after immunoprecipitation using an anti-human β-catenin antibody. C. Western detection of axin1 after immunoprecipitation using an anti-human axin1 antibody. D. Western detection of GSK-3β after immunoprecipitation after using an anti-human GSK-3β antibody. Lane 1: free MCF7 lysate. Lane 2: negative control: lysate subjected to immunoprecipitation without antibody. Lane 3: immunoprecipitation antibody and protein A/G plus agarose beads without lysate. Lane 4: immunoprecipitation sample.

To determine whether HSP90 was complexed to β-catenin, the samples of both HSP90α/β immunoprecipitation and β-catenin immunoprecipitation were resolved by SDS-PAGE and Western detection was performed for β-catenin in the HSP90α/β immunoprecipitation sample (Figure 4.3A), and HSP90α/β in the β-catenin immunoprecipitation sample (Figure 4.3B).

A signal was detected in the immunoprecipitation sample that corresponded to the same molecular weight as total β-catenin (Figure 4.3A, lane 4 and lane 1). A faint signal of the same molecular weight was also detected in the negative control (Figure 4.3A, lane 2) indicating that there was some non-specific binding of β-catenin to the protein A/G PLUS agarose beads. The signal in the immunoprecipitation sample (Figure 4.3A, lane 4) did, however, appear to be darker than that in the negative control (Figure 4.3A, lane 2). When the anti-human β-catenin antibody was used to immunoprecipitate the complex in MCF7 cells, followed by Western detection for HSP90α/β, a clean signal was detected in the immunoprecipitation sample (Figure 4.3B, lane 4) which corresponds to the same molecular weight as HSP90α/β in the positive control (Figure 4.3B, lane 1). No signal of the same molecular weight was detected in either of the negative controls (Figure 4.3B, lanes 2 and 3).

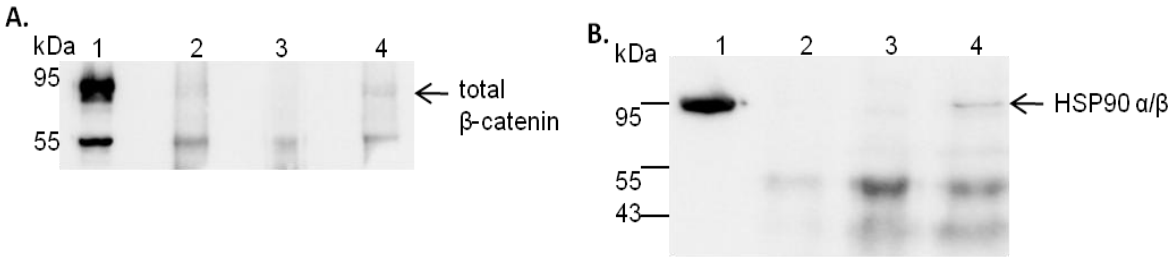

Figure 4.3. HSP90α/β and β-catenin co-immunoprecipitate. A. Western detection for total β-catenin in HSP90α/β immunprecipitate. B. Western detection for HSP90α/β in β-catenin immunoprecipitate. Lane 1: free MCF7 lysate. Lane 2: negative control: MCF7 lysate subjected to immunoprecipitation without antibody. Lane 3: immunoprecipitation antibody and protein A/G PLUS agarose beads without lysate. Lane 4: immunoprecipitation sample using antibody and MCF7 lysate.

Axin1 appeared to co-immunoprecipitate with HSP90α/β since a signal for axin was detected in the HSP90α/β immunoprecipitation sample (Figure 4.4A, lane 4) and HSP90α/β was detected in the axin immunoprecipitation sample (Figure 4.4C, lane 4). No signals of the same molecular weight as HSP90 (approximately 90 kDa) of axin1 (approximately 95 kDa) were detected in either of the negative controls (Figure 4.4A, lane 2 and 3 and Figure 4.4C, lane 2 and 3) indicating that both HSP90α/β and axin1 were isolated by the relevant immunoprecipitation antibody. P-β-catenin was also detected in the HSP90α/β immunoprecipitate (Figure 4.4B, lane 4) and axin immunoprecipitate (Figure 4.4D, lane 4). A

signal of the same intensity at the same molecular weight (approximately 94 kDa) was not identified in either of the negative controls for both immunoprecipitation experiments (Figure 4.4B and D, lanes 2 and 3).

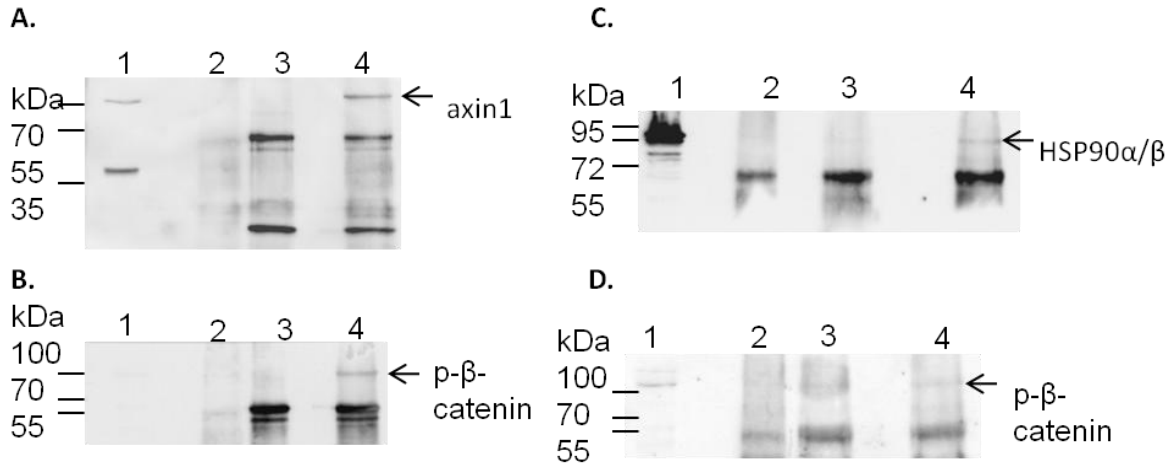

Figure 4.4. HSP90α/β co-immunoprecipitates with axin1 and p-β-catenin. A. Western detection for axin1 in HSP90α/β immunoprecipitation. B. Western detection for p-β-catenin ($pSer^{33}/pSer^{37}$) in HSP90α/β immunoprecipitate. C. Western detection of HSP90α/β in axin1 immunoprecipitate. D. Western detection of p-β-catenin ($pSer^{33}/pSer^{37}$) in axin1 immunoprecipitate. Lane 1. Free MCF7 lysate. Lane 2. Negative control of MCF7 lysate subjected to immunoprecipitation without the antibody. Lane 3: immunoprecipitation antibody and protein A/G PLUS-agarose beads. Lane 4. Immunoprecipitation sample using antibody and MCF7 lysate. Arrows point towards the protein of interest.

To further identify whether HSP90α/β was in a common complex with GSK-3β in MCF7 cells, immunoprecipitation using anti-human GSK-3β antibodies with protein A/G PLUS agarose was carried out and the samples were probed for HSP90α/β (Figure 4.5). The same immunoprecipitation experiment was carried out using anti-human HSP90α/β antibodies instead of anti-human GSK-3β antibodies to isolate the complex, but no conclusions could be made from the Western detections for GSK-3β since the heavy chain IgG masked any possible GSK-3β signal in the immunoprecipitation sample.

A signal corresponding to the same molecular weight as HSP90α/β (about 95 kDa) appeared in the immunoprecipitation sample (Figure 4.5, lane 3) and free lysate sample (Figure 4.5, lane 1), but did not appear in the negative control (Figure 4.5, lane 2).

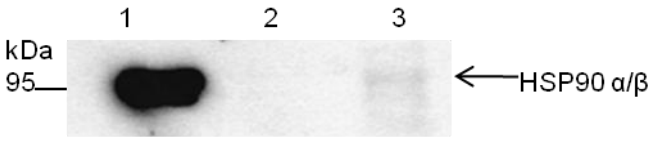

Figure 4.5. Potential co-immunoprecipitation of GSK-3β and HSP90α/β. Immunoprecipitation was performed using anti-human GSK-3β antibodies with protein A/G PLUS agarose beads. Western detection for HSP90α/β using an anti-human HSP90α/β antibody. Lane 1. Free MCF7 lysate. Lane 2. MCF7 lysate subjected to immunoprecipitation without antibody. Lane 3. Immunoprecipitate sample using antibody and MCF7 lysate.

To test whether the anti-human GSK-3β antibody was indeed working efficiently in isolating complexes, and to overcome any possible signals being masked by the heavy chain IgG, the immunoprecipitation experiment was performed using the Dynal Bead Separations Dynabeads co-immunoprecipitation kit (Dynal Bead Separations). This kit uses antibodies coupled to Dynabeads® M-270 Epoxy instead of protein A/G PLUS agarose to isolate any possible complexes. The antibody is thus coupled permanently to the Dynabeads® M-270 Epoxy, and will not dissociate, therefore preventing the detection of the heavy and light chain IgG. The anti-human GSK-3β antibody was coupled to the Dynabeads® M-270 Epoxy beads according to manufacturer's instructions, and the resulting eluted complexes were resolved by SDS-PAGE for Western blot analysis (Figure 4.6).

It appeared that the anti-human GSK-3β antibody coupled to Dynabeads® M-270 Epoxy successfully isolated GSK-3β (Figure 4.6A, lane 3). Although p-β-catenin co-immunoprecipitated with GSK-3β (Figure 4.6B, lane 3), it appeared that the amount of p-β-catenin detected in the immunoprecipitation sample (Figure 4.6B, lane 3) was much less than that in the free lysate (Figure 4.6B, lane 1).

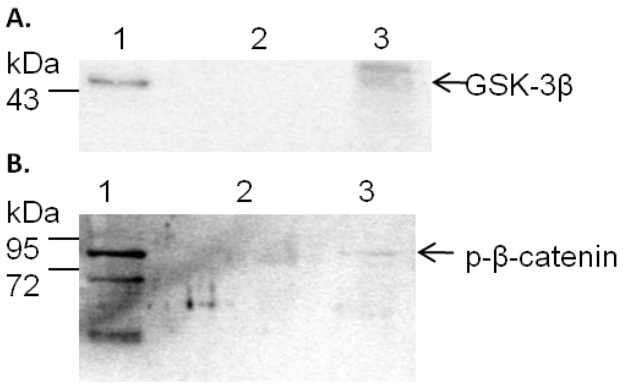

Figure 4.6. Potential co-immunoprecipitation of GSK-3β and p-β-catenin. GSK-3β immunoprecipitation was performed with GSK-3β antibody coupled to Dynabeads® M-270 Epoxy. A. Western detection for human GSK-3β. B. Western detection for p-β-catenin. Lane 1. Free MCF7 lysate. Lane 2. Negative control of MCF7 lysate subjected to immunoprecipitation with BSA coupled to Dynabeads® M-270 Epoxy instead of antibody. Lane 4. Immunoprecipitation sample.

4.3 Discussion

The proteins, HSP90α/β, axin1, total β-catenin and p-β-catenin were successfully detected in both MCF7 cells and HT29 cells by Western Blot analysis (Figure 4.1), thus allowing for further studies on these proteins to be carried out. When a comparison of these protein expression levels was made between the 2 cells lines, it was found that HT29 cells had higher

levels of both total β-catenin and p-β-catenin compared to MCF7 cells. Since both cell lines have an activated Wnt pathway (Morin *et al*., 1996; Yang *et al*., 2006; Schlange *et al*., 2007), it was interesting to note that HT29 cells had a higher expression level of both total β-catenin and its phosphorylated form. This was unexpected since p-β-catenin gets targeted for ubiquitination and degradation and thus the levels should be low. A possible explanation for this is that although the Wnt pathway may be aberrantly activated in the HT29 cells, β-catenin may still be getting phosphorylated, but the phosphorylated form is being prevented from being degraded. In contrast to this, another explanation could be that although there might be a mutation in the *APC* gene, which is associated with colorectal cancer (Yang *et al*., 2006), the overexpression of axin in the absence of APC in HT29 cells has allowed for the destruction complex's activity to return to normal (reviewed in Clevers, 2006). Furthermore, it can be said that cancer cells are heterogeneous thus pathways are constantly being stimulated and inhibited at different time periods, thus a certain time point study of protein expression levels might not be indicative of what the protein levels are throughout the cell cycle. In addition to this, the qualitative Western analysis did not allow for the proportion of β-catenin to p-β-catenin to be determined nor absolute levels to be identified. This was because the antibodies might have different sensitivities to the proteins that they detect therefore no comparative analysis could be done. Although a qualitative analysis was performed on the protein expression levels, a quantitative analysis comparing the protein expression levels between HT29 and MCF7 cells could not be performed. This was due to different protein amounts (as determined by Ponceau staining) being loaded for the two cell lines despite loading the same number of cells. These data confirmed that the Wnt pathway proteins were detectable by Western Analysis in MCF7 cells and thus made the cell line viable to continue with further studies to identify possible associations of the proteins with HSP90.

Using co-immunoprecipitation analysis of HSP90α/β and β-catenin, it was found that there was possible association between the two proteins. By isolating β-catenin using an antibody against HSP90α/β and performing the vice versa with a β-catenin antibody and isolating HSP90α/β (Figure 4.3), it can be said that HSP90α/β and β-catenin appeared to be associated in a common complex. Although there was apparent non-specific binding of β-catenin to the protein A/G PLUS agarose beads (Figure 4.3A, lane 2), densitometric analysis revealed that the β-catenin isolated by co-immunoprecipitation using anti-HSP90α/β (arbitrary unit: 1) was more than the β-catenin bound non-specifically to the beads (arbitrary unit: 0.8) (See

Appendix A4). Furthermore, since the reverse IP could be performed, this association between HSP90α/β and β-catenin was specific.

Co-immunoprecipitation, using an anti-HSP90α/β antibody, successfully isolated p-β-catenin (Figure 4.4B), thus giving preliminary evidence that p-β-catenin and HSP90α/β are associated in a common complex. This association was not a result of non-specific binding of the p-β-catenin to the protein A/G PLUS agarose beads since no signal was detected in either of the negative controls (Figure 4.4B, lane 2 and 3).

A possible association between axin1 and HSP90α/β was identified by co-immunoprecipitation (Figure 4.4). Axin1 was successfully isolated by immunoprecipitation using anti-HSP90α/β antibodies (Figure 4.4A); and the reverse was also seen with HSP90α/β being isolated by anti-axin1 antibodies (Figure 4.4C). This therefore revealed that for the first time, HSP90α/β has found to occur in a common complex with axin1. Furthermore, anti-axin1 and anti-HSP90α/β antibodies successfully isolated p-β-catenin, a by-product of the Wnt destruction complex (Clevers, 2006). It can thus be proposed that HSP90α/β is potentially involved in the destruction complex in the Wnt pathway.

A possible association was shown between GSK-3β and HSP90α/β by co-immunoprecipitation since HSP90α/β was isolated using an anti-GSK-3β antibody (Figure 4.5). The signal detected in the immunoprecipitation sample (Figure 4.5, lane 3) corresponded to the same molecular weight as HSP90α/β in the free lysate (Figure 4.5, lane 1), indicating that HSP90α/β was isolated by GSK-3β antibodies. This signal was not present in the negative control (Figure 4.5, lane 2), therefore was not a result of HSP90α/β binding non-specifically to the beads. It was difficult to identify whether GSK-3β was isolated from the MCF7 lysate by immunoprecipitation using anti-human GSK-3β antibodies, since the signal (43 kDa) was potentially masked by the signal for the heavy chain IgG (55 kDa) (Figure 4.2D, lane 4).

Using anti-human GSK-3β antibodies coupled to Dynabeads® M-270 Epoxy, p-β-catenin was successfully isolated (Figure 4.6B). However, the signal for p-β-catenin was faint, indicating that the level of p-β-catenin isolated was low. No signal was detected for HSP90α/β in the immunoprecipitation sample using anti-human GSK-3β antibodies coupled to Dynabeads® M-270 Epoxy (data not shown). A possible explanation for this is that the association between HSP90α/β and GSK-3β was only transient, therefore only small amounts

of HSP90α/β co-immunoprecipitated with GSK-3β which were too low to be detected by Western blot analysis, especially since the large volume of elution buffer required by the Dynal Bead Separations Dynabeads co-immunoprecipitation kit to elute the complexed proteins would have reduced the concentration of HSP90α/β to untraceable amounts. It would therefore be necessary to concentrate the IP fractions so that detection of signals could be performed. Another explanation could be that the association between GSK-3β and HSP90 was unstable, as has been reported of HSP90 with other clients (Arlander *et al*., 2006). This means the association between HSP90 and GSK-3β could not withstand the lysis or washing conditions that were performed during immunoprecipitation.

In conclusion, the protein expression study of the Wnt pathway proteins confirmed that β-catenin, p-β-catenin, axin1, GSK-3β and HSP90α/β were all detectable by Western analysis in MCF7 cells, thus allowing for further biochemical experiments to be performed. The co-immunoprecipitation data gave the first preliminary evidence that HSP90α/β is associated with axin1, p-β-catenin, β-catenin and GSK-3β. In the next chapter, HSP90 inhibition studies, will be used to confirm the possible association of HSP90α/β with the Wnt destruction in MCF7 cells.

Chapter 5: Effects on the Wnt pathway proteins by HSP90 inhibition

5.1 Introduction

Numerous HSP90 inhibitors have been investigated for their potential therapeutic uses in cancer. The HSP90 client oncoproteins that are being targeted for drug interventions include HER-2, Akt, polo-like kinase, EGFR, Src, Abl, c-Met and RAF-1 (Sreedhar *et al*., 2004). HSP90 inhibitors have been found to have a higher affinity for HSP90 in tumour cells, which could be due to HSP90 existing mainly in the complexed form in tumour cells (Kamal *et al*., 2003), and the HSP90 inhibitors preferentially associating with the HSP90 chaperone complex. HSP90 inhibitors not only have clinical uses, but also provide excellent research tools to study the HSP90-client and co-chaperone activity..

5.1.1 Geldanamycin and geldanamycin analogues

Geldanamycin, a naturally occurring antibiotic, is also an ansamycin with a benzoquinone moiety that makes it selective for HSP90 (Figure 5.1) (Zhang and Burrows, 2004). Geldanamycin was initially identified as an anti-tumour agent when it could inhibit the phosphorylation of v-Src, thus reversing the v-Src transformation in cells (Uehara *et al*., 1986). It was later discovered that geldanamycin binds to the ATP-binding pocket of HSP90 (Prodromou *et al*., 1997; Roe *et al*., 1999), preventing the mature HSP90 complex from forming and thus linking it to the degradation of the client proteins previously shown by Whitesell *et al*. (1994). Although geldanamycin showed promising anti-tumour activity, it was quite hepatotoxic in animals, preventing its further use in humans (Supko *et al*., 1995). This therefore lead to the development of the geldanamycin derivative, 17-AAG, which is a geldanamycin analog that has an allyl amino group instead of the methoxy group in the position 17 (Figure 5.1) (Goetz *et al*., 2003). 17-AAG was less hepatotoxic in animals than geldanamycin, but had similar antitumour activity (Schulte and Neckers, 1998; Workman *et al*., 2007). It has an IC_{50} value of about 128 nM for MCF7 cells (Maroney *et al*., 2006). 17-AAG is being investigated in clinical trials in the USA and the United Kingdom (Goetz *et al*., 2003). Other inhibitors include GA derivative (17-dimethylaminoethylamino-17-demethoxygeldanamycin (17-DMAG) and hydroquinone hydrochloride analogue of 17-AAG, 17-allylamino-17-demethoxygeldanamycin hydroquinone hydrochloride (IPI-504) (Workman *et al*., 2007). 17-DMAG is more water soluble than 17-AAG and has entered Phase 1 and 2 clinical testing with lower toxicity in comparison to 17-AAG (Hollingshead *et al*., 2005). IPI-504 is in Phase 1 and 2 clinical trials for treating chemotherapy-resistant cancer (Peng *et al*., 2007). Radicicol, a macrocyclic natural antibiotic, also competes for the

N-terminal HSP90 ATP pocket (Roe *et al*., 1999). It is however chemically and metabolically unstable and therefore had anti-cancer activity *in vitro* but not *in vivo* (Pearl *et al*., 2008). Derivatives are currently being investigated (Li *et al*., 2009).

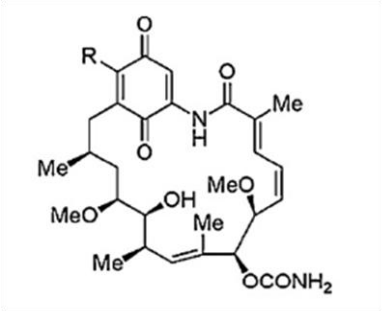

Geldanamycin R = OCH_3
17-AAG R = $NHCH_2CH{=}CH_2$
17-DMAG R = $NHCH_2CH_2N(CH_3)_2$

Figure 5.1. Chemical structure of geldanamycin and its derivatives 17-Allylamino-17-demethoxygeldanamycin (17-AAG), and 17-dimethylaminoethylamino-17- demethoxygeldanamycin (17-DMAG) (Li *et al*., 2009).

5.1.2 Novobiocin

Novobiocin is a coumarin antibiotic (Figure 5.2) that binds weakly to the ATP binding site of HSP90 at its C-terminus, disrupting the HSP90 chaperone complex and resulting in the degradation of HSP90 clients (Marcu *et al*., 2000). Inhibition with novobiocin had similar effects as N-terminal inhibitors, such as the degradation of client proteins, HER-2, RAF-1 and p53 (Marcu *et al*., 2000; Allan *et al*., 2006; McConkey and Zhu, 2008). The IC_{50} of novobiocin for MCF7 cells is quite high (260 μM) (Radanyi *et al*., 2008) therefore for an effect to be seen, a high concentration would be required *in vivo,* which could have detrimental effects on other pathways for the normal functioning of the cell. Other related coumarin analogs include chlorobiocin and coumermycin A1 which bind to the HSP90 C-terminus and have better activity in comparison to novobiocin (Marcu *et al*., 2000; Burlison and Blagg, 2006).

In this study, the HSP90 inhibitors, geldanamycin, 17-AAG and novobiocin were used to treat MCF7 to identify whether HSP90 inhibition would have an effect on the expression levels of the Wnt proteins, β-catenin, axin1 and GSK-3β. The data presented in this chapter will provide further insight into the associations that have already been identified (Chapter 3 and 4) between HSP90α/β and these Wnt pathway proteins.

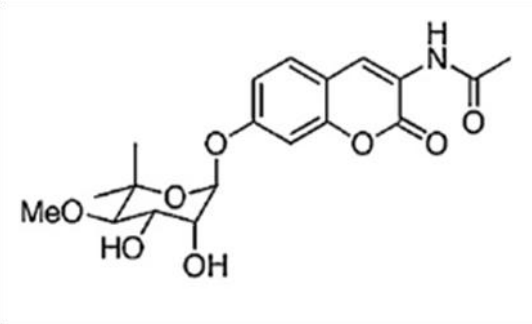

Figure 5.2. Chemical structure of novobiocin (Li *et al*., 2009).

5.2 Results

5.2.1 Determination of HSP90 protein expression levels by inhibition

5.2.1.1 Geldanamycin and 17-AAG inhibition

A range of geldanamycin and 17-AAG concentrations were used to treat MCF7 cells (Figure 5.3A and B) for 24 hours and 72 hours respectively. No treatment (Figure 5.3A, 0 and Figure 5.3B, 0) was used as the control in both experiments. In addition to this, cells treated with media supplemented with DMSO, were also used as a control in geldanamycin treatment (Figure 5.3A, DMSO).

When MCF7 cells were treated with geldanamycin and 17-AAG (Figure 5.3), little or no change occurred in the HSP90α/β expression levels with increasing concentrations of both geldanamycin (Figure 5.3A) and 17-AAG (Figure 5.3B).

Figure 5.3. HSP90α/β expression levels in MCF7 cells treated with 17-AAG and geldanamycin. A. Western detection for HSP90α/β in geldanamycin treated MCF cells. B. Western detection for HSP90α/β in 17-AAG treated MCF7 cells. Actin was used as the loading control. Control cells were treated in normal growth media (0) or media containing only DMSO (DMSO), in the absence of 17-AAG or geldanamycin.

5.2.1.2 Novobiocin

MCF7 cells were treated with increasing concentrations of novobiocin (Figure 5.4, 100 µM, 260µM, 500µM) for 24 hours. No treatment (Figure 5.4, 0) was used as the control. Treatment of MCF7 cells with increasing concentrations of novobiocin resulted in a slight increase in HSP90α/β (Figure 5.4) at 100 µM novobiocin concentration, whilst the other

concentrations, 260 and 500 μM had expression levels similar to no treatment, 0 μM. It may therefore be concluded that no apparent change in HSP90α/β expression occurred after novobiocin treatment.

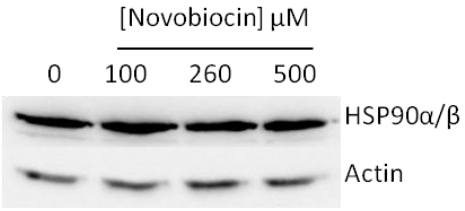

Figure 5.4. HSP90α/β expression levels in MCF7 cells treated with novobiocin. Western detection for HSP90α/β in novobiocin treated MCF cells. Actin was used as the loading control. Control cells were treated in normal growth media in the absence of novobiocin (0).

5.2.2 Effect of HSP90 inhibition on client proteins

The effects of geldanamycin, 17-AAG and novobiocin were tested on known client proteins STAT3, p-STAT3, and Akt, so as to establish an experimental framework from which to test if β-catenin, p-β-catenin, GSK-3β and axin1 were client proteins. The client proteins have previously been found to have decreased expression levels when treated with HSP90 inhibitors such as geldanamycin (Basso *et al*., 2002A and B; Sato *et al*., 2003). HSP90 stabilizes its client proteins so that they can be activated (Sato *et al*., 2003). It is involved in the activation of client proteins by bringing them in contact with their kinases (Fujita *et al*., 2002). Therefore, disruption of this association by geldanamycin, 17-AAG or novobiocin would cause a decrease in the phosphorylated, active forms of the client proteins.

5.2.2.1 STAT3

5.2.2.1.1 Total STAT3

A range of geldanamycin and 17-AAG concentrations were used to treat MCF7 cells (Figure 5.5A and B) for 24 hours and 72 hours respectively. No treatment (Figure 5.5A, 0 and Figure 5.5B, 0) was used as the control in both experiments. In addition to this, cells treated with media supplemented with DMSO were also used as a control in geldanamycin treatment (Figure 5.5A, DMSO).

When MCF7 cells were treated with geldanamycin, a decrease in the level of STAT3 expression was seen at the higher concentrations of geldanamycin (Figure 5.5A); however this decrease was very slight for 1 and 10 μM geldanamycin when normalized to actin

(Appendix, Figure A4.1A). On the other hand, there was very little or no change in the STAT3 levels with increasing concentrations of 17-AAG (Figure 5.5B).

MCF7 cells were treated with increasing concentrations of novobiocin (Figure 5.6, 100 μM, 260 μM, 500 μM) for 24 hours. No treatment (Figure 5.6, 0) was used as the control. There was a decrease in the expression of STAT3 with increasing concentrations of novobiocin (Figure 5.6). Although less protein was loaded in lane 4 and 5 (Figure 5.6, 260 and 500 μM concentrations), the densitometric analysis confirmed that there was an overall decrease in STAT3 with increasing novobiocin concentrations (Appendix, Figure A4.1C).

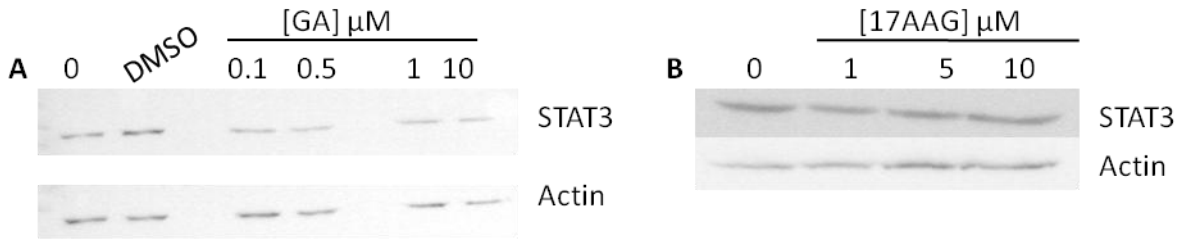

Figure 5.5. Total STAT3 expression levels in MCF7 cells treated with 17-AAG and geldanamycin. A. Western detection for STAT3 in geldanamycin treated MCF cells. B. Western detection for STAT3 in 17-AAG treated MCF7 cells. Actin was used as the loading control. Control cells were treated in normal growth media (0) or media containing only DMSO (DMSO), in the absence of 17-AAG or geldanamycin.

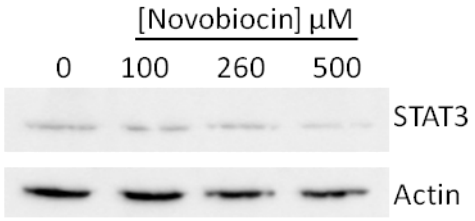

Figure 5.6. Total STAT3 expression levels in MCF7 cells treated with novobiocin. Western detection for STAT3 in novobiocin treated MCF cells. Actin was used as the loading control. Control cells were treated in normal growth media in the absence of novobiocin (0)**.**

5.2.2.1.2 P-STAT3

MCF7 cells were exposed to increasing concentrations of 17-AAG and novobiocin for 72 and 24 hours respectively (Figure 5.7 and 5.8). No treatment (Figure 5.7, 0) was used as the control. The relative levels of p-STAT3 were analyzed by Western blot analysis of total protein lysates after the 17-AAG treatments (Figure 5.7) and novobiocin (Figure 5.8) treatments. There was a decrease in the p-STAT3 signal at 10 μM 17-AAG (Figure 5.7A), which was also shown when the densitometric analysis was performed (Appendix, Figure A4.3).

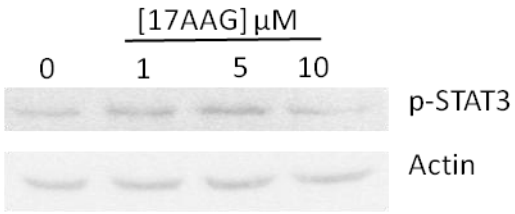

Figure 5.7. p-STAT3 expression levels in MCF7 cells treated with 17-AAG. Western detection for p-STAT3 in 17-AAG treated MCF7 cells. Actin was used as the loading control. No Control cells were treated in normal growth media (0) or media containing only DMSO (DMSO), in the absence of 17-AAG.

The level of p-STAT3 decreased with increasing concentration of novobiocin (Figure 5.8A), with 260 and 500 µM novobiocin causing more of a decrease in the p-STAT3 than 100 µM (Figure 5.8B).

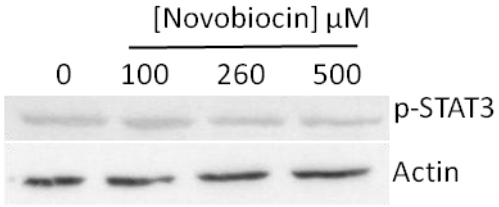

Figure 5.8. P-STAT3 expression levels in MCF7 cells treated with novobiocin. Western detection for STAT3 in novobiocin treated MCF cells. Actin was used as the loading control. Control cells were treated in normal growth media in the absence of novobiocin (0)**.**

5.2.2.2 Akt

Akt is another client protein that was used as a control to test the effects of the HSP90 inhibitors on client proteins (Figure 5.9). HSP90 binds to the active form of Akt, allowing for its phosphorylation (Basso *et al*., 2002A and 2002B). Inhibition of HSP90 by geldanamycin and other derivatives results in a decrease in Akt activity and protein expression as shown by previous studies (Basso *et al*., 2002A and B).

There was not much change in the expression of Akt with 17-AAG treatment (Figure 5.9). On the other hand there was a decreasing trend in the Akt expression level with increasing concentrations of novobiocin (Figure 5.10).

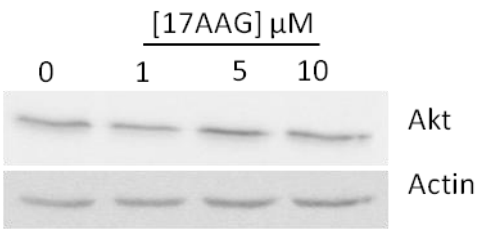

Figure 5.9. Akt expression levels in MCF7 cells treated with 17-AAG. A. Western detection for Akt in 17-AAG treated MCF7 cells. Actin was used as the loading control. Control cells were treated in normal growth media (0) or media containing only DMSO (DMSO), in the absence of 17-AAG.

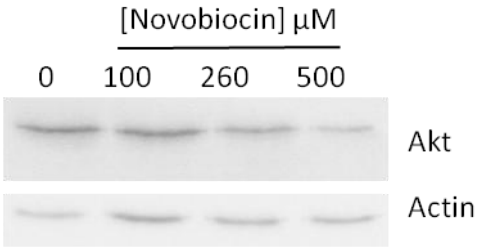

Figure 5.10. Akt expression levels in MCF7 cells treated with novobiocin. A. Western detection for Akt in novobiocin treated MCF cells. Actin was used as the loading control. Control cells were treated in normal growth media in the absence of novobiocin (0).

5.2.2.3 GSK-3β

Different concentrations of geldanamycin and 17-AAG were used to treat MCF7 cells (Figure 5.11A and B) for 24 hours and 72 hours respectively. No treatment (Figure 5.11A, 0 and Figure 5.11B, 0) was used as the control in both experiments. In addition to this, cells treated with media supplemented with DMSO were also used as a control in geldanamycin treatment (Figure 5.11A, DMSO).

Treatment with geldanamycin resulted in a decrease in GSK-3β expression at high concentrations (Figure 5.11A, 10 μM concentration). HSP90-induced inhibition by 17-AAG in MCF7 cells did not result in a notable change in the expression levels of GSK-3β (Figure 5.11B).

After treatment of MCF7 cells with varying concentrations of novobiocin, there was a decrease in the expression level of GSK-3β at the higher concentrations (Figure 5.12, 500 μM).

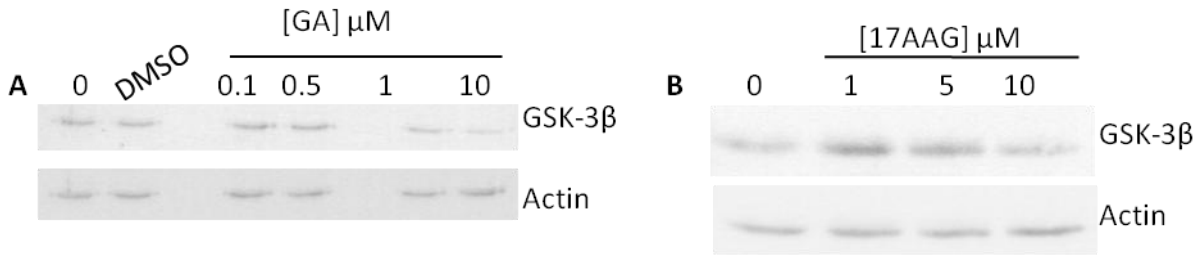

Figure 5.11. GSK-3β expression levels in MCF7 cells treated with 17-AAG and geldanamycin. A. Western detection for GSK-3β in geldanamycin treated MCF cells. B. Western detection for GSK-3β in 17-AAG treated

MCF7 cells. Actin was used as the loading control. Control cells were treated in normal growth media (0) or media containing only DMSO (DMSO), in the absence of 17-AAG or geldanamycin.

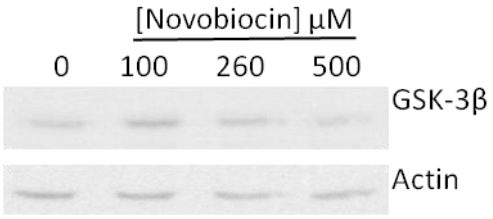

Figure 5.12. GSK-3β expression levels in MCF7 cells treated with novobiocin. Western detection for GSK-3β in novobiocin treated MCF cells. Actin was used as the loading control. Control cells were treated in normal growth media in the absence of novobiocin (0).

5.2.3 β-catenin

There is preliminary evidence that HSP90 and total β-catenin associated by co-immunoprecipitation (Chapter 4, Section 4.2.2); therefore exposure of MCF7 cells to HSP90 inhibitors could have an effect on the protein expression level of β-catenin.

MCF7 cells were treated with increasing concentrations of geldanamycin (Figure 5.13A) and 17-AAG (Figure 5.13B). No treatment (Figure 5.13, lane 0) and media supplemented with DMSO (Figure 5.13A, DMSO) were used as the controls. Treatment with geldanamycin (Figure 5.13A) and 17-AAG (Figure 5.13B) did not decrease the level of total β-catenin, and seemed to cause a very slight increase in protein expression level at the higher concentration of 17-AAG (Figure 5.13B, 10 μM). Although it appeared that the level of β-catenin had decreased at the high concentration of 17-AAG (Figure 5.13B, 10 μM), densitometric analysis of triplicate studies revealed that there was actually a slight increase in the β-catenin level (Appendix, Figure A4.6C).

A decrease in protein expression level of β-catenin was seen at higher concentrations (500 μM) of novobiocin treatment (Figure 5.14, 500 μM). This decrease was also reflected in the densitometric study (Appendix, Figure A4.6B).

Figure 5.13. β-catenin expression levels in MCF7 cells treated with 17-AAG and geldanamycin. A. Western detection for β-catenin in geldanamycin treated MCF cells. B. Western detection for β-catenin in 17-

AAG treated MCF7 cells. Actin was used as the loading control. Control cells were treated in normal growth media (0) or media containing only DMSO (DMSO), in the absence of 17-AAG or geldanamycin.

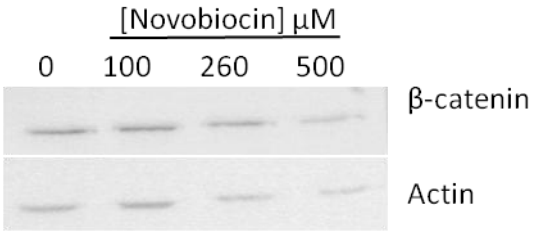

Figure 5.14. β-catenin expression levels in MCF7 cells treated with novobiocin. Western detection for β-catenin in novobiocin treated MCF cells. Actin was used as the loading control. Control cells were treated in normal growth media in the absence of novobiocin (0).

5.2.3.1 p-β-catenin

HSP90α/β co-immunoprecipitated with the phosphorylated form of β-catenin (Chapter 4, section 4.2.2), therefore giving the first preliminary evidence that there was potential association between HSP90α/β and p-β-catenin. Western analysis for p-β-catenin was performed on MCF7 cells treated with HSP90 inhibitors at increasing concentrations. MCF7 cells were treated with geldanamycin (Figure 5.15A, 0.1 μM, 0.5 μM, 1 μM, 10 μM) and novobiocin (Figure 5.16, 100 μM, 260 μM, 500 μM) for 24 hours. Treatment with 17-AAG (Figure 5.15B, 0.05 μM, 0.1 μM, 0.5 μM, 1 μM) occurred for 72 hours. No treatment (Figure 5.15 and 5.16, lane 0) and media supplemented with DMSO (Figure 5.15A, DMSO) were used as the controls.

Each HSP90 inhibitor treatment resulted in a decrease in the protein expression level of p-β-catenin (Figure 5.15A and B; 5.16). At the high concentration of geldanamycin (Figure 5.15A, 10 μM), the p-β-catenin level had also decreased in comparison to no treatment and the DMSO control (Figure 5.15A, DMSO). p-β-catenin protein expression levels also decreased with increasing 17-AAG (Figure 5.15B), from a concentration as low as 0.5 μM.

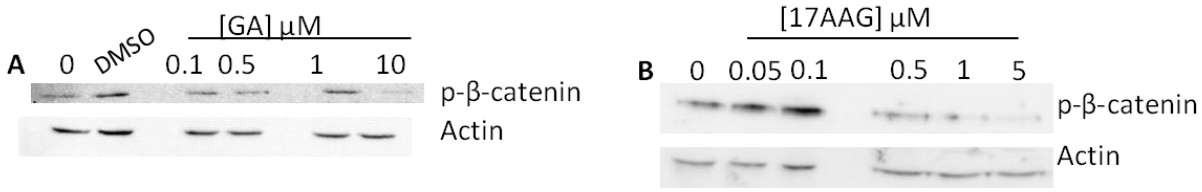

Figure 5.15. p-β-catenin expression levels in MCF7 cells treated with 17-AAG and geldanamycin. A. Western detection for p-β-catenin in geldanamycin treated MCF cells. B. Western detection for p-β-catenin in 17-AAG treated MCF7 cells. Actin was used as the loading control. Control cells were treated in normal growth media (0) or media containing only DMSO (DMSO), in the absence of 17-AAG or geldanamycin.

Increasing the concentration of novobiocin decreased the concentration of p-β-catenin (Figure 5.16) such that at 500 μM novobiocin, the p-β-catenin signal was much less than that of no treatment (Figure 5.16, 500 μM).

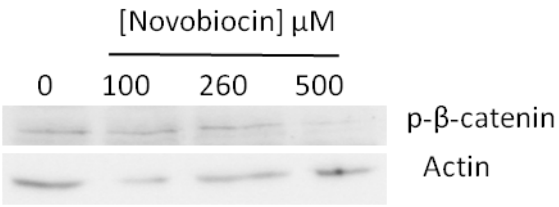

Figure 5.16. P-β-catenin expression levels in MCF7 cells treated with novobiocin. A. Western detection for p-β-catenin in novobiocin treated MCF cells. Actin was used as the loading control. Control cells were treated in normal growth media in the absence of novobiocin (0).

5.3 Discussion

The compound, 17-AAG binds to the N-terminus of HSP90, and results in a degradation of client proteins. HSP90α/β expression levels were not affected although the 17-AAG was preventing ATP from binding to the N-terminus (Roe *et al*., 1999). The known client proteins, STAT3, Akt and p-STAT3 were tested in this study to ensure that the efficacy of the compound was not compromised and also to provide a framework to which a comparison of the effect of the inhibitors on the Wnt proteins could be made. There was very little change in the expression levels of STAT3 (Figure 5.5) and Akt (Figure 5.9) with increasing concentrations of 17-AAG, whilst the expression of the phosphorylated form of STAT3 decreased slightly with increasing concentrations of 17-AAG (Figure 5.7). Interestingly, studies have found that client proteins that degrade slowly are more likely to interact with HSP90 in a transient manner during conformational maturation and therefore become degraded at rates according to their protein half life (Liu *et al*., 1993; Xu *et al*., 2001). Furthermore, HSP90 inhibition prevented the client protein from becoming activated, such as STAT3 from being phosphorylated (Sato *et al*., 2003). 17-AAG did not have an effect on the expression levels of β-catenin (Figure 5.13C) and GSK-3β (Figure 5.11C). In contrast to this, the expression level of p-β-catenin decreased with increasing concentrations of 17-AAG thus illustrating that p-β-catenin was a potential client of HSP90 and was sensitive to HSP90 inhibition. It can be suggested that 17-AAG efficiency was only sub-optimal for some of the experiments since an effect on the client protein, p-STAT3, was only seen at very high concentrations such as 10 μM.

To further validate the effects that 17-AAG inhibition had on the Wnt proteins, geldanamycin was used. Similar to 17-AAG, increasing concentrations of geldanamycin did not have an effect on the expression levels of HSP90, nor did it cause a change in the total β-catenin expression. Interestingly, there was only a slight decrease in GSK-3β at high geldanamycin concentrations (Figure 5.11A and B); whilst in literature GSK-3β has been found to be sensitive to geldanamycin concentrations in Hep3B cells (Banz *et al*., 2009). P-β-catenin also decreased with increasing geldanamycin concentrations (Figure 5.15B) which concurs with the study done by Banz *et al*. (2009). Banz *et al.* (2009) suggested that geldanamycin-induced HSP90 inhibition can also affect the kinases upstream of GSK-3β, such as Akt. This would result in the inhibition of GSK-3β, preventing GSK-3β from phosphorylating p-β-catenin.

Treatment of MCF7 cells with the compound novobiocin did not cause a change in the expression level of HSP90α/β (Figure 5.4). On the other hand, the client proteins, STAT3 (Figure 5.6), p-STAT3 (Figure 5.8) and Akt (Figure 5.10) decreased with increasing concentrations of novobiocin. Interestingly, the members of the Wnt pathway, GSK-3β (Figure 5.12), β-catenin (Figure 5.14) and p-β-catenin (Figure 5.16) also decreased with increasing concentrations of novobiocin.

Overall, the results obtained in this study are consistent with the data obtained from co-localization (Chapter 3) and immunoprecipitation (Chapter 4) studies, suggesting that HSP90α/β associates with GSK-3β, p-β-catenin and β-catenin. Although previous studies (Banz *et al*., 2009; Kurashina *et al*., 2009) have described a decrease in p-β-catenin after HSP90 inhibition as an indirect result of the inhibition of GSK-3β, the data presented here have shown that p-β-catenin and HSP90α/β associate in a common complex.

Chapter 6: Conclusion and future work

6.1 HSP90 association with Wnt members

Aberrant activation of the Wnt pathway has been found in cancer, whereby stabilized β-catenin can translocate to the nucleus and activate and maintain oncogenesis (Hoppler and Kavanagh, 2007). This can be due to mutations in genes encoding proteins involved in the destruction complex, such as APC, axin and even β-catenin (Polakis, 2000; Fodde *et al*., 2001) or autocrine signaling. In colon cancer, the Wnt pathway is known to be stimulated due to a mutation in the *APC* gene (Bienz and Clevers, 2000; Yang *et al*., 2006). However, in breast cancer, it is thought that other factors influence the upregulation of stabilized β-catenin (Veeck *et al*., 2006). A study of the expression levels of axin1, β-catenin, p-β-catenin, GSK-3β between the breast cancer cell line MCF7 and the colorectal cancer line HT29 confirmed that the MCF7 cell line had detectable levels of these proteins by Western analysis, making it a viable cell line to work with. These results concurred with literature as the Wnt pathway has been found to be "switched on" in breast cancer (Schlange *et al*., 2007).

Previous studies have linked HSP90α/β to the Wnt pathway via association with GSK-3β (Lochhead *et al*., 2006), however little is known about the association of HSP90α/β with other members of the Wnt pathway in MCF7 cells. For the first time, in this study, an association of HSP90α/β with other members of the Wnt pathway, axin1, p-β-catenin and β-catenin was shown in MCF7 cells.

HSP90 plays a role in the maturation and stabilization of numerous client proteins, many of which are involved in oncogenesis (Grbovic *et al*., 2006). Of particular interest is that HSP90 plays a role in many signal transduction pathways, but the mechanistic involvement of HSP90 in the Wnt signaling pathway has not been clearly defined. Although an association of HSP90 has been found with GSK-3β (Lochhead *et al*., 2006), it is argued that this association is only transient (Banz *et al*., 2009). Our studies of co-localization by confocal microscopy confirmed that there was a possible association between HSP90 and GSK-3β. This was later confirmed by HSP90 inhibition whereby treatment of the cells with high geldanamycin concentrations resulted in a disruption of this association, leading to a decrease in detectable levels of GSK-3β. Furthermore, treatment with novobiocin, an HSP90 inhibitor, that binds to the C-terminus and disrupts co-chaperone interaction (Allan *et al*., 2006), resulted in the decrease in detectable levels of GSK-3β. This illustrated that without the stabilization of the chaperone complex, GSK-3β became unstable and was potentially degraded. Co-immunoprecipitation analyses confirmed the association of GSK-3β and

HSP90 by isolating HSP90 by immunoprecipitation with GSK-3β. However the reverse was difficult to analyze by Western detection since the signal was masked by the heavy chain IgG. At the same time, a definitive association between GSK-3β and HSP90 was difficult to confirm by co-immunoprecipitation possibly because there was steric hindrance between the antibody used to isolate the complex and the protein being detected (Tsaytler *et al*., 2009). It could be argued that the association between GSK-3β and HSP90 is only transient therefore the weak interaction did not withstand the stringent lysis and washing conditions that occur during immunoprecipitation, as has been reported before for other HSP90 clients (Arlander *et al*., 2006). To confirm that the association between GSK-3β and HSP90 was not transient, other techniques could be employed. These could include using another technique of co-immunoprecipitation to isolate the HSP90 complex, such as the magnetic DynaBeads® therefore preventing any signal of GSK-3β being masked by the antibody's heavy and light chain.

Immunofluorescence and confocal microscopy revealed that the expression level of axin1 was very low in MCF-7 cells which concurs with literature since axin1 is the limiting protein of the destruction complex therefore expressed at low levels (Lee *et al*., 2003). Furthermore, axin1 was found to be in a similar location to HSP90 suggesting association which was confirmed by co-immunoprecipitation. Taking into account that axin1 is the scaffolding protein of the Wnt destruction complex, and gets sequestered to the membrane in the presence of a Wnt signal, and thereafter degraded (Willert *et al*., 1999), it was interesting to note that HSP90 inhibition by novobiocin resulted in accumulation of axin1 at the membrane (confocal analysis) and a reduction in the expression level (Western analysis). A possible explanation for this is that due to the destruction complex being disrupted by HSP90 inhibition, axin1 is sequestered to the membrane and degraded. It would be important to make a comparison between the localization pattern and expression levels of axin1 in normal epithelial cells as well as cells that have the Wnt pathway "switched on" such as HT29 to see if there is a difference. Furthermore, by stimulating the Wnt pathway in MCF7 cells, confocal analysis would reveal whether a similar change in localization of axin1 as that of HSP90-inhibition would occur, to prove the hypothesis.

HSP90 was found to have a possible association with the destruction complex via the proteins, GSK-3β and axin1, total β-catenin and its phosphorylated form. Co-immunoprecipitation analyses revealed that HSP90 is associated with both total β-catenin and p-β-catenin, with a strong association being found with the p-β-catenin. Furthermore,

inhibition by 17-AAG and geldanamycin resulted in a rapid degradation of p-β-catenin, thus suggesting its reliance on HSP90 for stabilization, either directly or in the complexed form. Novobiocin treatment, at high concentrations resulted in both the total β-catenin and p-β-catenin expression levels decreasing. This suggested that since the co-chaperone activity of HSP90 was being inhibited by novobiocin, β-catenin was not able to enter the destruction complex to get phosphorylated. These results could indicate that HSP90 inhibition is disrupting a pathway upstream of the Wnt pathway, which could result in the Wnt pathway being activated so that axin1 is sequestered to the membrane after novobiocin treatment. This theory opposes that of Kurashina and colleagues (2009), who suggested that 17-AAG treatment inhibits the Wnt pathway by activating GSK-3β via Akt.

These data collected in this study support a possible schematic model of the association of HSP90α/β with the destruction complex (Figure 6.1). The immunoprecipitation data suggest that HSP90α/β associates in a common complex with p-β-catenin (Figure 6.1A), which becomes disrupted upon treatment with an HSP90 inhibitor, such as novobiocin (Figure 6.1B). β-catenin was therefore prevented from associating with the destruction complex (Figure 6.1B) and thus prevented from being phosphorylated. On the other hand, p-β-catenin was released from the destruction complex and degraded (Figure 6.1B), whilst the other destruction complex members, GSK-3β and axin1 were no longer stabilized by HSP90 which resulted in their degradation. If this model is true then p-β-catenin constitutes a small proportion of the total β-catenin detected. This could explain why there was a notable decrease in the expression level of p-β-catenin after novobiocin treatment (Figure 5.16), whilst only a small decrease in total β-catenin expression levels (Figure 5.14). If this model is true, then care must be taken in designing HSP90 inhibitor drugs since there is a possibility of activating the Wnt pathway by HSP90 inhibition, and thus potentially increasing the aggressiveness of the cancer. Furthermore, by activating the Wnt pathway, there is potential that dormant cancer stem cell-like cells will be activated, since the Wnt pathway is linked to stem cell proliferation (Lindvall *et al*., 2007)

Taken together, these results suggest that HSP90 is directly involved in the destruction complex of HSP90 in the Wnt pathway, in contrast to previous studies which suggest its involvement in upstream pathways influencing the Wnt pathway (Banz *et al*., 2009). It can therefore be said, that there is a possible involvement of HSP90 in the modulation or

stabilization of p-β-catenin in the Wnt pathway by association with the proteins axin1, GSK-3β and p-β-catenin.

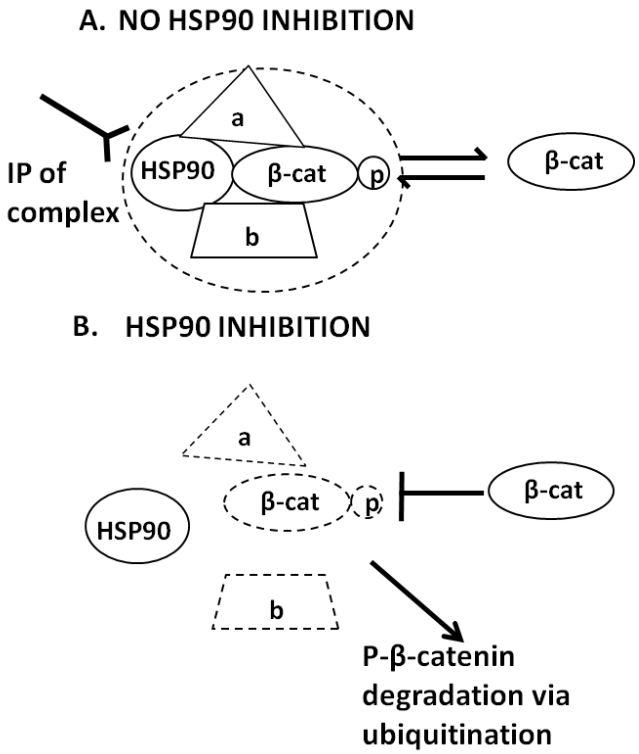

Figure 6.1. Schematic model of the association of HSP90α/β with p-β-catenin in the destruction complex in Wnt pathway in MCF7 cells. In the absence of HSP90 inhibition (A), there is a dynamic interaction between β-catenin and its phosphosphorylated form p-β-catenin. Immunoprecipitation (IP) studies have shown that HSP90α/β associates with p-β-catenin in a common complex (dotted line around complex). In the presence of HSP90 inhibitors (B), such as novobiocin, the HSP90 association with the destruction complex is disrupted and the proteins get degraded. β-catenin is prevented from being phosphorylated shown by blunted line. Primary antibody shown schematically detecting IP complex. Arrows point towards direction of pathway. Dotted lines in (B) represent protein degradation. 'a' and 'b' represent proteins within destruction complex.

6.2 Future work

An interesting study that could be performed in the future would be to compare the expression levels of the Wnt pathway proteins between a normal breast epithelial cell line and MCF7 cells to see if there is a difference, and then to stimulate the Wnt pathway in the normal breast epithelial cell line to see if the expression levels of proteins such as β-catenin are upregulated to a comparable level.

Another interesting study would be to identify which other proteins in the Wnt pathway could be associated with HSP90. Many questions need to be answered in order to fully understand

the role of HSP90 in the Wnt pathway. For example, since HSP90 has been found to be associated with the destruction complex via axin1 and GSK-3β, is it also involved with the other members, such as APC? Where is HSP90 involved with the destruction complex? How strong are the associations of HSP90 with these proposed client proteins? If HSP90 is associated with axin1, which is proposed to be also involved in the transport of β-catenin in and out of the nucleus, is HSP90 also involved in the nuclear transport of β-catenin?

These questions could be answered by co-immunoprecipitation studies, as well as cross-linking HSP90 with other proteins involved in the destruction complex such as APC prior to immunoprecipitation. Treatment of the cells with HSP90 inhibitors prior to co-immunoprecipitation would further reveal dependency of the complexes on HSP90 for stabilization and at which terminus the client proteins interact with HSP90. Furthermore, by treating MCF7 cells with a compound that is known to stimulate the Wnt pathway, confocal analysis could be performed to test if there is an association of HSP90 with the nuclear fraction of β-catenin, and whether other associations would change. Co-immunoprecipitations on subcellular fractionations would reveal where in the cell the associations with HSP90 occur. Furthermore, pTopflash reporter assays, which measure the TCF/LEF transcription, could be performed to identify whether the Wnt pathway is activated or inhibited after HSP90 treatment.

An alternative method for identifying the protein-protein interactions, such as those between HSP90 and the APC destruction complex, would be to synthesize a histidine tagged version of HSP90 and using it affinity purification of the MCF7 lysate. The resulting isolated complex could then be probed for the respective proteins within the APC destruction complex. The reverse could be performed by synthesizing histidine tagged versions of the APC complex proteins and probing for HSP90.

Lastly, this is the first study that provides a possible association of HSP90 with the Wnt pathway in MCF7 cells. This mechanistic understanding of the involvement of HSP90 in the Wnt pathway is important since it gives a framework for studying the association of HSP90 in the Wnt pathway in cancer stem cells, thus allowing for the development of therapeutic drugs targeted at inhibiting the Wnt pathway.

REFERENCES

Aguilera O, Fraga MF, Ballestar E, Paz MF, Herranz M, Espada J, Garcia JM, Muñoz A, Esteller M and González-Sancho JM (2006). Epigenetic inactivation of the Wnt antagonist *Dickkopf-1* (*Dkk-1*) gene in human colorectal cancer: Dkk-1 methylation in human colorectal cancer. *Oncogene* **25**: 4116–4121.

Alberts B, Johnson A, Lewis J, Raff M, Roberts K and Walter P (2002). Cancer. In: *Molecular Biology of the Cel*l, 4th Edition, Alberts B, Johnson A, Lewis J, Raff M, Roberts K, Walter P (eds), 1313−1362. New York: Garland Science Textbooks.

Al-Hajj M, Wicha MS, Benito-Hernandez A, Morrison SJ and Clarke MF (2003). Prospective identification of tumourigenic breast cancer cells. *Proc. Natl. Acad. Sci. USA* **100**: 3983–8.

Ali MMU, Roe SM, Vaughan CK, Meyer P, Panaretou B, Piper PW, Prodromou C and Pearl LH (2006). Crystal structure of an Hsp90-nucleotide-p23/Sba1 closed chaperone complex. *Nature* **440**: 1013–1017.

Allan RK, Mok D, Ward BK and Ratajczak T (2006). Modulation of chaperone function and cochaperone interaction by novobiocin in the C-terminal domain of Hsp90: evidence that coumarin antibiotics disrupt Hsp90 dimerization. *J. Biol. Chem*. **281**: 7161–7171.

Alves-Guerra MC, Ronchini C and Capobianco AJ (2007). Mastermind-like 1 is a specific coactivator of β-catenin transcription activation and is essential for colon carcinoma cell survival. *Cancer Res.* **67**: 8690–8698.

Amit S, Hatzubai A, Birman Y, Andersen JS, Ben-Shushan E, Mann M, Ben-Neriah Y and Alkalay I (2002). Axin-mediated CK1 phosphorylation of β-catenin at Ser 45: a molecular switch for the pathway. *Genes Dev.* **16**: 1066 – 1076.

Angers S and Moon RT (2009). Proximal events in Wnt signal transduction. *Nature* **10**: 468-477.

Arlander SJ, Felts SJ, Wagner JM, Stensgard B, Toft DO and Karnitz LM (2006). Chaperoning checkpoint kinase 1 (Chk1), an Hsp90 client, with purified chaperones. *J. Biol. Chem***. 281**: 2989–2998.

Ayyanan A, Civenni G, Ciarloni L, Morel C, Mueller N, Lefort K, Mandinova A, Raffoul W, Fiche M, Dotto GP and Brisken C (2006). Increased Wnt signaling triggers oncogenic conversion of human breast epithelial cells by a Notch-dependent mechanism. *Proc. Natl. Acad. Sci. USA* **103**: 3799-3804.

Banz VM, Medová M, Keogh A, Furer C, Zimmer Y, Candinas D and Stroka D (2009). Hsp90 transcriptionally and post-translationally regulates the expression of NDRG1 and maintains the stability of its modifying kinase GSK3beta. *Biochim. Biophys. Acta* **1793**: 1597-1603.

Barth AI, Pollack AL, Altschuler Y, Mostov KE and Nelson WJ (1997). NH2-terminal deletion of β-catenin results in stable colocalization of mutant β-catenin with adenomatous polyposis coli protein and altered MDCK cell adhesion. *J. Cell. Biol.* **136**: 693-706.

Basso AD, Solit DB, Chiosis G, Giri B, Tsichlis P and Rosen N (2002B). Akt forms an intracellular complex with heat shock protein 90 (Hsp90) and Cdc37 and is destabilized by inhibitors of Hsp90 function. *J. Biol. Chem*. **277**: 39858–39866.

Basso AD, Solit DB, Munster PN and Rosen N (2002A). Ansamycin antibiotics inhibit Akt activation and cyclin D expression in breast cancer cells that overexpress HER2. *Oncogene* **21**: 1159– 1166.

Behrens J, Jerchow BA, Würtele M, Grimm J, Asbrand C, Wirtz R, Kühl M, Wedlich D and Birchmeier W (1998). Functional interaction of an axin homolog, conductin, with beta-catenin, APC, and GSK-3beta. *Science* **280**: 596–599.

Bennet LB, Taurog JD and Bowcock AM (1999). Hereditary breast cancer genes. In: Breast Cancer: Molecular Genetics, Pathogenesis, and Therapeutics, Bowcock AM (ed), pp 199–224. Totowa, NJ: Humana Press Inc.

Bienz M and Clevers H (2000). Linking colorectal cancer to Wnt signaling. *Cell*: **103**: 311–320.

Bilić J, Huang YL, Davidson G, Zimmermann T, Cruciat CM, Bienz M and Niehrs C (2007). Wnt induces LRP6 signalosomes and promotes Dishevelled-dependent LRP6 phosphorylation. *Science* **316**: 1619-1622.

Blagg BS and Kerr TD (2006). Hsp90 inhibitors: small molecules that transform the Hsp90 protein folding machinery into a catalyst for protein degradation. *Med. Res. Rev*. **26**: 310–338.

Borkovich KA, Farrelly FW, Finkelstein DB, Taulien J and Lindquist S (1989). Hsp82 is an essential protein that is required in higher concentrations for growth of cells at higher temperatures. *Mol. Cell. Biol***. 9**: 3919–3930.

Bovolenta P, Esteve P, Ruiz JM, Cisneros E and Lopez-Rios J (2008). Beyond Wnt inhibition: new functions of secreted Frizzled-related proteins in development and disease. *J. Cell Sci*. 121: 737–746.

Brabletz T, Jung A, Reu S, Porzner M, Hlubek F, Kunz-Schughart LA, Knuechel R and Kirchner T (2001). Variable β-catenin expression in colorectal cancers indicates tumour progression driven by the tumour environment. *Proc. Natl. Acad. Sci. USA* **98**: 10356-10361.

Brown (2001). Wnt signaling in breast cancer: have we come a full circle? *Breast Cancer Res*. **3**: 351 – 5.

Brown MA, Zhu L, Schmidt C and Tucker PW (2007). HSP90 – from signal transduction to cell transformation. *Biochem. Biophys. Res. Commun*. **363**: 241-246.

Brugge JS (1983). Interaction of the Rous sarcoma virus protein pp60src with cellular proteins pp50 and pp90. *Curr. Top. Microbiol. Immunol.* **123**: 1-22.

Bui TD, Rankin J, Smith K, Huguet EL, Ruben S, Strachan T, Harris AL and Lindsay S (1997). A novel human Wnt gene, WNT10B, maps to 12q13 and is expressed in human breast carcinomas. *Oncogene* **14**: 1249-1253.

Burlison JA and Blagg BS (2006). Synthesis and evaluation of coumermycin A1 analogues that inhibit the Hsp90 protein folding machinery. *Org. Lett*. **8**: 4855– 4858.

Cairns J (2002). Somatic stem cells and the kinetics of mutagenesis and carcinogenesis. *Proc. Natl. Acad. Sci. USA* **99**: 10567 – 70.

Calvocoressi L, Sun A, Kasl SV, Claus EB and Jones BA (2008). Mammography screening of women in their 40s: impact of changes in screening guidelines. *Cancer* **112**: 473 – 480.

Campbell Marotta LL and Polyak K (2009). Cancer stem cells: a model in the making. *Curr. Opin. Genet. Dev*. **19**: 44-50.

Cariati M and Purushotham AD (2008). Stem cells and breast cancer. *Histopathology* **52**: 99 – 107.

Caspi M, Zilberberg A, Eldar-Finkelman H and Rosin-Arbesfeld R (2008). Nuclear GSK-3β inhibits the canonical Wnt signaling pathway in a β-catenin phosphorylation-independent manner. *Oncogene* **27**: 3546-3555.

Cavalieri EL, Stack DE, Devanesan PD, Todorovic R, Dwivedy I, Higginbotham S, Johansson SL, Patil KD, Gross ML, Gooden JK, Ramanathan R, Cemy RL and Rogan EG (1997). Molecular origin of cancer: catechol estrogen-3,4-quinones as endogenous tumour initiators. *Proc. Natl. Acad. Sci. USA* **94**:10937–10942.

Chamorro MN, Schwartz DR, Vonica A, Brivanlou AH, Cho KR and Varmus HE (2005). FGF-20 and DKK1 are transcriptional targets of β-catenin and FGF-20 is implicated in cancer and development. *EMBO J*. **24**: 73–84.

Chan TA, Wang Z, Dang LH, Vogelstein B and Kinzler KW (2002). Targeted inactivation of *CTNNB1* reveals unexpected effects of β-catenin mutation. *Proc. Natl. Acad. Sci. USA* **99**: 8265–8270.

Chen G, Cao P and Goeddel DV (2002). TNF-induced recruitment and activation of the IKK complex require Cdc37 and Hsp90. *Mol. Cell* **9**: 401–410.

Chen MS, Woodward WA, Behbod F, Peddibhotla S, Alfaro MP, Buchholz TA and Rosen JM (2007). Wnt/β-catenin mediates radiation resistance of Sca1+ progenitors in an immortalized mammary gland cell line. *J. Cell Sci*. **120**: 468–477.

Chen WY, Chang FR, Huang ZY, Chen JH, Wu YC and Wu CC (2008). Tubocapsenolide A, a novel withanolide, inhibits proliferation and induces apoptosis in MDA-MB-231 cells by thiol oxidation of heat shock proteins. *J. Biol. Chem.* **283**: 17184–17193.

Chiosis G and Neckers L (2006). Tumour selectivity of Hsp90 inhibitors: the explanation remains elusive. *ACS Chem. Biol*. **1**:279–284.

Chung GG, Provost E, Kielhorn EP, Charette LA, Smith BL and Rimm DL. (2001). Tissue microarray analysis of β-catenin in colorectal cancer shows nuclear p-β-catenin is associated with a better prognosis. *Clin. Cancer Res*. **7**: 4013–4020.

Ciani L, Krylova O, Smalley MJ, Dale TC and Salinas PC (2004). A divergent canonical WNT-signaling pathway regulates microtubule dynamics: dishevelled signals locally to stabilize microtubules. *J. Cell. Biol.* **164**: 243–253.

Clevers H (2006). Wnt/β-catenin signaling in development and disease. *Cell* **127**: 469–480.

Cole AR and Sutherland C (2008). Measuring GSK3 expression and activity in cells. *Methods Mol. Biol.* **468**: 45-65.

Coles C, Condie A, Chetty U, Steel CM, Evans HJ and Prosser J (1992). *p53* mutations in breast cancer. *Cancer Res.* 52: 5291–5298.

Collu GM, Meurette M and Brennan K (2009). Is there more to Wnt signaling in breast cancer than stabilisation of β-catenin? *Breast Cancer Res*. **11**: 105.

Cong F and Varmus H (2004A). Nuclear-cytoplasmic shuttling of Axin regulates subcellular localization of β-catenin . *Proc. Natl. Acad. Sci. USA* **101**: 2882–7.

Cong F, Schweizer L and Varmus H (2004B). Wnt signals across the plasma membrane to activate the β-catenin pathway by forming oligomers containing its receptors, Frizzled and LRP. *Development* **131**: 5103-5115.

Covey TM, Edes K, Coombs GS, Virshup DM and Fitzpatrick FA (2010). Alkylation of the tumour suppressor PTEN activates Akt and β-catenin signaling: a mechanism linking inflammation and oxidative stress with cancer. *PLoS ONE* **5**: e13545.

Crawford HC, Fingleton BM, Rudolph-Owen LA, Goss KJ, Rubinfeld B, Polakis P and Matrisian LM (1999). The metalloproteinase matrilysin is a target of β-catenin transactivation in intestinal tumours. *Oncogene* **18**: 2883–2891.

Cress RD, Morris C, Ellison GL, Goodman MT (2006). Secular changes in colorectal cancer incidence by subsite, stage at diagnosis and race/ ethnicity, 1992 – 2001. *Cancer* **107**: 1142 – 52.

Cross DA, Alessi DR, Cohen P, Andjelkovich M and Hemmings BA (1995). Inhibition of glycogen synthase kinase-3 by insulin mediated by protein kinase B. *Nature* **378**:785–9.

Cselenyi CS, Jernigan KK, Tahinci E, Thorne CA, Lee LA and Lee E (2008). LRP6 transduces a canonical Wnt signal independently of Axin degradation by inhibiting GSK3's phosphorylation of β-catenin. *Proc. Nat. Acad. Sci.* **105**: 8032-8037.

Daidone MG, Luisi A, Veneroni S, Benini E and Silvestrini R (1999). Clinical studies of Bcl-2 and treatment benefit in breast cancer patients. *Endocr. Relat. Cancer* **6**:61–68.

Daniels DL and Weis WI (2005). β-catenin directly displaces Groucho/TLE repressors from Tcf/Lef in Wnt-mediated transcription activation. *Nat. Struct. Mol. Biol*. **12**: 364–371.

Darnell JE, Kerr IM and Stark GR (1994). Jak-STAT pathways and transcriptional activation in response to IFNs and other extracellular signaling proteins. *Science* **264**: 1415 – 1421.

Davidson G, Wu W, Shen J, Bilić J, Fenger U, Stannek P, Glinka A and Niehrs C (2005). Casein kinase 1γ couples Wnt receptor activation to cytoplasmic signal transduction. *Nature* **438**: 867–872.

Debruin LS and Josephy PD (2002). Perspectives on the chemical etiology of breast cancer. *Environ. Health Perspect*. **110** (suppl. 1): 119-128.

Dolled-Filhart M, McCabe A, Giltnane J, Cregger M, Camp RL and Rimm DL (2006). Quantitative *in situ* analysis of β-catenin expression in breast cancer shows decreased expression is associated with poor outcome. *Cancer Res.* **66**: 5487–5494.

Dollins DE, Warren JJ, Immormino RM, Gewirth DT (2007). Structures of GRP94-nucleotide complexes reveal mechanistic differences between the hsp90 chaperones. *Mol. Cell* **28**: 41–56.

Dontu G, El-Ashry D and Wicha MS (2004). Breast cancer, stem/progenitor cells and the estrogen receptor. *Trends Endocrinol. Metab.* **15**: 193 – 197.

Dutta R and Inouye M (2000) GHKL, an emergent ATPase/kinase superfamily. *Trends Biochem. Sci*. **25**: 24–28.

Eaton L (2003). World cancer rates set to double by 2020. *BMJ* **326**: 728

Eleftheriou A, Yoshida M and Henderson BR (2001). Nuclear export of human β-catenin can occur independent of CRM1 and the adenomatous polyposis coli tumour suppressor. *J. Biol. Chem*. **276**: 25883 – 25888.

Espinosa L, Inglés-Esteve J, Aguilera C and Bigas A (2003). Phosphorylation by glycogen synthase kinase-3β down-regulates Notch activity, a link for Notch and Wnt pathways. *J. Biol. Chem*. **278**: 32227–32235.

Eyler CE and Rich JN (2008). Survival of the fittest: cancer stem cells in therapeutic resistance and angiogenesis. *J. Clin. Oncol.* **26**: 2839 – 2845.

Fan X, Matsui W, Khaki L, Stearns D, Chun J, Li YM and Eberhart CG (2006). Notch pathway inhibition depletes stem-like cells and blocks engraftment in embryonal brain tumours. *Cancer Res*. **66**: 7445 – 7452.

Faux MC, Coates JL, Catimel B, Cody S, Clayton AHA, Layton MJ and AW Burgess (2008). Recruitment of adenomatous polyposis coli and β-catenin to axin-puncta. *Oncogene* **27**: 5808–5820.

Feinberg AP, Ohlsson R and Henikoff S (2006). The epigenetic progenitor origin of human cancer. *Nat. Rev. Genet.* **7**: 21-33.

Felts SJ, Owen BA, Nguyen P, Trepel J, Donner DB and Toft DO (2000). The hsp90-related protein TRAP1 is a mitochondrial protein with distinct functional properties. *J. Biol. Chem*. **275**: 3305–3312.

Ferrarini M, Heltai S, Zocchi MR and Rugarli C (1992). Unusual expression and localization of heat-shock proteins in human tumour cells. *Int. J. Cancer* **51**: 613 – 619.

Fodde R, Smits R and Clevers H (2001). APC, signal transduction and genetic instability in colorectal cancer. *Nat. Rev. Cancer* **1**: 55 – 67.

Frisén J and Lendahl U (2001). Oh no, Notch again! *Bioessays* **23**: 3–7.

Fujita N, Sato S, Ishida A and Tsuruo T (2002). Involvement of Hsp90 in signaling and stability of 3-phosphoinositide-dependent kinase-1. *J. Biol. Chem.* **277**: 10346-10353.

Gehrke I, Gandhirajan RK and Kreuzer KA (2009). Targeting the WNT/β-catenin/TCF/LEF1 axis in solid and haematological cancers: multiplicity of therapeutic options. *Eur. J. Cancer* **45**: 2759 –2767.

Gillett CE, Miles DW, Ryder K, Skilton D, Liebman RD, Springall RJ, Barnes DM and Hanby AM (2001). Retention of the expression of E-cadherin and catenins is associated with shorter survival in grade III ductal carcinoma of the breast. *J. Pathol.* **93**: 433–441.

Goetz MP, Toft DO, Ames MM and Erlichman C (2003) The Hsp90 chaperone complex as a novel target for cancer therapy. *Annal. Oncol*. **14**: 1169-1176.

Grammatikakis N, Vultur A, Ramana CV, Siganou A, Schweinfest CW, Watson DK and Raptis L. (2002). The role of Hsp90N, a new member of the Hsp90 family, in signal transduction and neoplastic transformation. *J. Biol. Chem*. **277**: 8312–8320.

Graziano A, d'Aquino R, Tirino V, Desiderio V, Rossi A and Pirozzi G (2008). The stem cell hypothesis in head and neck cancer. *J. Cell. Biochem*. **103**: 408 – 412.

Grbovic OM, Basso AD, Sawai A, Ye Q, Friedlander P, Solit D, Rosen N (2006). V600E B-Raf requires the Hsp90 chaperone for stability and is degraded in response to Hsp90 inhibitors. *Proc. Natl. Acad. Sci. USA* **103**: 57–62.

Hambardzumyan D, Becher OJ and Holland EC (2008). Cancer stem cells and survival pathways. *Cell Cycle* **7**: 1371 – 1378.

Harada N, Tamai Y, Ishikawa T, Sauer B, Takaku K, Oshima M. and Taketo MM (1999). Intestinal polyposis in mice with a dominant stable mutation of the β-catenin gene. *EMBO J*. **18**: 5931–5942.

Haraguchi N, Ohkima M, Sakashita H, Matsuzaki S, Tanaka F, Mimori, K, Kamohara Y, Inoue H and Mori M (2008). CD133+CD44+ population efficiently enriches colon cancer initiating cells. *Ann. Surg. Oncol*. **15**: 2927 – 2933.

Hawle P, Siepmann M, Harst A, Siderius M, Reusch HP and Obermann WM (2006). The middle domain of Hsp90 acts as a discriminator between different types of client proteins. *Mol. Cell. Biol*. **26**:8385–8395.

Hayward P, Balayo T and Martinez Arias A (2006). Notch synergizes with axin to regulate the activity of armadillo in Drosophila. *Dev. Dyn*. **235**: 2656–2666.

He TC, Sparks AB, Rago C, Hermeking H, Zawel L, da Costa LT, Morin PJ, Vogelstein B and Kinzler KW (1998). Identification of c-MYC as a Target of the APC Pathway. *Science* **281**: 1509–1512.

Helmbrecht K, Zeise E and Rensing L (2000). Chaperones in cell cycle regulation and mitogenic signal transductions: a review. *Cell Prolif*. **33**: 341 – 365

Henderson BE and Feigelson HS (2000). Hormonal carcinogenesis. *Carcinogenesis* **21**:427–43.

Henderson BR (2000). Nuclear-cytoplasmic shuttling of APC regulates β-catenin subcellular localization and turnover. *Nat. Cell. Biol*. **2**: 653 – 660.

Henderson BR and Fagotto F (2000). The ins and outs of APC and β-catenin nuclear transport. *EMBO re*. **3**: 834-839.

Henderson BR, Galea M, Schuechner S and Leung L (2002). Lymphoid Enhancer Factor-1 blocks APC-mediated nuclear export and degradation of β-catenin: regulation by Histone Deacetylase 1. *J. Biol. Chem*. **277**: 24258–24264.

Hinz M, Broemer M, Arslan SC, Otto A, Mueller EC, Dettmer R and Scheidereit C (2007). Signal responsiveness of IκB kinases is determined by Cdc37-assisted transient interaction with Hsp90. *J. Biol. Chem*. **282**: 32311-32319.

Hirschmann-Jax C, Foster AE, Wulf GG, Nuchtern JG, Jax TW, Gobel U, Goodell MA and Brenner MK (2004). A distinct "side population" of cells with high drug efflux capacity in human tumour cells. *Proc. Natl. Acad. Sci. USA* **101**:14228–14233.

Hiscox S, Jiang WG, Obermeier K, Taylor K, Morgan L, Burmi R, Barrow D and Nicholson RI (2006). Tamoxifen resistance in MCF7 cells promotes EMT-like behaviour and involves modulation of β-catenin phosphorylation. *Int. J. Cancer* **118**: 290–301.

Hocevar BA, Mou F, Rennolds JL, Morris SM, Cooper JA and Howe PH (2003). Regulation of the Wnt signaling pathway by disabled-2 (Dab2). *EMBO J*. **22**: 3084 – 3094.

Hoffmans R and Basler K (2007). BCL9-2 binds Arm/β-catenin in a Tyr142-independent manner and requires Pygopus for its function in Wg/Wnt signaling. *Mech. Dev*. **124**: 59-67.

Hollingshead M, Alley M, Burger AM, Borgel S, Pacula-Cox C, Fiebig HH and Sausville EA (2005). *In vivo* antitumour efficacy of 17-DMAG (17-dimethylaminoethylamino-17-demethoxygeldanamycin hydrochloride), a water-soluble geldanamycin derivative. *Cancer Chemother. Pharmacol*. **56**: 115-125.

Hoppler S and Kavanagh CL (2007). Wnt signaling: variety at the core. *J. Cell Sci*. **120**: 385-393.

Hovanes K, Li TW, Munguia JE, Truong T, Milovanovic T, Lawrence Marsh J, Holcombe R F and Waterman ML (2001). β-catenin-sensitive isoforms of lymphoid enhancer factor-1 are selectively expressed in colon cancer. *Nat. Genet*. **28**: 53-57.

Howard BA (2000). Human breast development. *J. Mammary Gland Biol. Neoplasia* **5**: 119 – 137.

Howard EM, Lau SK, Lyles RH, Birdsong GG, Tadros TS, Umbreit JN and Kochhar R (2004). Correlation and expression of p53, HER-2, vascular endothelial growth factor (VEGF), and e-cadherin in a high-risk breast-cancer population. *Int. J. Clin. Oncol.* **9**: 154-60.

Huang H and He X (2008). Wnt/β-catenin signaling: new (and old) players and new insights. *Curr. Opin. Cell Biol*. **20**: 119–125.

Huber AH andWeis WI (2001). The structure of the β-catenin/E-cadherin complex and the molecular basis of diverse recognition by β-catenin. *Cell* **105**: 391 – 402.

Hung MC and Lau YK (1999). Basic science of HER-2/neu: a review. *Semin. Oncol*. **26**: 51–59.

Ingham PW and McMahon AP (2001). Hedgehog signaling in animal development: paradigms and principles. *Genes Dev*. **15**: 3059 – 87.

Inoki K, Ouyang H, Zhu T, Lindvall C,Wang Y, Zhang X, Yang Q, Bennett C, Harada Y, Stankunas K, Wang CY, He X, MacDougald OA, You M, Williams BO and Guan KL (2006). TSC2 integrates Wnt and energy signals via a coordinated phosphorylation by AMPK and GSK3 to regulate cell growth. *Cell* **126**: 955–968.

Iozzo RV, Eichstetter I and Danielson KG (1995). Aberrant expression of the growth factor Wnt-5A in human malignancy. *Cancer Res.* **55**: 3495 – 3499.

Jemal A, Siegal R, Ward E, Hao Y, Xu J, Murray T and Thun MJ (2008). Cancer statistics, 2010. *CA Cancer J. Clin*. **58**: 71-96.

Jin LH, Shao QJ, Luo W, Ye ZY, Li Q, Lin SC (2003). Detection of point mutations of the *Axin1* gene in colorectal cancers. *Int. J. Cancer* **107**: 696–699.

Jones PA and Baylin (2002). The fundamental role of epigenetic events in cancer. *Nat. Rev. Genet*. **3**: 415 – 428.

Kakarala M and Wicha MS (2008). Implications of the cancer stem-cell hypothesis for breast cancer prevention and therapy. *J. Clin. Oncol*. **26**: 2813 – 2820.

Kam Y and Quaranta Y (2009). Cadherin-Bound β-catenin feeds into the Wnt Pathway upon Adherens junctions dissociation: evidence for an intersection between β-catenin pools. *PLoS ONE* **4**: e4580.

Kamal A, Boehm MF and Burrows FJ (2004). Therapeutic and diagnostic implications of Hsp90 activation. *Trends Mol. Med.* **10**: 283–290.

Kamal A, Thao L, Sensintaffar J, Zhang L, Boehm MF, Fritz LC and Burrows FJ (2003). A high-affinity conformation of Hsp90 confers tumour selectivity on Hsp90 inhibitors. *Nature* **425**: 407–410.

Kanwar SS, Yu Y, Nautiyal J, Patel BB and Majumdar APN (2010). The Wnt/β-catenin pathway regulates growth and maintenance of colonospheres. *Mol. Cancer* **9**:212

Katoh M and Katoh M (2007). STAT3 induced WNT5A signaling loop in embryonic stem cells, adult normal tissues, chronic persistent inflammation, rheumatoid arthritis and cancer (review). *Int. J. Mol. Med.* **19**: 273 – 278.

Katschinski DM, Le L, Heinrich D, Wagner KF, Hofer T, Schindler SG and Wenger RH (2002). Heat induction of the unphosphorylated form of hypoxia-inducible factor-1α is dependent on heat shock protein-90 activity. *J. Biol. Chem.* **277**: 9262-9267.

Kelleher FC, Fennelly D, Rafferty M (2006). Common critical pathways in embryogenesis and cancer. *Acta Oncologica* **45**: 375-388.

Khan Z, Vijayakumar S, de la Torre TV, Rotolo S and Bafico A (2007). Analysis of endogenous LRP6 function reveals a novel feedback mechanism by which Wnt negatively regulates its receptor. *Mol. Cell. Biol*. **27**: 7291–7301.

Kielhorn E, Provost E, Olsen D, D'Aquila TG, Smith BL, Camp RL and Rimm DL**.** (2003). Tissue microarray-based analysis shows p-β-catenin expression in malignant melanoma is associated with poor outcome. *Int. J. Cancer* **103**: 652–656.

Kikuchi A (2000). Regulation of β-catenin signaling in the Wnt pathway. *Biochem. Biophys. Res. Commun*. **268**: 243–248.

Kim HL, Cassone M, Otvos L Jr and Vogiatzi P (2008). HIF-1α and STAT3 client proteins interacting with the cancer chaperone HSP90. *Cancer Biol. and Therapy* **7**: 10 -14.

Kim YS, Alarcon SV, Lee S, Lee MJ, Giaccone G, Neckers L and Trepel JB (2009). Update on HSP90 inhibitors in clinical trial. *Curr. Top. Med. Chem*. **9**: 1479 – 1492.

Kimelman D and Xu W (2006). β-Catenin destruction complex: insights and questions from a structural perspective. *Oncogene* **25**: 7482–7491.

Kirchner T and Brabletz T (2000). Patterning and nuclear β-catenin expression in the colonic adenoma-carcinoma sequence. Analogies with embryonic gastrulation. *Am. J. Pathol*. **157**: 1113-1121.

Kitagawa M, Hatakeyama S, Shirane M, Matsumoto M Ishida N, Nakamichi I, Kikuchi A, Nakayama K and Nakayama K (1999). An Fbox protein FWD1 mediates ubiquitin dependent proteolysis of β-catenin. *EMBO J.* **18**: 2401 – 2410.

Kohler EM, Chandra SHV, Behrens J and Schneikert (2009). β-Catenin degradation mediated by the CID domain of APC provides a model for the selection of APC mutations in colorectal, desmoid and duodenal tumours. *Human Mol. Genet.* **18**: 213-226.

Kondo T, Setoguchi T and Taga T (2004). Persistence of a small subpopulation of cancer stem-like cells in the C6 glioma cell line. *Proc. Natl. Acad. Sci. USA* **101**:781–786.

Kopper L and Hadju M (2004). Tumour stem cells. *Pathol. Oncol. Res.* **10**: 69 - 73.

Korinek V, Barker N, Morin PJ, van Wichen D, de Weger R, Kinzler KW, Vogelstein B and Clevers H (1997). Constitutive transcriptional activation by a β-catenin -Tcf complex in APC-/- colon carcinoma. *Science* **275**:1784–1787.

Korkaya H and Wicha MS (2007). Selective targeting of cancer stem cells: a new concept in cancer therapeutics. *Biodrugs* **21**: 299 – 310.

Kotiligam D, Lazar AJ, Pollock RE and Lev D (2008). Desmoid tumour: a disease opportune for molecular insights. *Histol. Histopathol.* **23**:117-26.

Kroboth K, Newton IP, Kita K, Dikovskaya D, Zumbrunn J, Waterman-Storer CM and Näthke IS (2007). Lack of adenomatous polyposis coli protein correlates with a decrease in cell migration and overall changes in microtubule stability. *Mol. Biol. Cell.* **18**: 910-8.

Kubo M, Nakamura M, Tasaki A, Yamanaka N, Nakashima H, Nomura M, Kuroki S and Katano M (2004). Hedgehog signaling pathway is a new therapeutic target for patients with breast cancer. *Cancer Res*. **64**: 6071 – 6074.

Kumar S and Weaver VM (2009). Mechanics, malignancy, and metastasis: the force journey of a tumour cell. *Cancer Metastasis Rev.* **28**: 113–127.

Kurashina R, Ohyashiki JH, Kobayashi a C, Hamamuraa R, Zhang Y, Hirano T and Ohyashiki K (2009). Anti-proliferative activity of heat shock protein (Hsp) 90 inhibitors via β-catenin/TCF7L2 pathway in adult T cell leukemia cells. *Cancer Letters* **284**: 62–70.

Laemmli UK (1970). Cleavage of structural proteins during the assembly of the head of bacteriophage T4. *Nature* **227**: 680-685.

Lagerstedt Robinson K, Liu T, Vandrovcova J, Halvarsson B, Clendenning M, Frebourg T, Papadopoulos N, Kinzler KW, Vogelstein B, Peltomäki P, Kolodner RD, Nilbert M and Lindblom A (2007). Lynch Syndrome (Hereditary Nonpolyposis Colorectal Cancer) Diagnostics. *J. Natl. Cancer Inst.* 99: 291-299.

Lamberti C, Lin KM, Yamamoto Y, Verma IM, Byers S and Gaynor RB (2001). Regulation of beta-catenin function by the IkappaB kinases. *J. Biol. Chem*. **276**: 42276 – 42286.

Lammi L, Arte S, Somer M, Järvinen H, Lahermo P, Thesleff I, Pirinen S and Nieminen P (2004). Mutations in AXIN2 cause familial tooth agenesis and predispose to colorectal cancer. *Am. J. Hum. Genet*. **74**: 1043–1050.

Lang SA, Moser C, Gaumann A, Klein D, Glockzin G, Popp FC, Dahkle MH, Piso P, Schlitt HJ, Geissler EK and Stoeltzing O (2007). Targeting heat shock protein 90 in pancreatic cancer impairs insulin-like growth factor-1 receptor signaling, disrupting an interleukin 6/ signal transducer and activator of transcription 3/ hypoxia inducible factor 1 (alpha) autocrine loop and reduces orthotopic tumour growth. *Clin. Cancer Res.* **13**: 6459 – 68.

Langer T, Rosmus S and Fasold H (2003). Intracellular localization of the 90 kDA heat shock protein (HSP90α) determined by expression of a EGFP-HSP90α-fusion protein in unstressed and heat stressed 3T3 cells. *Cell Biol. Int*. **27**: 47-52.

Lawson JC, Blatch GL and Edkins AL (2009). Cancer stem cells in breast cancer and metastasis. *Breast Cancer Res. Treat*. **118**: 241-54.

Lee E, Salic A, Krüger R, Heinrich R and Kirschner MW (2003). The roles of APC and Axin derived from experimental and theoretical analysis of the Wnt pathway. *PLoS Biol*. **1**: e10.

Leung JY, Kolligs FT, Wu R, Zhai Y, Kuick R, Hanash S, Cho KR, Fearon ER (2002). Activation of AXIN2 expression by β-catenin-T cell factor. A feedback repressor pathway regulating Wnt signaling. *J. Biol. Chem*. **277**: 21657 – 21665.

Levina E, Oren M and Ben-Ze'ev A (2004). Downregulation of β-catenin by p53 involves changes in the rate of β-catenin phosphorylation and Axin dynamics. *Oncogene* **23**: 4444–4453.

Li L, Yuan H, Weaver CD, Mao J, Farr GH 3rd, Sussman DJ, Jonkers J, Kimelman D and Wu D (1999). Axin and Frat1 interact with dvl and GSK, bridging Dvl to GSK in Wnt-mediated regulation of LEF-1. *EMBO J.* **18**: 4233–4240

Li X, Zhang Y, Kang H, Liu W, Liu P, Zhang J, Harris SE and Wu D (2005). Sclerostin binds to LRP5/6 and antagonizes canonical Wnt signaling. *J. Biol. Chem*. **280**: 19883–19887.

Li Y, Zhang T, Schwartz SJ and Sun D (2009). New developments in Hsp90 inhibitors as anti-cancer therapeutics: Mechanisms, clinical perspective and more potential. *Drug Res. Updat*. **12**: 17–27.

Lichtenstein P, Holm NV, Verkasalo PK, Iliadou A, Kaprio J, Koskenvuo M, Pukkala E, Skytthe A and Hemminki K (2000). Environmental and heritable factors in the causation of cancer - analyses of cohorts of twins from Sweden, Denmark, and Finland. *N. Engl. J. Med*. **343**:78–85.

Lin J, Tang H, Jin X, Jia G and Hsieh JT (2002). p53 regulates Stat3 phosphorylation and DNA binding activity in human prostate cancer cells expressing constitutively active Stat3**.** *Oncogene*. **21**:3082-3088.

Lin SY, Xia W, Wang JC, Kwong KY, Spohn B, Wen Y, Pestell RG and Hung MC (2000). β-catenin, a novel prognostic marker for breast cancer: its roles in cyclin D1 expression and cancer progression. *Proc. Natl. Acad. Sci. USA*. **97**: 4262-4266.

Lindvall C, Bu W, Williams BO and Li Y (2007). Wnt signaling, stem cells, and the cellular origin of breast cancer. *Stem Cell Rev*. **3**:157–168.

Liu G, Yuan X, Zeng Z, Tunici P, Ng H, Abdulkadir IR, Lu L, Irvin D, Black KL and Yu JS (2006). Analysis of gene expression and chemoresistance of CD133+ cancer stem cells in glioblastoma. *Mol. Cancer* **5**: 67.

Liu S and Carpenter G (1993). Differential heat stress stability of epidermal growth factor receptor and erbB-2 receptor tyrosine kinase activities. *J. Cell. Physiol*. **157**: 237–242.

Liu S, Dontu G and Wicha MS (2005). Mammary stem cells, self-renewal pathways and carcinogenesis. *Breast Cancer Res.* **7**: 86 – 95

Liu S, Dontu G, Mantle ID, Patel S, Ahn N, Jackson KW, Suri P and Wicha MS (2006). Hedgehog signaling and Bmi-1 Regulate self-renewal of normal and malignant human mammary stem cells. *Cancer Res*. **66**: 6063-71.

Liu W, Dong X, Mai M, Seelan RS, Taniguchi K, Krishnadath KK, Halling KC, Cunningham JM, Boardman LA, Qian C, Christensen E, Schmidt SS, Roche PC, Smith DI and Thibodeau SN (2000). Mutations in AXIN2 cause colorectal cancer with defective mismatch repair by activating β-catenin /TCF signaling. *Nat. Genet*. **26**: 146–147.

Lochhead PA, Kinstrie R, Sibbet G, Rawjee T, Morrice N and Cleghon V (2006). A chaperone-dependent GSK3β transitional intermediate mediates activation-loop autophosphorylation. *Mol. Cell* **24**: 627-633.

Logan CY and Nusse R (2004). The Wnt signaling in development and disease. *Annu. Rev. Cell. Dev. Biol*. **20**: 781-810.

López-Knowles E, Zardawi SJ, McNeil CM, Millar EK, Crea P, Musgrove EA, Sutherland RL and O'Toole SA (2010). Cytoplasmic localization of beta-catenin is a marker of poor outcome in breast cancer patients. *Cancer Epidemiol. Biomarkers Prev*. **19**:301-9.

Luo W, Peterson A, Garcia BA, Coombs G, Kofahl B, Heinrich R, Shabanowitz J, Hunt DF, Yost HJ and Virshup DM (2007). Protein phosphatase 1 regulates assembly and function of the β-catenin degradation complex. *EMBO J*. **26**: 1511-1521.

Lustig B, Jerchow B, Sachs M, Weiler S, Pietsch T, Karsten U, van de Wetering M, Clevers H, Schlag PM, Birchmeier W and Behrens J (2002). Negative feedback loop of Wnt signaling through upregulation of conductin/axin2 in colorectal and liver tumours. *Mol. Cell. Biol*. **22**: 1184–93.

Luu HH, Zhang R, Haydon RC, Rayburn E, Kang Q, Si W, Park JK, Wang H, Peng Y, Jiang W and He TC (2004). Wnt/β-catenin signaling pathway as a novel cancer drug target. *Curr. Cancer Drug Targets* **4**: 653–71.

Ma H, Nguyen C, Lee LS and Kahn M (2005). Differential roles for the coactivators CBP and p300 on TCF/beta-catenin-mediated *survivin* gene expression. *Oncogene* **24**: 3619–3631.

Mai M, Qian C, Yokomizo A, Smith DI and Liu W (1999). Cloning the human homolog of conductin (AXIN2), a gene mapping to chromosome 17 q23-24. *Genomics* **55**: 341 – 344.

Major MB, Camp ND, Berndt JD, Yi X, Goldenberg SJ, Hubbert C, Biechele TL, Gingras AC, Zheng N, MacCoss MJ, Angers S and Moon RT (2007). Wilms tumour suppressor WTX negatively regulates WNT/β-catenin signaling. *Science* **316**:1043-1046.

Manders EM, Stap MJ, Brakenhoff GJ, Van Driel R and Aten JA (1992). Dynamics of three-dimensional replication patterns during the S-phase, analyzed by double labeling of DNA and confocal microscopy. *J. Cell Sci*. **103**: 857–862.

Mann B, Gelos M, Siedow A, Hanski ML, Gratchev A, Ilyas M, Bodmer WF, Moyer MP, Riecken EO, Buhr HJ and Hanski C (1999). Target genes of beta-catenin T-cell-factor/lymphoid-enhancer-factor signaling in human colorectal carcinomas. *Proc. Natl. Acad. Sci. USA* **96**: 1603–1608.

Manoukian AS and Woodgett JR (2002). Role of glycogen synthase kinase-3 in cancer: regulation by Wnts and other signaling pathways. *Adv. Cancer Res*. **84**: 203-229.

Mao J, Wang J, Liu B, Pan W, Farr GH 3rd, Flynn C, Yuan H, Takada S, Kimelman D, Li L and Wu D (2001). Low-density lipoprotein receptor-related protein-5 binds to Axin and regulates the canonical Wnt signaling pathway. *Mol. Cell* **7**: 801-809.

Marcu MG, Schulte TW and Neckers L (2000). Novobiocin and related coumarins and depletion of heat shock protein 90- dependent signaling proteins. *J. Natl. Cancer Inst*. **92**: 242–248.

Maroney AC, Marugan JJ, Mezzasalma TM, Barnakov AN, Garrabrant TA, Weaner LE, Jones WJ, Barnakova LA, Koblish HK, Todd MJ, Masucci JA, Deckman IC, Galemmo RA Jr and Johnson DL (2006). Dihydroquinone ansamycins: toward resolving the conflict between low in vitro affinity and high cellular potency of geldanamycin derivatives. *Biochemistry* **45**: 5678-5685.

Martinez-Climent JA, Andreu EJ and Prosper F (2006). Somatic stem cells and the origin of cancer. *Clin. Transl. Oncol*. **8**: 647 – 663.

Mastroianni M, Kim S, Kim YC, Esch A, Wagner C and Alexander CM (2010). Wnt signaling can substitute for estrogen to induce division of ERα-positive cells in a mouse mammary tumour model. *Cancer Letters* **289**: 23-31.

Matsuda Y, Schlange T, Oakeley EJ, Boulay A and Hynes NE (2009). WNT signaling enhances breast cancer cell motility and blockade of the WNT pathway by sFRP1 suppresses MDA-MB-231 xenograft growth. *Breast Cancer Res*. **11**:R32.

McConkey DJ and Zhu K (2008). Mechanisms of proteasome inhibitor action and resistance in cancer. *Drug Resist. Updates* **11**: 164–179.

Messaoudi S, Peyrat JF, Brion JD, Alami M (2008). Recent advances in Hsp90 inhibitors as antitumour agents. *Anticancer Agents Med. Chem.***8**:761–782.

Meyer P, Prodromou C, Liao C, Hu B, Roe SM, Vaughan CK, Vlasic I, Panaretou B, Piper PW and Pearl LH. (2004). Structural basis for recruitment of the ATPase activator Aha1 to the Hsp90 chaperone machinery. *EMBO J*. **23**:1402-1410.

Milovanovic T, Planutis K, Nguyen A, Marsh JL, Lin F, Hope C and Holcombe RF (2004). Expression of Wnt genes and frizzled 1 and 2 receptors in normal breast epithelium and infiltrating breast carcinoma. *Int. J. Oncol*. **25**: 1337–1342.

Miniño AM, Heron MP, Murphy SL and Kochanek KD (2007). Deaths: final data for 2004. *Natl. Vital Stat. Rep*. **55**: 1–120.

Miyagi K, Yamazaki T, Tsujino I, Takahashi N, Koya Y, Masutani M, Sawada U and Horie T (2001). Application of hypothermia to autologous stem cell purging. *Cryobiology* **42**: 190 – 195.

Miyata Y (2009). Protein kinase CK2 in health and disease: CK2: the kinase controlling the Hsp90 chaperone machinery. *Cell. Mol. Life Sci*. **66**: 1840-1849.

Miyata Y and Yahara I (1992). The 90-kDa heat shock protein, HSP90, binds and protects casein kinase 2 from self-aggregation and enhances its kinase activity. *J. Biol. Chem.* **267**: 7042 – 7047.

Miyoshi Y, Nagase H, Ando H, Horii A, Ichii S, Kakatsuru S, Aoki T, Miki Y, Mori R and Nakamura Y (1992). Somatic mutations of the *APC* gene in colorectal tumours: mutation cluster region in the *APC* gene. *Hum. Mol. Genet*. **1**: 229-233.

Modi S, Stopeck AT, Gordon MS, Mendelson D, Solit DB, Bagatell R, Ma W, Wheler J, Rosen N, Norton L, Cropp GF, Johnson RG, Hannah AL and Hudis CA (2007). Combination of trastuzumab and tanespimycin (17-AAG, KOS-953) is safe and active in trastuzumab-refractory HER-2 overexpressing breast cancer: a phase I dose-escalation study. *J. Clin. Oncol.* **25**:5410–5417.

Moon RT, Kohn AD, De Ferrari GV and Kaykas A (2004). Wnt and β-catenin signaling: diseases and therapies. *Nat. Rev. Genet*. **5**: 691-701.

Morin PJ (1999). β-catenin signaling and cancer. *Bioessays* **21**: 1021–1030.

Morin PJ, Sparks AB, Korinek V, Barker N, Clevers H, Vogelstein B and Kinzler KW (1997). Activation of β-catenin-Tcf signaling in colon cancer by mutations in β-catenin or APC. *Science* **275**: 1787-1790.

Morin PJ, Vogelstein B and Kinzler KW (1996). Apoptosis and APC in colorectal tumourigenesis. *Proc. Natl. Acad. Sci. USA* **93**: 7950-7954.

Morrow D, Cullen JP, Liu W, Guha S, Sweeney C, Birney YA, Collins N, Walls D, Redmond EM and Cahill PA (2009). Sonic Hedgehog induces Notch target gene expression in vascular smooth muscle cells via VEGF-A. *Arterioscler. Thromb. Vasc. Biol*. **29**: 1112–1118.

Moser AR, Hegge LF and Cardiff RD (2001). Genetic background affects susceptibility to mammary hyperplasias and carcinomas in Apc(min)/+ mice. *Cancer Res*. 61: 3480-3485.

Moserle L, Ghisi M, Amadori A and Indraccolo S (2010). Side population and cancer stem cells: therapeutic implications. *Cancer Letters* **288**: 1–9.

Nagahata T, Shimada T, Harada A, Nagai H, Onda M, Yokoyama S, Shiba T, Jin E, Kawanami O and Emi M (2003). Amplification, up-regulation and over-expression of DVL-1, the human counterpart of the Drosophila disheveled gene, in primary breast cancers. *Cancer Sci*. **94**: 515–518.

Nakopoulou L, Mylona E, Papadaki I, Kavantzas N, Giannopoulou I, Markaki S, Keramopoulos A (2006). Study of phospho-β-catenin subcellular distribution in invasive breast carcinomas in relation to their phenotype and the clinical outcome. *Mod. Pathol*. **19**: 556–563.

Neckers L (2003). Development of small molecule Hsp90 Inhibitors: utilizing both forward and reverse chemical genomics for drug identification. *Curr. Med. Chem*.**10**: 733–739.

Neckers L (2006). Chaperoning oncogenes: Hsp90 as a target of geldanamycin. *Handb. Exp. Pharmacol*. **172**: 259–277.

Neckers L, Minnaugh E and Schulte TW (1999). HSP90 as an anti-cancer target. *Drug Res. Updates* **2**: 165 – 172.

Neo SY, Zhang Y, Yaw LP, Li P and Lin SC. (2000). Axin-induced apoptosis depends on the extent of its JNK activation and its ability to down-regulate β-catenin levels. *Biochem. Biophys. Res. Commun.* **272**:144–50.

Neufeld KL, Zhang F, Cullen BR and White RL (2000). APC mediated downregulation of β-catenin activity involves nuclear sequestration and nuclear export. *EMBO re*. **1**: 519 – 523.

Ni M and Lee AS (2007). ER chaperones in mammalian development and human diseases. *FEBS Lett.* **581**: 3641–3651.

Niu G, Wright KL, Ma Y, Wright GM, Huang M, Irby R, Briggs J, Karras J, Cress WD, Pardoll D, Jove R, Chen J, Yu H (2005). Role of Stat3 in regulating p53 expression and function. *Mol. Cell. Biol*. **25**:7432-40.

Nusse R and Varmus HE (1992). Wnt genes. *Cell* **69**: 1073-1087.

Oates NA, van Vliet J, Duffy DL, Kroes HY, Martin NG, Boomsma DI, Campbell M, Coulthard MG, Whitelaw E and Chong S (2006). Increased DNA methylation at the AXIN1 gene in a monozygotic twin from a pair discordant for a caudal duplication anomaly. *Am. J. Hum. Genet*. **79**: 155–162.

Ossewaarde, JM, de Vries A, Bestebroer T and Angulo AF (1996). Application of *Mycoplasma* group-specific PCR for monitoring decontamination of *Mycoplasma*-infected *Chlamydia* sp. Strains. *Appl. Environ. Microbiol*. **62**: 328–331.

Ozaki S, Ikeda S, Ishizaki Y, Kurihara T, Tokumoto N, Iseki M, Arihiro K, Kataoka T, Okajima M and Asahara T (2005). Alterations and correlations of the components in the Wnt signaling pathway and its target genes in breast cancer. *Oncol. Rep*. **14**: 1437–43.

Pacey S, Banerji U, Judson I and Workman P (2006). Hsp90 inhibitors in the clinic. *Handb. Exp. Pharmacol.* **172**: 331–358.

Paddock SW (2005). Microscopy. In: *Principles and techniques of biochemistry and molecular biology*. Sixth edition Wilson K and Walker J (ed), pp 133-151. Cambridge: Cambridge University Press.

Park JW, Yeh MW, Wong MG, Lobo M, Hyun WC, Duh QY and Clark OH (2003). The heat shock protein 90 binding geldanamycin inhibits cancer cell proliferation, down regulates oncoproteins and inhibits epidermal growth facton induced invasion in thyroid cancer cell lines. *J. Clin. Endocrinol. Metab.* **88**: 3346 – 3353.

Parker DS, Ni YY, Chang JL, Li J and Cadigan KM (2008). Wingless signaling induces widespread chromatin remodeling of target loci. *Mol. Cell. Biol.* **28**: 1815–1828.

Patrawala L, Calhoun T, Schneider-Broussard R, Zhou J, Claypool K and Tang DG (2005). Side population is enriched in tumourigenic, stem-like cancer cells, whereas ABCG2+ and ABCG2– cancer cells are similarly tumourigenic. *Cancer Res*. 65:6207–6219.

Pearl LH and Prodromou C (2001) Structure, function and mechanism of the Hsp90 molecular chaperone. *Adv. Protein Chem.* **59**: 157-186.

Pearl LH and Prodromou C (2006). Structure and mechanism of the Hsp90 molecular chaperone machinery (2006). *Annu. Rev. Biochem*. **75**: 271–294.

Pearl LH, Prodromou C and Workman P (2008). The Hsp90 molecular chaperone: an open and shut case for treatment. *Biochem. J.* **410**: 439–453.

Peifer M and Polakis P (2000). Wnt signaling in oncogenesis and embryogenesis - a look outside the nucleus. *Science* **287**: 1606– 1609.

Peng C, Brain J, Hu Y, Goodrich A, Kong L, Grayzel D, Pak R, Read M and Li S. (2007). Inhibition of heat shock protein 90 prolongs survival of mice with BCR-ABL-T315I-induced leukemia and suppresses leukemic stem cells. *Blood* **110**: 678–685.

Periyasamy S, Warrier M, Tillekeratne MP, Shou W and Sanchez ER (2007). The immunophilin ligands cyclosporin A and FK506 suppress prostate cancer cell growth by androgen receptor-dependent and -independent mechanisms. *Endocrinology* **148**:4716-26.

Picard D (2002). Heat-shock protein 90, a chaperone for folding and regulation. *Cell. Mol. Life Sci.* **59**: 1640–1648.

Pick E, Kluger Y, Giltnane JM, Moeder C, Camp RL, Rimm DL and Kluger HM (2007). High HSP90 expression is associated wwith decreased survival in breast cancer. *Cancer Res.* **67**: 2932 – 2937.

Polakis P (2000). Wnt signaling and cancer. *Genes Dev*. **14**: 1837-1851.

Polakis P (2007). The many ways of Wnt in cancer. *Curr. Opin. Genet. Dev*. **17**: 45–51.

Prasad CP, Mirza S, Sharma G, Prashad R, DattaGupta S, Rath G and Ralhan R (2008). Epigenetic alterations of CDH1 and APC genes: relationship with activation of Wnt/β-catenin pathway in invasive ductal carcinoma of breast. *Life Sci.* **83**: 318–325.

Price MA (2006). CK1, there's more than one: casein kinase 1 family members in Wnt and Hedgehog signaling. *Genes Dev*. **20**: 399–410.

Prinsloo E, Cooper LC, Moyo B, de la Mare J, Lawson JC, Edkins A and Blatch GL (2010). Heat shock proteins in normal and cancer stem cell biology: implications for regenerative and chemotherapeutic medicine. In: *Stem Cell, Regenerative Medicine and Cancer*, Singh SR (ed), pp 693-713. New York: Nova Science Publishers Inc.

Prodromou C, Roe SM, O'Brien R, Ladbury JE, Piper PW and Pearl LH (1997). Identification and structural characterization of the ATP/ADP-binding site in the Hsp90 molecular chaperone. *Cell* **90**: 65–75.

Radanyi C, Le Bras G, Messaoudi S, Bouclier C, Peyrat JF, Brion JD, Marsaud V, Renoir JM and Alami M (2008). Synthesis and biological activity of simplified denoviose-coumarins related to novobiocin as potent inhibitors of heat-shock protein 90 (hsp90). *Bioorg. Med. Chem. Lett*. **18**: 2495-2498.

Restall IJ and Lorimer IAJ (2010). Induction of premature senescence by Hsp90 inhibition in small cell lung cancer. *PLoS ONE* **5**: e11076.

Reya T and Clevers H (2005). Wnt signaling in stem cells and cancer. *Nature* **434**: 843 – 850.

Reya T, Morrison SJ, Clarke MF and Weissman IL (2001). Stem cells, cancer, and cancer stem cells. *Nature* **414**: 105 – 111.

Richter K and Buchner J (2001). Hsp90: chaperoning signal transduction. *J. Cell. Physiol.* **188**: 281-90.

Richter K, Soroka J, Skalniak L, Leskovar A, Hessling M, Reinstein J and Buchner J (2008). Conserved conformational changes in the ATPase cycle of human Hsp90. *J. Biol. Chem*. **283**: 17757– 17765.

Rodilla V, Villanueva A, Obrador-Hevia A, Robert-Moreno A, Fernández-Majada V, Grilli A, López-Bigas N, Bellora N, Albà MM, Torres F, Duñach M, Sanjuan X, Gonzalez S, Gridley T, Capella G, Bigas A and Espinosa L (2009). Jagged1 is the pathological link between Wnt and Notch pathways in colorectal cancer. *Proc. Natl. Acad. Sci. USA* **106**: 6315–20.

Roe SM, Prodromou C, O'Brien R, Ladbury JE, Piper PW and Pearl LH (1999). Structural basis for inhibition of the Hsp90 molecular chaperone by the antitumour antibiotics radicicol and geldanamycin. *J. Med. Chem*. **42**: 260–266.

Ronnen EA, Kondagunta GV, Ishill N, Sweeney SM, Deluca JK, Schwartz L, Bacik J and Motzer RJ (2006). A phase II trial of 17-(Allylamino)-17-demethoxygeldanamycin in patients with papillary and clear cell renal cell carcinoma. *Invest. New Drugs* **24**:543–546.

Rubinfeld B, Robbins P, El-Gamil M, Albert I, Porfiri E and Polakis P (1997). Stabilization of β-catenin by genetic defects in melanoma cell lines. *Science* **275**: 1790–1792.

Russo J and Russo IH (2001). The pathway of neoplastic transformation of human breast epithelial cells. *Radiat. Res*. **155**: 151–154.

Sadot E, Conacci-Sorrell M, Zhurinsky J, Shnizer D, Lando Z, Zharhary D, Kam Z, Ben-Ze'ev A and Geiger B (2002). Regulation of S33/S37 phosphorylated β-catenin in normal and transformed cells. *J. Cell Sci*. **115**: 2771-2780.

Salahshor S and Woodgett JR (2005). The links between axin and carcinogenesis. *J. Clin. Pathol*. **58** : 225-236.

Sato N, Yamamoto T, Sekine Y, Yumioka T, Junicho A, Fuse H, Matsuda T (2003). Involvement of heat-shock protein 90 in the interleukin-6-mediated signaling pathway through STAT3. *Biochem. Biophys. Res. Commun*. **300**: 847–852.

Satoh S, Daigo Y, Furukawa Y, Kato T, Miwa N, Nishiwaki T, Kawasoe T, Ishiguro H, Fujita M, Tokino T, Sasak Y, Imaoka S, Murata M, Shimano T, Yamaoka Y and Nakamura Y (2000). AXIN1 mutations in hepatocellular carcinomas, and growth suppression in cancer cells by virus-mediated transfer of AXIN1. *Nat. Genet*. **24**: 245–250.

Schatzkin A, Freedman LS, Dawsey SM and Lanza E (1994). Interpreting precursor studies: what polyp trials tell us about large-bowel cancer. *J. Natl. Cancer Inst*. 86: 1053–7.

Schlange T, Matsuda Y, Lienhard S, Huber A and Hynes NE (2007). Autocrine WNT signaling contributes to breast cancer cell proliferation via the canonical WNT pathway and EGFR trans-activation. Breast *Cancer Res*. **9**: R63.

Schlosshauer PW, Brown SA, Eisinger K, Yan Q, Guglielminetti ER, Parsons R, Hedrick Ellenson L and Kitajewski J (2000). APC truncation and increased β-catenin levels in a human breast cancer cell line. *Carcinogenesis* **21**: 1453–1456.

Schorr K, Li M, Krajewski S, Reed JC and Furth PA (1999). *Bcl-2* gene family and related proteins in mammary gland involution and breast cancer. *J. Mammary Gland Biol. Neoplasia* **4**:153–164.

Schulte TW and Neckers LM (1998). The benzoquinone ansamycin 17-allylamino-17-demethoxygeldanamycin binds to HSP90 and shares important biologic activities with geldanamycin. *Cancer Chemother. Pharmacol*. **42**: 273–279.

Schulte TW, Blagoklonny MV, Ingui C and Neckers L (1995). Disruption of Raf-1-Hsp90 molecular complex results in destabilization of Raf-1 and loss of Raf-1-Ras association. *J. Biol. Chem*. **270**: 24585-24588.

Schwarz-Romond T, Merrifield C, Nichols BJ and Bienz M (2005). The Wnt signaling effector Dishevelled forms dynamic protein assemblies rather than stable associations with cytoplasmic vesicles. *J. Cell Sci*. **118**: 5269-5277.

Schwarz-Romond T, Fiedler M, Shibata N, Butler PJ, Kikuchi A, Higuchi Y and Bienz M (2007A). The DIX domain of Dishevelled confers Wnt signaling by dynamic polymerization. *Nat. Struct. Mol. Biol*. **14**: 484–492.

Schwarz-Romond T, Metcalfe C and Bienz M (2007B). Dynamic recruitment of axin by Dishevelled protein assemblies. *J. Cell Sci*. **120**: 2402–2412.

Sell S (2004). Stem cell origin of cancer and differentiation therapy. *Crit. Rev. Oncol. Hematol*. **51**: 1-28.

Semënov MV, Tamai K, Brott BK, Kuhl M, Sokol S and He X (2001). Head inducer Dickkopf-1 is a ligand for Wnt coreceptor LRP6. *Curr. Biol*. **11**: 951–961.

Sharma S, Kelly TK and Jones PA (2010). Epigenetics in cancer. *Carcinogenesis* **31**: 27 – 36.

Shiras A, Chettiar ST, Shepal V, Rajendran G, Prasad GR and Shastry P (2007). Spontaneous transformation of human adult nontumourigenic stem cells to cancer stem cells is driven by genomic instability in a human model of glioblastoma. *Stem Cells* **25**: 1478–1489.

Shtutman M, Zhurinsky J, Simcha I, Albanese C, D'Amico M, Pestell R and Ben-Ze'ev A (1999). The cyclin D1 gene is a target of the β-catenin/LEF-1 pathway. *Proc. Natl. Acad. Sci. USA* **96**: 5522-5527.

Simcha I, Shtutman M, Salomon D, Zhurinsky J, Sadot E, Geiger B and Ben-Ze'ev A (1998). Differential nuclear translocation and transactivation potential of β-catenin and plakoglobin. *J. Cell. Biol*. **141**: 1433-1448.

Solit DB and Chiosis G (2008). Development and application of Hsp90 inhibitors. *Drug Discov. Today* **13**: 38– 43.

Spira AI and Carducci MA (2003). Differentiation therapy. *Curr. Opin. Pharmacol*. **3**: 338 – 43.

Sreedhar AS, Soti C and Csermely P (2004). Inhibition of Hsp90: a new strategy for inhibiting protein kinases. *Biochim. Biophys. Acta* **1697**: 233-42.

Staal FJT, Noort MV, Strous, GJ and Clevers HC (2002). Wnt signals are transmitted through N-terminally dephosphorylated β-catenin. *EMBO rep*. **3**: 63-68.

Städeli R and Basler K (2005). Dissecting nuclear Wingless signaling: recruitment of the transcriptional co-activator Pygopus by a chain of adaptor proteins. *Mech. Dev*. **122**: 1171– 1182.

Stepanova L, Leng X, Parker SB and Harper JW (1996). Mammalian p50Cdc37 is a protein kinase-targeting subunit of HSP90 that binds and stabilizes Cdk4. *Genes Dev*. **10**: 1491 – 1502.

Stepanova L, Yang G, DeMayo F, Wheeler TM, Finegold M, Thompson TC and Harper JW (2000). Induction of human Cdc37 in prostate cancer correlates with the ability of targeted Cdc37 expression to promote prostatic hyperplasia. *Oncogene* **19**:2186–2193.

Stewart SL, Wike JM, Kato I, Lewis DR and Michaud F (2006). A population-based study of colorectal cancer histology in the United States, 1998-2001. *Cancer* **107**: 1128 – 41.

Strange R, Metcalfe T, Thackray L, and Dang M (2001). Apoptosis in normal and neoplastic mammary gland development. *Micros. Res. Tech*. **52**: 171 – 181.

Stylianou S, Clarke RB and Brennan K (2006). Aberrant activation of notch signaling in human breast cancer. *Cancer Res*. **66**: 1517– 25.

Supko JG, Hickman RL, Grever MR and Malspeis L (1995). Preclinical pharmacological evaluation of geldanamycin as an antitumor agent. *Cancer Chemother. Pharmacol*. **36**: 305–315.

Suzuki H, Toyota M, Caraway H, Gabrielson E, Ohmura T, Fujikane T, Nishikawa N, Sogabe Y, Nojima M, Sonoda T, Mori M, Hirata K, Imai K, Shinomura Y, Baylin SB and Tokino T (2008). Frequent epigenetic inactivation of Wnt antagonist genes in breast cancer. *Brit. J. Cancer* **98**: 1147 – 1156

Suzuki H, Watkins DN, Jair KW, Schuebel KE, Markowitz SD, Chen WD, Pretlow TP, Yang B, Akiyama Y, Van Engeland M, Toyota M, Tokino T, Hinoda Y, Imai K, Herman JG and Baylin SB (2004). Epigenetic inactivation of SFRP genes allows constitutive WNT signaling in colorectal cancer. *Nat. Genet*. **36**: 417-422.

Taherian A, Krone PH and Ovsenek N (2007). A comparison of Hsp90α and Hsp90β interactions with cochaperones and substrates. *Biochem. Cell Biol*. **86**: 37-45.

Takayama S, Reed JC and Homma S (2003). Heat-shock proteins as regulators of apoptosis. *Oncogene* **22**: 9041 – 9047.

Tamai K, Zeng X, Liu C, Zhang X, Harada Y, Chang Z and He X (2004). A mechanism for Wnt coreceptor activation. *Mol. Cell* **13**: 149–156.

Terasawa K, Minami M, Minami Y (2005). Constantly updated knowledge of Hsp90. *J. Biochem*. **137**: 443– 447.

Thiery JP (2002). Epithelial-mesenchymal transitions in tumour progression. *Nat. Rev. Cancer* **2**: 442-454.

Towbin H, Staehelin T, and Gordon J (1979). Electrophoretic transfer of proteins from polyacrylamide gels to nitrocellulose sheets: procedure and some applications. *Proc. Natl. Acad. Sci. USA* **76**: 4350-4354

Tsaytler PA, Krijgsveld J, Goerdayal SS, Rüdiger S and Egmond MR (2009). Novel Hsp90 partners discovered using complementary proteomic approaches. *Cell Stress Chaperones* **14**: 629- 638.

Tutter AV, Fryer CJ and Jones KA (2001). Chromatin-specific regulation of LEF-1-beta-catenin transcription activation and inhibition *in vitro*. *Genes Dev*. **15**: 3342-54.

Uehara Y, Hori M, Takeuchi T, Umezawa H (1986). Phenotypic change from transformed to normal induced by benzoquinonoid ansamycins accompanies inactivation of p60src in rat kidney cells infected with Rous sarcoma virus. *Mol. Cell. Biol*. **6**: 2198– 2206.

van Amerongen R, Mikels A and Nusse R (2008). Alternative Wnt signaling is initiated by distinct receptors. *Sci. Signal*. **1**:re9.

Vasen HFA, Möslein G, Alonso A, Bernstein I, Bertario L, Blanco I, Burn J, Capella G, Engel C, Frayling I, Freidl W, Hes FJ, Hodgson S, Mecklin JP, Møller P, Nagengast F, Parc Y, Renkonen- Sinisalo L, Sampson JR, Stormorken A and Wijnen J (2007). Guidelines for the clinical management of Lynch syndrome (hereditary non-polyposis cancer). *J. Med. Genet*. **44**: 353-362.

Veeck J, Geisler C, Noetzel E, Alkaya S, Hartmann A, Knuchel R and Dahl E (2008). Epigenetic inactivation of the secreted frizzled-related protein-5 (SFRP5) gene in human breast cancer is associated with unfavorable prognosis. *Carcinogenesis* **29**: 991–998.

Veeck J, Niederacher D, An H, Klopocki E, Wiesmann F, Betz B, Galm O, Camara O, Dürst M, Kristiansen G, Huszka C, Knüchel R and Dahl E (2006). Aberrant methylation of the Wnt antagonist SFRP1 in breast cancer is associated with unfavourable prognosis. *Oncogene* **25**: 3479–3488.

Venezia TA, Merchant AA, Ramos CA, Whitehouse NL, Young AS, Shaw CA and Goodell MA (2004). Molecular signatures of proliferation and quiescence in hematopoietic stem cells. *PLoS Biol* **2**:e301.

Vignjevic D, Schoumacher M, Gavert N, Janssen KP, Jih G, Lae M, Louvard D, Ben-Ze'ev A and Robine S (2007). Fascin, a novel target of β-catenin-TCF signaling, is expressed at the invasive front of human colon cancer. *Cancer Res*. **67**: 6844–6853.

Vivanco I and Sawyers CL (2002). The phosphatidylinositol 3-kinase AKT pathway in human cancer. *Nat. Rev. Cancer* **2**:489– 501.

Von Kleist S, Chany E, Burtin P, King M and Fogh J (1975). Immunohistology of the antigenic pattern of a continuous cell line from a human colon tumour. *J. Natl. Cancer Inst*. **55**: 555 – 560.

Vousden KH and Lu X (2002). Live or let die: the cell's response to p53. *Nat. Rev. Cancer* **2**: 594–604.

Wadhwa R, Takano S, Robert M, Yoshida A, Nomura H, Reddel RR, Mitsui Y and Kaul SC (1998). Inactivation of tumour suppressor p53 by mot-2, a hsp70 family member. *J. Biol Chem*. **273**: 29586-29591.

Wandinger SK, Richter K. and Buchner J (2008). The Hsp90 chaperone machinery. *J. Biol. Chem*. **283**: 18473–18477.

Wang H, Zeng ZC, Bui TA, DiBiase SJ, Qin W, Xia F, Powell SN and Iliakis G (2001). Nonhomologous end-joining of ionizing radiation-induced DNA double-stranded breaks in human tumour cells deficient in BRCA1 or BRCA2. *Cancer Res*. **61**: 270–277.

Westerheide SD and Morimoto RI (2005). Heat shock response modulators as therapeutic tools for diseases of protein conformation. *J. Biol. Chem.* **280**: 33097 – 33100.

Wharton KA Jr (2003). Runnin' with Dvl: proteins that associate with Dsh/Dvl and their significance to Wnt signal transduction. *Dev. Biol*. **253**: 1 -17.

Whitesell L and Lindquist S (2005). Hsp90 and the chaperoning of cancer. *Nature Rev. Cancer* 5:761–772.

Whitesell L, Mimnaugh EG, De Costa B, Myers CE and Neckers LM (1994). Inhibition of heat shock protein HSP90-pp60v-src heteroprotein complex formation by benzoquinone ansamycins: essential role for stress proteins in oncogenic transformation. *Proc. Natl. Acad. Sci. USA* **91**: 8324–8328.

Wicha MS, Liu S, Dontu G (2006). Cancer stem cells: an old idea – a paradigm shift. *Cancer Res.* **66**: 1883 – 1890.

Wiechens N, Heinle K, Englmeier L, Schohl A and Fagotto F (2004). Nucleo-cytoplasmic shuttling of Axin, a negative regulator of the Wnt–β-catenin pathway. *J. Biol. Chem*. **279**: 5263–5267.

Willert K, Shibamoto S and Nusse R (1999). Wnt-induced dephosphorylation of axin releases β-catenin from the axin complex. *Genes and Dev*. 13: 1768–1773.

Wissmann C, Wild PJ, Kaiser S, Roepcke S, Stoehr R, Woenckhaus M, Kristiansen G, Hsieh JC, Hofstaedter F, Hartmann A, Knuechel R, Rosenthal A and Pilarsky C (2003). WIF-1, a component of the Wnt pathway, is down-regulated in prostate, breast, lung, and bladder cancer. *J. Pathol*. **201**: 204-212.

Wong CM, Fan ST and Ng IO (2001). β-Catenin mutation and overexpression in hepatocellular carcinoma: clinicopathologic and prognostic significance. *Cancer* **92**: 136–145.

Wong HC, Bourdelas A, Krauss A, Lee HJ, Shao Y, Wu D, Mlodzik M, Shi DL and Zheng J (2003). Direct binding of the PDZ domain of Dishevelled to a conserved internal sequence in the C-terminal region of Frizzled. *Mol. Cell* **12**: 1251–1260.

Wong SC, Lo SF, Lee KC, Yam JW, Chan JK and Wendy Hsiao WL (2002). Expression of frizzled-related protein and Wnt-signaling molecules in invasive human breast tumours. J. Pathol. 196: 145–153.

Woodgett JR (1990). Molecular cloning and expression of glycogen synthase kinase-3/factor A. *EMBO J*. **9**: 2431–2438.

Woodward WA, Chen MS, Behbod F, Alfaro MP, Buchholz TA and Rosen JM (2007). WNT/β-catenin mediates radiation resistance of mouse mammary progenitor cells. *Proc. Natl. Acad. Sci USA*. **104**: 618-623.

Woodward WA, Chen MS, Behbod F, Rosen JM (2005). On mammary stem cells. *J. Cell Sci*. **118**: 3585 – 3594.

Workman P, Burrows F, Neckers L and Rosen N (2007). Drugging the cancer chaperone HSP90:combinatorial therapeutic exploitation of oncogene addiction and tumour stress. *Ann. NY Acad. Sci*. **1113**: 202–216.

Wullschleger S, Loewith R and Hall MN (2006). TOR signaling in growth and metabolism. *Cell* **124**: 471–484.

Xu W, Mimnaugh E, Rosser MF, Nicchitta C, Marcu M, Yarden Y and Neckers L (2001). Sensitivity of mature Erbb2 to geldanamycin is conferred by its kinase domain and is mediated by the chaperone protein Hsp90. *J. Biol. Chem.* **276**: 3702–3708.

Yan D, Wiesmann M, Rohan M, Rohan M, Chan V, Jefferson AB, Guo L, Sakamoto D, Caothien RH, Fuller JH, Reinhard C, Garcia PD, Randazzo FM, Escobedo J, Fantl WJ and Williams LT (2001). Elevated expression of axin2 and hnkd mRNA provides evidence that Wnt/β-catenin signaling is activated in human colon tumours. *Proc. Natl. Acad. Sci. USA* **98**: 14973–8.

Yang J, Zhang W, Evans PM, Chen X, He X and Liu C (2006). Adenomatous polyposis coli (APC) differentially regulates β-catenin phosphorylation and ubiquitination in colon cancer cells. *J. Biol. Chem*. **281**: 17751–17757.

Yoo CB and Jones PA (2006). Epigenetic therapy of cancer: past, present and future. *Nat. Rev. Drug Discovery* **5**: 37-50.

Young JC, Moarefi I and Hartl FU (2001). Hsp90: a specialized but essential protein-folding tool. *J. Cell Biol*. **154**: 267–273.

Zeng L, Fagotto F, Zhang T, Hsu W, Vasicek TJ, Perry WL 3rd, Lee JJ, Tilghman SM, Gumbiner BM and Costantini F (1997). The mouse Fused locus encodes Axin, an inhibitor of the Wnt signaling pathway that regulates embryonic axis formation. *Cell* **90**: 181–192.

Zeng X, Huang H, Tamai K, Zhang X, Harada Y, Yokota C, Almeida K, Wang J, Doble B, Woodgett J, Wynshaw-Boris A, Hsieh JC and He X (2008). Initiation of Wnt signaling: control of Wnt coreceptor LRP6 phosphorylation/ activation via frizzled, dishevelled and axin functions. *Development* **135**: 367-375.

Zeng X, Tamai K, Doble B, Li S, Huang H, Habas R, Okamura H, Woodgett J and He X (2005). A dual-kinase mechanism for Wnt co-receptor phosphorylation and activation. *Nature* **438**: 873–877.

Zhang H and Burrows F (2004). Targeting multiple signal transduction pathways through inhibition of Hsp90. *J. Mol. Med.* **82**: 488-499.

Zhang T, Li Y, Yu Y, Zou P, Jiang Y and Sun D (2009B)**.** Characterization of celastrol to inhibit hsp90 and cdc37 interaction. *J. Biol. Chem.* **284**:35381-35389.

Zhang T, Otevrel T, Gao Z, Gao Z, Ehrlich SM, Fields JZ and Boman BM (2001). Evidence that APC regulates *survivin* expression, a possible mechanism contribution to the stem cell origin of colon cancer. *Cancer Res.* **61**: 8664–8667.

Zhang W, Yang J, Liu Y, Chen X, Yu T, Jia J and Liu C (2009A). PR55 alpha, a regulatory subunit of PP2A, specifically regulates PP2A-mediated beta-catenin dephosphorylation. *J. Biol. Chem.* **284**: 22649-56.

Zhou J, Wulfkuhle J, Zhang H, Gu P, Yang Y, Deng J, Margolick JB, Liotta LA, Ill EP and Zhang Y (2007). Activation of the PTEN/mTOR/STAT3 pathway in breast cancer stem-like cells is required for viability and maintenance. *Proc. Nat. Acad. Sci. USA* **104**: 16158 – 1613.

Zinchuk V and Zinchuk O (2008). Quantitative colocalization analysis of confocal fluorescence microscopy images. *Curr. Protoc. Cell Biol*. 4.19.1-4.19.16

Zinchuk V, Zinchuk O and Okada T (2007). Quantitative colocalization analysis of multicolour confocal immunofluorescence microscopy images: pushing pixels to explore biological phenomena. *Acta. Histochem. Cytochem.* **40**: 101-111.

WEBSITES REFERENCED

Reference	Website name and address	Date accessed
Website 1	CANSA, www.cansa.org.za.	December 2010
Website 2	IARC, www.iarc.fr.	December 2010
Website 3	The WNT signaling pathway and its role in human solid tumours. Atlas of genetics and cytogenetics in oncology and haematology, http://atlasgeneticsoncology.org/Deep/WNTSignPathID20042.html.	December 2010
Website 4	PICARD LIST OF HSP90 INTERACTORS http://www.picard.ch/downloads/downloads.htm	December 2010

APPENDIX

A1 *Mycoplasma* detection protocol

Briefly, Mycoplasma were tested for using immunofluorescent microscopy and amplification of a fragment of the 16S rRNA gene.

Detection by confocal microscopy

- Seed cells and grow on sterile glass cover slips overnight at 37 °C
- Remove media, and wash with PBS
- Fix cells with ice cold methanol (add briefly)
- Dip cover slip into Hoechst 33342 (1:1000 dilution in water) for 15 seconds
- Leave cover slip to dry on paper towel
- Mount cover slip onto glass slide with mounting medium and seal with nail varnish

Negative detection:

- Clean blue nuclei without any other speckled staining around

Positive detection:

- Blue specks (nuclear staining) around and on top of the area on the cytoplasm (Figure A1).

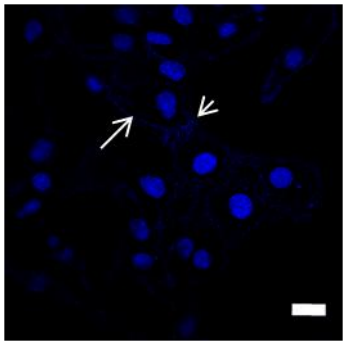

Figure A1.1 Confocal microscopy image of Caco2 cells contaminated with *Mycoplasma*. Caco2 cell nuclei stained with Hoechst. Scale bar represents 20 µM. Arrows point toward *Mycoplasma*.

Detection by PCR

1. **Isolation of DNA by boiling cells**

- T25 flask of cells trypsinized (approx 280 000 cells)
- Inhibited further trypsinization by adding media
- Transferred cells in TE buffer into eppendorf
- Centrifuged 2000 rpm, 2 mins
- Resuspended cells in 50 µl TE buffer
- Boiled samples in kettle for 15 minutes to lyse cells (viscosity)
- DNA used for PCR reaction

2. PCR Reaction

NB Dilute forward and reverse primers stock 1:10 in water before PCR

***Mycoplasma* primers**

Specific for 16S rRNA gene

Forward (XXIDT 60298391)

Upstream primer GPO-3 5'-GGG AGC AAA CAG GAT TAG ATA CCC T-3')

Position 774-798 on gene (Ossewaarde *et al*., 1996).

Reverse (XXIDT 60298392)

Downstream primer MGSO 5' – TGC ACC ATC TGT CAC TCT GTT AAC CTC -3')

Position 1029-1055 on gene (Ossewaarde *et al*., 1996).

Table A1.1 PCR reaction

Reagent	in 50 µl final volume	Final concentration	Company of reagent
Buffer 5 X Green GoTaq	10 µl	1 X	Promega, M 791A
dNTP	2 µl	0.4 mM	Roche, 13873400
forward primer (diluted)	5 µl	1 µM	XXIDT, 60298391
reverse primer (diluted)	5 µl	1 µM	XXIDT, 60298392
GoTaq polymerase (5 U/ µl)	0.25 µl	1.25 U	Promega, 9PIM300
DNA	5 µl		
Water	22.75 µl		

Table A1.2 PCR Conditions (adapted from Ossewaarde *et al*., 1996)

Temperature	Time
94 °C (denaturation)	1 min
72 °C (extension)	1 min
65 °C (annealing)	1 min
every 2 cycles annealing temperature decreased by 2 °C until 55 °C	
55 °C (final annealing)	30 cycles
4 °C	α

Set up water control, substituting DNA with water

3. Resolving PCR samples on 2 % agarose gel

2 % = 1 g agarose in 50 ml TAE buffer

The size of the PCR product of *Mycoplasma* contaminated cells is approximately 270 bp (Figure A1.2).

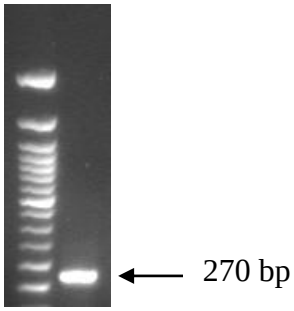

Figure A1.2. AGE (2 % acrylamide) of PCR product of cells contaminated with *Mycoplasma*. Positive signal is detected at 270 bp.

A2 ORIGINAL, UNEDITED CONFOCAL IMAGES

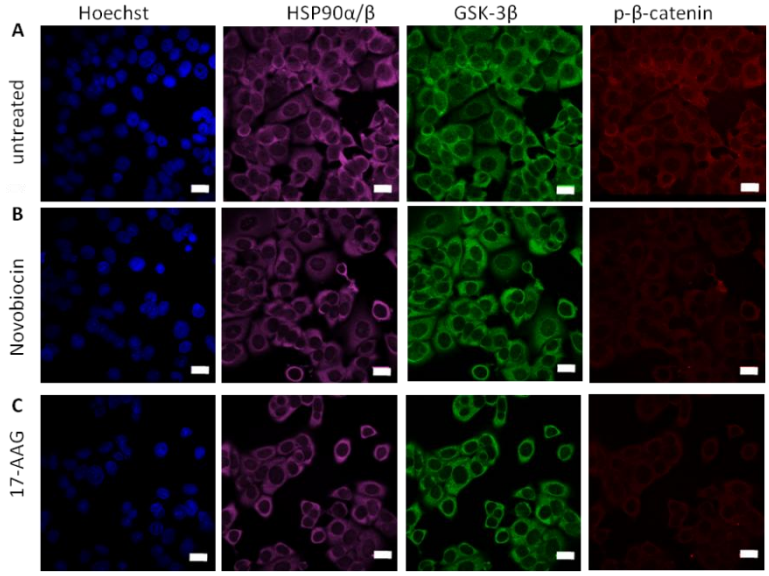

Figure A2.1. Unedited confocal images showing the effects of HSP90 inhibitors on the localization of HSP90α/β, GSK-3β and p-β-catenin. MCF7 cells were serum-starved for 1 hour prior to 5 hour treatment with inhibitors. Confocal microscopy images of stained MCF7 cells were captured using a Zeiss LSM 510 confocal microscope. A. Untreated MCF7 cells. B. Novobiocin (500 μM) treated MCF7 cells. C. 17-AAG (10 μM) treated MCF7 cells. Hoechst: blue nuclear staining. HSP90α/β (purple) using anti-human HSP90α/β antibody. GSK-3β (green) using anti-human GSK-3β antibody. P-β-catenin (red) using anti-human p-β-catenin. Scale bars represent 20 μM.

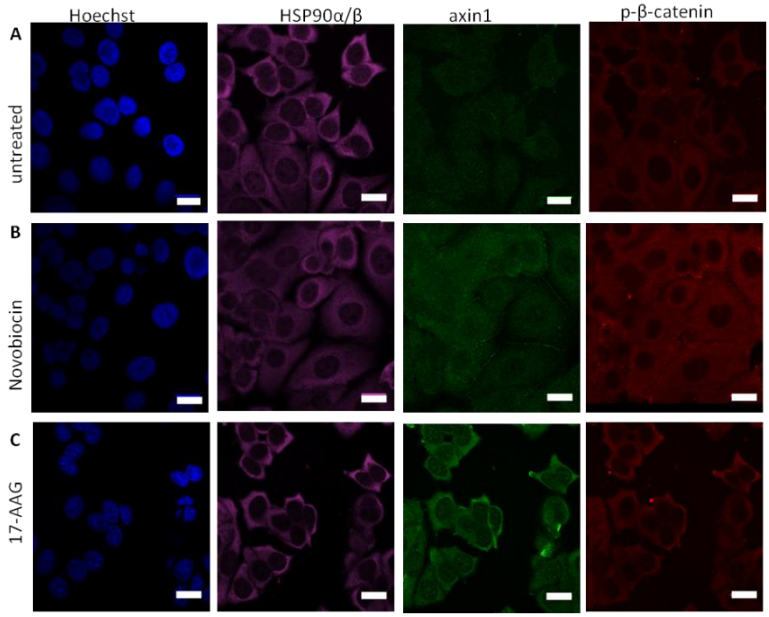

Figure A2.2 Unedited confocal images showing the effects of HSP90 inhibitors on the localization of HSP90α/β, axin1 and p-β-catenin. MCF7 cells were serum-starved for 1 hour prior to 5 hour treatment with inhibitors. Immunofluorescence confocal microscopy images of stained MCF7 cells captured using a Zeiss LSM 510 confocal microscope. A. Untreated MCF7 cells. B. Novobiocin (500 μM) treated MCF7 cells. C. 17-AAG (10 μM) treated MCF7 cells. Hoechst: blue nuclear staining. HSP90α/β (purple) using anti-human HSP90α/β antibody. Axin1 (green) using anti-human axin1 antibody. P-β-catenin (red) using anti-human p-β-catenin. Scale bars represent 20 μM.

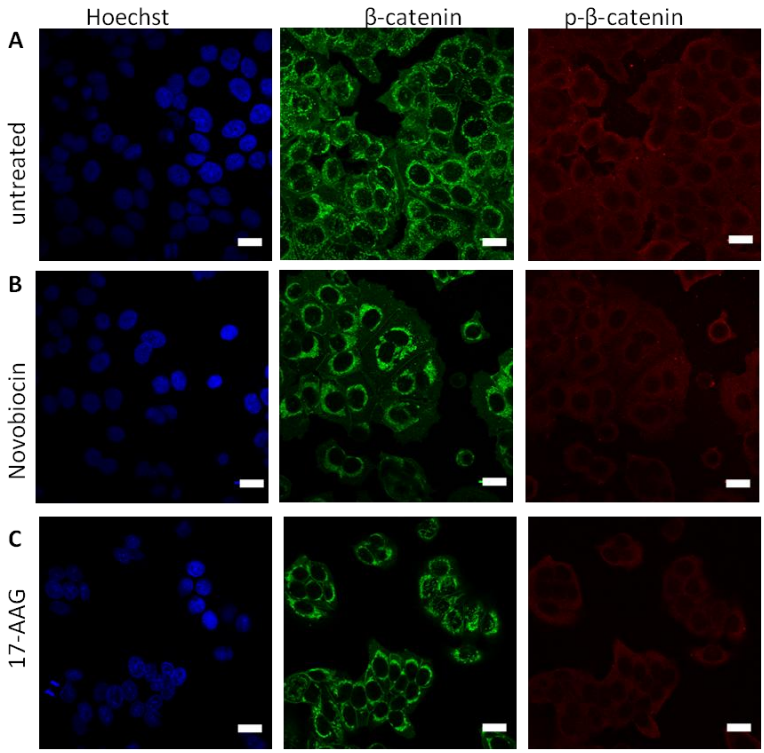

Figure A2.3. Unedited confocal images showing the effect of HSP90 inhibitors on β-catenin and p-β-catenin localization. MCF7 cells were serum-starved for 1 hour prior to 5 hour treatment with inhibitors. Immunofluorescence confocal microscopy images of stained MCF7 cells captured using a Zeiss LSM 510 confocal microscope. A. Untreated MCF7 cells. B. Novobiocin (500 μM) treated MCF7 cells. C. 17-AAG (10 μM) treated MCF7 cells. Hoechst: blue nuclear staining. β-catenin (green) using anti-human β-catenin antibody. p-β-catenin (red) using anti-human p-β-catenin antibody. Scale bars represent 20 μm.

A3 DENSITOMETRIC ANALYSIS SHOWING TOTAL β-CATENIN ISOLATED BY HSP90 IMMUNOPRECIPITATION WAS GREATER THAN NON-SPECIFIC PROTEIN

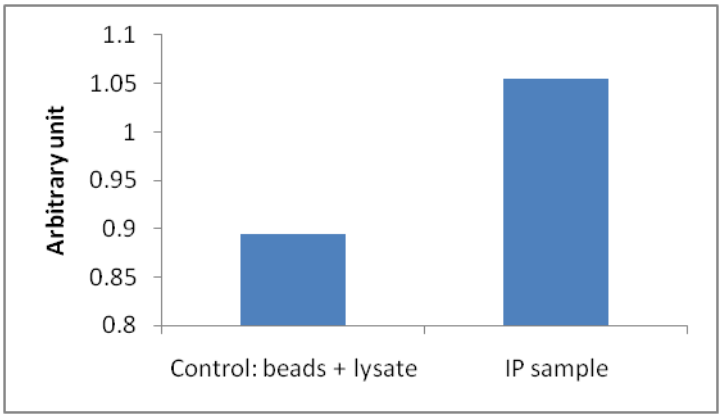

Figure A3.1. Western detection signal representing total β-catenin was higher than the non-specific signal. Densitometric analysis of signals representing β-catenin and non-specific bands detected in HSP90 immunoprecipitation. Control: protein A/G agarose-PLUS beads in the absence of antibody. IP sample: Signal representing β-catenin isolated by HSP90α/β immunoprecipitation.

A4 DENSITOMETRIC ANALYSIS OF PROTEINS NORMALIZED AGAINST ACTIN IN HSP90 INHIBITION STUDY

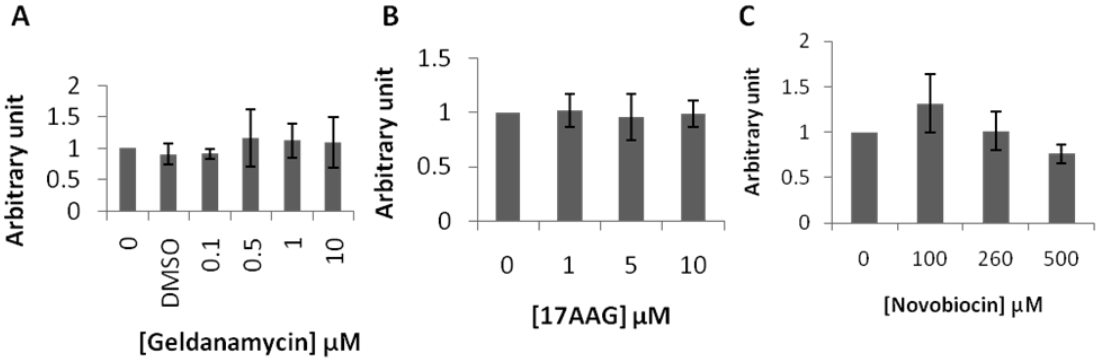

Figure A4.1. Densitometric analysis of HSP90α/β normalized against actin in geldanamycin (A), 17-AAG (B) and novobiocin (C) treated MCF7 cells. No treatment (0) and DMSO were used as the controls.

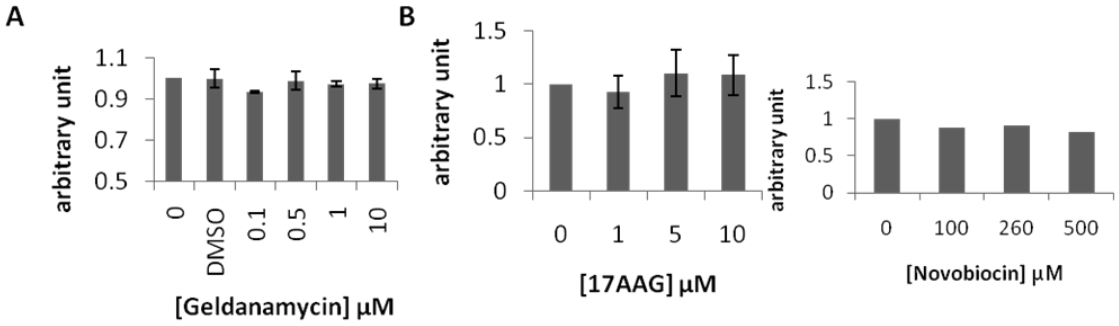

Figure A4.2. Densitometric analysis of STAT3 normalized against actin in geldanamycin (A), 17-AAG (B) and novobiocin (C) treated MCF7 cells. No treatment (0) and DMSO were used as the controls.

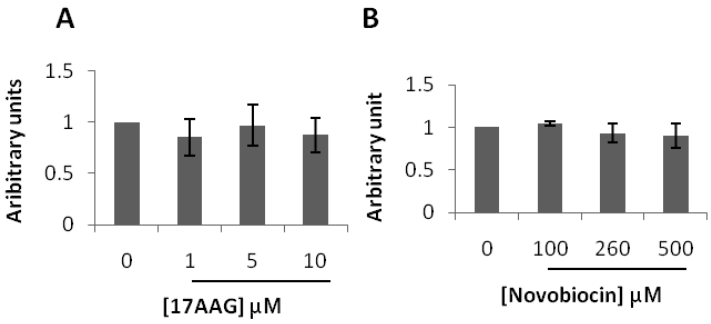

Figure A4.3. Densitometric analysis of p-STAT3 normalized against actin in geldanamycin (A) and 17-AAG (B) treated MCF7 cells. No treatment (0) was used as the control.

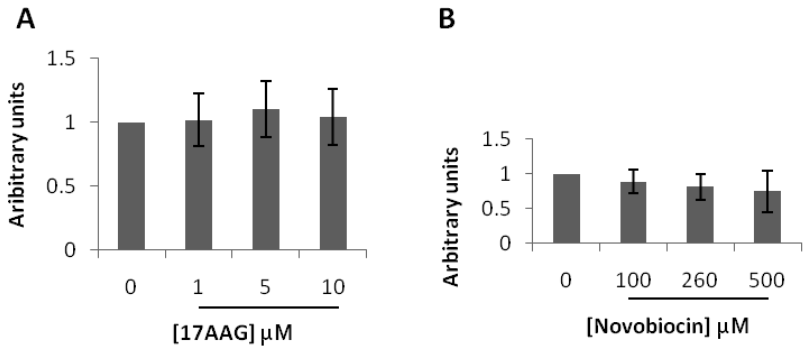

Figure A4.4. Densitometric analysis of Akt normalized against actin in geldanamycin (A), 17-AAG (B) and novobiocin (C) treated MCF7 cells. No treatment (0) was used as the control.

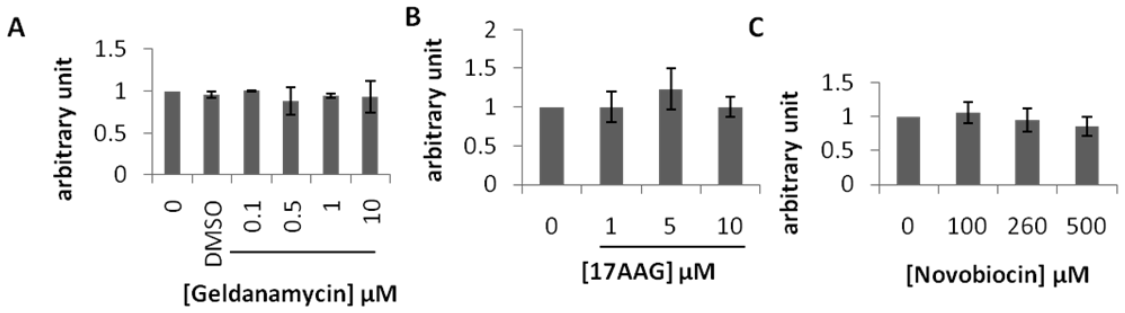

Figure A4.5. Densitometric analysis of GSK-3β normalized against actin in geldanamycin (A), 17-AAG (B) and novobiocin (C) treated MCF7 cells. No treatment (0) and DMSO were used as the controls.

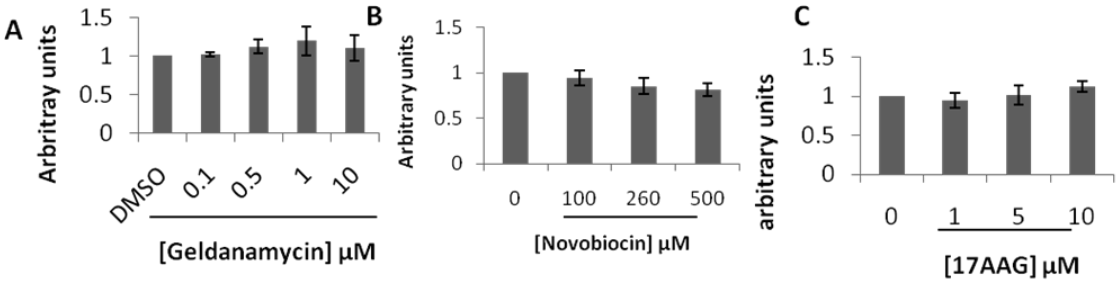

Figure A4.6. Densitometric analysis of β-catenin normalized against actin in geldanamycin (A), novobiocin (B) 17-AAG (C) treated MCF7 cells. No treatment (0) and DMSO were used as the controls.

A5 MEDIA AND SOLUTION PREPARATION

10 X phosphate buffered saline (PBS) pH 7.4

Dilute stock 10 X to make 1 X

Reagent	**Final Concentration (in 1L)**	**Mass (g)**
NaCl	1.37 M	80
KCl	0.03 M	2
Na_3HPO_4	0.16 M	11.5
KH_2PO_4	0.02 M	2

RIPA lysis buffer

Protease inhibitor cocktail added according to the vendor's instructions (1 % v/v)

Reagent	**Final concentration (in 200 µl)**	**volume (µl)**
Tris-HCl and NaCl solution	50 mM and 150 mM	189.8
EGTA/EDTA	1 mM	2
Na_3VO_4	1 mM	2.2
NP40	1 % (v/v)	2
Na deoxycholate	1 mM	2
PMSF	1 mM	2
protease inhibitor	2 µg/ml	2

A6 SDS-PAGE PAGE BUFFERS AND GEL PREPARATIONS

Reagent	**volume**
dH_20	3.55 ml
0.5 M Tris-HCl pH 6.8	1.25 ml
glycerol	2.5 ml
10 % (w/v) SDS	2 ml
0.5 % (w/v) bromophenol blue	0.2 ml

Add 50 µl β-mercaptoethanol to 950 µl prior to use to make 5 X sample treatment buffer

SDS-PAGE gel preparation

12 % acrylamide resolving gel

Reagent	**Volume**
dH_20	3.35 ml
1.5 M Tris-HCl (Ph 8.8)	2.5 ml
10 % SDS	100 µl
Bis-acrylamide	4 ml
10 % ammonium persulphate	100 µl
TEMED	20 µl

4 % acrylamide stacking gel

Reagent	**Volume**
dH_20	3.05 ml
0.5 M Tris-HCl (Ph 6.8)	1.25 ml
10 % SDS	50 µl
Bis-acrylamide	665 µl
10 % ammonium persulphate	100 µl
TEMED	20 µl

10 X SDS-PAGE running buffer

Reagent	**mass (in 1 L water)**
glycine	144 g
SDS	10 g
Tris	30.3 g

Dilute to 1 X prior to use

A7 REAGENTS, CHEMICALS AND SOURCES

Tissue culture

Reagent	Company	Country
4 well culture plates (Nunclon^{TM})	NUNC	USA
6 well culture plates	Corning	USA
Dako fluorescent mounting medium	Dako	USA
dimethyl sulphoxide (DMSO)	Sigma-Aldrich	USA
Dulbecco's Modified Eagle Medium (DMEM) with 4.5 g/L D-glucose, L-glutamine, pyruvate	Gibco, Invitrogen	USA
Fetal calf serum (FCS)	PAA Laboratories	USA
Hoechst 33342	Invitrogen	USA
L-glutamine	Gibco	USA
Penicillin-Streptomycin solution stabilizer (5 000U and 5 mg strep)	Sigma-Aldrich	USA
T25 (25 cm^3) tissue culture flasks	Corning	USA
T75 (75 cm^3) tissue culture flasks	Corning	USA
Trypan Blue solution (0.4 %)	Sigma-Aldrich	USA
Trypsin/ ethylenediaminetetraacetic acid (EDTA)	Sigma-Aldrich	USA

General reagents

Reagents	Vendor	Country
17-AAG	Sigma-Aldrich	USA
2-mercaptoethanol	MERCK	South Africa
50 bp marker	New England BioLabs	UK
Acetic acid	SAARCHEM, MERCK	South Africa
Acrylamide	BioRad	USA
Agarose	Whitehead Scientific	South Africa
Ammonium persulphate	SAARCHEM	South Africa
Bromophenol blue	Sigma-Aldrich	USA
BSA	Roche Diagnostics	Germany
Coomassie Brilliant Blue-R250	Sigma-Aldrich	USA

Disodium hydrogen orthophosphate	Merck	South Africa
Dynabeads® co-immunoprecipitation kit	Invitrogen	USA
ECL kit	GE Healthcare, Amersham	USA
EDTA	Saarchem	USA
Ethidium bromide	Sigma-Aldrich	USA
Fermentas Marker Plus	Fermentas	USA
geldanamycin	BioMol International	USA
Glacial acetic acid	SAARCHEM	South Africa
Glycerol	SAARCHEM	South Africa
Glycine	Sigma-Aldrich	South Africa
HCl	Merck	South Africa
KCl	SAARCHEM	South Africa
NaCl	Sigma-Aldrich	South Africa
NP40	Roche	Germany
PBS tablets	Sigma-Aldrich	USA
pEQ Gold Marker IV	peQ-Lab	Germany
Ponceau S	Sigma-Aldrich	USA
Potassium diydrogen phosphate	Merck	South Africa
protease inhibitor cocktail	Sigma-Aldrich	USA
protein A/G PLUS-agarose immunoprecipitation reagent	Santa Cruz Biotechnologies	USA
Sodium diodecyl sulphate	Sigma-Aldrich	USA
TEMED	Sigma-Aldrich	USA
Trans-Blot® nitrocellulose membrane	Bio-Rad	South Africa
trisodium citrate	Saarchem	South Africa
Triton X-100	Sigma-Aldrich	USA
Trizma base	Sigma-Aldrich	USA
Tryptone (pancreatic digestion of casein)	Biolab, Merck	UK
Tween-20	SAARCHEM, MERCK	South Africa

A8 Instruments and sources

Instrument	Source
Western blotting power pack	Bio-Rad, UK
Centrifuge 8000R	Centurion Scientific, UK
Centrifuge 5804R	Eppendorf, Germany
Centrifuge 5415R	Eppendorf, Germany

A9 PICARD LIST OF HSP90 INTERACTORS

(website 4)

Chaperones and relatives	Transcription factors
- Aha1 and its homolog Hch1 - Cdc37 (p50) and its relative Harc - p23 (=Sba1) - proteins with TPR motifs, including Hop (=Sti1), FKBP52 (and high MW plant homologs), FKBP51, FKBP8 (=FKBP38), FKBP36 (= FKBP6), Plasmodium FKBP35, cyclophilin-40 (Cpr6 and Cpr7), PP5 (and yeast Ppt1), Tom70, probably also related Tom71=Tom72, XAP-2 (=AIP=ARA9), Cns1 and its Drosophila and human relatives Dpit47 and TTC4, CHIP, GCUNC-45 (also UNC-45 and She4), DnaJC7 (=Tpr2=mDj11=CCRP), CRN, WISp39 (=FKBPL), Tah1 (=Spaghetti), NASP, Toc64, TPR1 (=Ttc1), SGT (=αSGT=SGTA), DYX1C1 - CS-containing p23 relatives SGT1 (=SUGT1), RAR1, Siah-1-interacting protein (SIP), Chp1/Morgana, B-ind1, melusin, CHORDC1 - Hsp60 - Hsc70/Hsp70/Hsp72 - Human DnaJ homolog Hsj1b - S100A1 - Sse1, Sse2 - valosin-containing protein (VCP)/p97 - NudC and NudCL2 - Pih1 (=Nop17) (mostly through Tah1) - Cullin5 - Tel2-Tti1-Tti2 complex	- 12(S)-HETE receptor - AF9/MLLT3 - all vertebrate steroid receptors (GR, MR, ERα, ERβ, PR, AR) - BCL-6 - CAR - cytoplasmic v-erbA - EcR - PPARα (PPARβ) - PXR - Hap1 - HSF-1 - IRF3 - Mal63 - p53 - PAS family members: Dioxin receptor (=AhR), Sim, HIF–1α, HIF-2α, HIF-3α - Sp1 - Stat3 (also in caveolin-1 complexes in rafts) - TonEBP/OREBP - Ure2 - VDR - water mold *Achlya* steroid (antheridiol) receptor

Kinases	
- Akt/PKB	- MOK, MAK, MRK
- ASK1	- c-Mos
- Aurora B	- NIK
- Bcr-Abl	- Nucleophosmin-Anaplastic Lymphoma Kinase
- casein kinase IIα catalytic subunit	
- Cdc2 (=Cdk1)	- p38
- Cdc25c	- p90RSK
- Cdk2, Cdk4, Cdk6, Cdk9, Cdk11	- platelet-derived growth factor receptor α
- Chk1	- PDK1
- Cot = Tpl-2	- Pim-1
- Death-associated kinases DAPK, DAPK2, DAPK3	- Pink1
	- PKCλ, PKCε and other PKCs
- death domain kinase RIP	- Plk1
- eEF-2 kinase	- pp60v-src, c-src
- eIF2-α kinases HRI, Gcn2, Perk, PKR	- src related tyrosine kinases: fer, fes, fgr, fps, lck, yes
- EphA2	
- ErbB2 (and mutant EGF receptor)	- Raf-1, B-Raf, Ste11
- ERK5	- RET
- Flt3	- RET/PTC1
- Fused	- Ron
- GRK2 and GRK6	- Ryk
- GSK3β	- SGK-1
- HER3	- Slt2
- IκB kinases α, β, γ, ε	- SRPK1
- Insulin receptor	- SSTK (= Tssk6)
- Insulin-like growth factor 1 receptor	- TAK1
- Integrin-linked kinase	- TBK1
- IP6K2	- TGFβ receptors I and II
- IRAK-1	- TrkB
- Ire1	- TrkAI and III
- JAK1	- Tyk2
- JNK	- VEGFR1, VEGFR2
- c-Kit	- Wee1, Swe1
- KSR	- ZAP-70
- Lkb1	
- LRRK2	
- MAPK6	
- MEK	
- MEKK1 and MEKK3	
- Mik1	
- MLK3	

Others	
- Annexin II	- glutathione S-transferase subunit 3 (KS type)
- ANP receptor	- HDAC6
- Apaf-1	Hepatitis E virus capsid protein
- apoB	- HERG
- Argonaute-1	- Histones H1, H2A, H2B, H3 and H4
- Argonaute-2 (= GERp95)	- c-IAP1
- Bcl-2	- Importin β
- Bcl-xL	- Inositol 1,4,5-trisphosphate receptor 3
- Bid	- KSHV K1
BLM helicase	- Kir6.2
- BRMS1	- knob complexes (in the membrane of Plasmodium-infected erythrocytes)
- calcineurin (Cna2; catalytic subunit)	- LAMP-2A
- calmodulin	- LAP
- calponin	- LIS1
- CB2 cannabinoid receptor	- macromolecular aminoacyl-tRNA synthetase complex
- CD91	- Macrophage scavenger receptor
- Cdc13	- Mdm2
- Cdk5 activator p35	- MMP2, MMP9
- CFTR (nascent polypeptide)	- MRE11/Rad50/NBS1 (MRN) complex
- Chronophin	- Msps/XMAP215/ch-TOG
- ClC-2 chloride channel	- MTG8
- COG complex	- MUC1
- CTA1	- Na+-K+-Cl- cotransporter 1
- Ctf13/Skp1 component of CBF3	- NB-LRR proteins: RPM1 and RPS2, Nod1, Nod2, NALP2, NALP3, NALP4, NALP12, IPAF
- Cup	- Neuropeptide Y
- cyclin B	- N-myc downstream-regulated gene 1 (NRDG1)
- cyclophilin D (mitochondrial)	- Nsl1
- cytoskelettal proteins: actin, tubulin (including ciliary β4-tubulin), myosin	- Nup62
- DEDD	- N-WASP
- Dengue virus protein E	- OsCERK1
- DNA polymerase α	- P1 (picornaviral capsid precursor protein P1)
- DNA polymerase η	- p300
- DNMT1	- P450 CYP2E1
- Dsn1	- P2X7 purinergic receptor
- eNOS, nNOS (?)	- PB2 subunit of influenza RNA pol.
- ether-a-gogo-related cardiac potassium channel	
- FLIPS and FLIPL	
- free βγ subunit of G protein	
- Gα0, Gα12	
- Hepatitis virus C protein NS3	

- perilipin - Mg2+-dependent phosphatidate phosphohydrolase - polysomal ribonuclease 1 (PMR1) - PRMT5 - prolactin receptor - prostacyclin synthase - proteasome - R2TP complex through Pih1 - Rab-αGDI - Rab11a - Rac/Rop GTPase Rac1 (rice) - Rac1 - Ral-binding protein 1 - Raptor - reovirus protein σ1 - reverse transcriptase of hepatitis B virus - ribosomal proteins S3 and S6 - ribosomal protein L2 (E. coli) - ricin catalytic A chain - RIG-I - Rpb1 - R-protein I-2 - SIR2 (SIR2RP1 in Leishmania) - SKP2 complexes - SMYD1, SMYD2, SMYD3 - snoRNP complexes - SREC-I - DNA helicase Ssl2 - SUR1 (subunit of β-cell ATP-sensitive potassium channel) - survivin - SV40 large T-antigen - α-synuclein - Tab2/3 - Tau protein - telomerase	- thiopurine S-methyltransferase - thrombin receptor (PAR-1) - thromboxane synthase - Tissue plasminogen activator (tPA) - TLR4/MD-2 complex - TOM40 - Trithorax (and ortholog MLL) - Tyrosine hydroxylase - UCH-L1 - Uroporphyrinogen decarboxylase (HemE) [in cyanobacteria] - Vaccinia core protein 4a - misfolded VHL - Vimentin